OCEANOGRAFI Nr 119, 2016

Model study on the variability of ecosystem parameters in the Skagerrak-Kattegat area, effect of load reduction in the North Sea and possible effect of BSAP on Skagerrak-Kattegat area

Ivan Kuznetsov, Kari Eilola, Christian Dieterich, Robinson Hordoir, Lars Axell, Anders Höglund and Semjon Schimanke

Cover: Fiskebäck, Gothenburg

ISSN: 0283-7714

OCEANOGRAFI Nr 119, 2016

Model study on the variability of ecosystem parameters in the Skagerrak-Kattegat area, effect of load reduction in the North Sea and possible effect of BSAP on Skagerrak-Kattegat area

Ivan Kuznetsov, Kari Eilola, Cristian Dieterich, Robinson Hordoir, Lars Axell, Anders Höglund and Semjon Schimanke

Summary

Newly developed ecosystem model NEMO-Nordic-SCOBI was applied to Skagerrak - Kattegat area to investigate the variability of some indicators of the ecosystem. Also, two sensitivity runs were performed to investigate possible effect of the Baltic Sea Action Plan (BSAP) and a river loads reduction scenario on the Skagerrak - Kattegat area. The performed investigation could be used "to provide a basis to assist with the interpretation of measurement data before the Intermediate Assessments Eutrophication status assessment". Comparison of simulation results with observations indicates acceptable model performance. Modeled sea surface salinity, temperature and dissolved inorganic phosphate (DIP) are in good agreement with observations. At the same time, the model has a bias in certain areas of the investigated region for dissolved inorganic nitrogen (DIN) and dissolved silicate during the winter season. However, the model in its current state shows good enough results for the performed investigation. Results of the two sensitivity studies show a decrease of sea surface nutrients concentrations during winter period in both regions. In the Skagerrak area the decrease is due to reduction in river nutrient loads in North Sea. In the Kattegat area there is a decrease of dissolved phosphate due to the implementation of BSAP. At the same time, in both scenarios, no significant changes were obtained for near bottom oxygen or surface layer Chl-a.

Sammanfattning

Den nyligen utvecklade ekosystemmodellen NEMO-Nordic-SCOBI användes för att studera variabiliteten av några indikatorer för ekosystemet i Skagerrak-Kattegatt området. Även två känslighetsstudier gjordes för att undersöka möjliga effekter av Baltic Sea Action Plan (BSAP) och en reduktion scenario av närsaltstillförsel på Skagerrak-Kattegatt området. Den utförda studien kan användas som underlag och stöd vid tolkningen av observationsdata inför utvärderingen ”Intermediate Assessments Eutrophication status assessment”. Jämförelsen mellan modelldata och observationer indikerar att modellens resultat är acceptabla. Modellerade ytvärden av salthalt, temperatur och löst fosfat (DIP) visar god överenskommelse med observerade värden. Samtidigt har modellresultaten avvikelser i vissa delområden vad gäller löst oorganiskt kväve (DIN) och löst kisel under vitertid. Dock visar modellen i sitt nuvarande tillstånd tillräckligt goda resultat för den aktuella studien. Resultaten från de två känslighetsstudierna visar en minskning av näringskoncentrationer i ytan under vintern i båda havsområdena. I Skagerrak är minskningen orsakad av reducerad närsaltstillförsel i Nordsjön. I Kattegatt minskar lösta fosfatet på grund av genomförandet av BSAP. Ingen av scenarierna visade någon signifikant påverkan på syre vid havsbotten eller på ytkoncentratiner av Chl-a.

Table of Contents

1. Introduction

The Skagerrak and Kattegat (Fig. 1) are situated in the transition area between the brackish Baltic Sea waters and the more oceanic waters in the North Sea (e.g. Rodhe et al. 2006). The physical conditions vary because of large differences in salinity, tidal stirring and topography. The characteristics of the North Sea and the Baltic Sea are separated especially due to the shallow sills at the Danish Sounds with a maximum depth of about 18m. The Kattegat is quite shallow (mean depth of 23 m) while the Skagerrak is deep with much higher salinity (mean depth of 230m and a deep trench in the northern parts) (eg. Leppäranta and Myrberg, 2009). The Baltic Sea is characterized by a long water residence time while the water exchange in the North Sea, Skagerrak and the Kattegat is much faster.

The outflow of fresher waters from the Baltic Sea takes place at the surface mainly along the eastern parts following the Swedish and Norwegian coasts and the salinity of the outflowing water increases on the way to the North Sea due to entrainment and upwelling of high saline waters from the deeper layers. The large salinity gradients between the Baltic Sea and the North Sea and the shifting atmospheric conditions cause frontal movements and large variations in the hydrographic conditions in the transition area. The preconditions for biogeochemical processes are therefore different in the different areas and the importance of the main sources of nutrients (supplies from land, upwelling or the open boundary) may differ as well (e.g. Rodhe et al. 2006).

In a previous model investigation Eilola and Sahlberg (2006) used a box model to represent the Kattegat and Skagerrak area. They followed largely the COMP (OSPAR common procedure) and assessed the eutrophication status in the Skagerrak and the Kattegat coastal and offshore areas and the following long-term effects on the ecosystem for nutrient reductions as suggested by the PARCOM Recommendation 88/2. In this case the open boundaries towards the North Sea and the Baltic Sea were forced by a combination of model data and observations. The volume transports were forced by model data while the concentrations were based on observations. Hence, the possibility to investigate the detailed spatial variations was limited.

Previous COMP (OSPAR Common Procedure) calculations of Good Environmental Status (GES) are based on observations that are available today (data 2001-2005) and new values for GES will be produced again at the next evaluation round of 2018. The uncertainty or confidence of these assessment numbers, based on discrete spatial and temporal data in the highly dynamic transition area, is not well known today. The aim of the present investigation is based on an agreement between the Swedish Agency for Marine and Water management (Svenska Havs- och Vattenmyndigheten HaV) and the Swedish Meteorological and Hydrological Institute (SMHI) to explore these uncertainties from results produced with a newly developed coupled physical-biogeochemical ecosystem model called NEMO-Nordic-SCOBI. The model covers both the North Sea and the Baltic Sea with high resolution and includes several of the components used in the COMP. More specifically we will check if there are spatial confidential errors based on the model reality, find information on data variability (assuming the model data is the reality, rather than the measured data) and perform sensitivity analyses based on proposed scenarios.

The work is divided into two main parts:

1. Describe statistical measures of available variables that give information on the OSPAR COMP causative effects, direct effects and indirect effects.
2. Cause and effect studies are used to explore if it is possible to detect changes in COMP assessments in specific areas following suggested reductions in the North Sea or a Baltic Sea that reach the state suggested by the Baltic Sea Action Plan.

The results from the investigation will mainly be provided as maps. More details and the proposed list of outcome are listed in the methods.

2. Methods

The ecosystem model NEMO-Nordic-SCOBI used in this study consist of two main parts: physical and biogeochemical models.

2.1 Physical model

The nucleus for European Modelling of the Ocean (NEMO) ocean engine is used here as the physical model. The setup of NEMO for the coupled North Sea - Baltic Sea system (called NEMO-Nordic) was developed by the Swedish Meteorological and Hydrological Institute. The model setup was well validated and the results were published by Dietrich et al. (2013) and Hordoir et al. (2013 a, b; 2015). The model has open boundaries in the English Channel in the south-west and in the section between Norway and Scotland (see Fig. 1) in the north-west. The model has a horizontal resolution of about 2 nm (3.7 km) and 56 vertical levels. Detailed description of the physical setup can be found in Hordoir et al. (2013 a, b; 2015) and Dietrich et al. (2013). Results of a downscaled ERA40 reanalysis by RCA4 atmospheric model were used as atmospheric forcing Wang et al. (2015). The river runoff forcing was provided by E-HYPE model (Donnelly et al. 2015).

2.2 Biogeochemical model

The biogeochemical model for this study was the Swedish Coastal and Ocean BIogeochemical (SCOBI) model (Marmefelt et al. 1999). The SCOBI model is a continuously developing model, see for example Eilola et al., (2009), Almroth-Rosell et al., (2011, 2015). At SMHI the SCOBI model has been used for many years in different physical model configurations e.g., the RCO (e.g. Almroth and Skogen, 2010; Eilola et al., 2011; 2012; 2013; 2014; Meier et al., 2012; Skogen et al., 2014), HIROMB (Eilola et al., 2006) and PROBE models (Sahlberg, 2009). The present NEMO-Nordic-SCOBI model has also been developed to include the dynamics of silicate. The present SCOBI model therefore describes cycles of nitrogen, phosphorus and silicate. Oxygen dynamics are also included and hydrogen sulfide concentrations are represented by "negative oxygen" equivalents (1 ml H_2S l^{-1} = –2 ml O_2 l^{-1}). Inorganic nutrients are represented by four state variables: nitrate, ammonia, phosphate and silicate. Nutrients are assimilated by three phytoplankton groups representing diatoms, flagellates and others, and cyanobacteria. Bulk zooplankton grazes on phytoplankton. Dead organic material, represented by separate variables for nitrogen, phosphorus and silicate, accumulates in detritus in the water column and in the sediments. Particulate organic matter can sink and resuspend from the sediments due to strong currents and waves. For detailed description of the SCOBI model see Eilola et al. (2009) and Almroth-Rosell et al. (2011, 2015).

2.3 Reference run

All model runs were performed from January 2007 to the end of 2012. Several data sets were used to force the biogeochemical model. Nutrient loads reconstruction from Savchuk et al. (2012) was used as a forcing for the SCOBI model in the Baltic Sea region. It includes atmospheric deposition, as well as loads from rivers and point sources. To force the model in the North Sea data from Morten D. Skogen, Institute of Marine Research (pers. Com.) were used (see Fig. 2). Initial conditions for 2007 were derived from previous hindcast simulations (1961-2007) (Kuznetsov et al., 2015 (in preparation)). The boundary conditions for biogeochemical model were extracted from the ICES data base (ICES, 2009) and interpolated on the model grid.

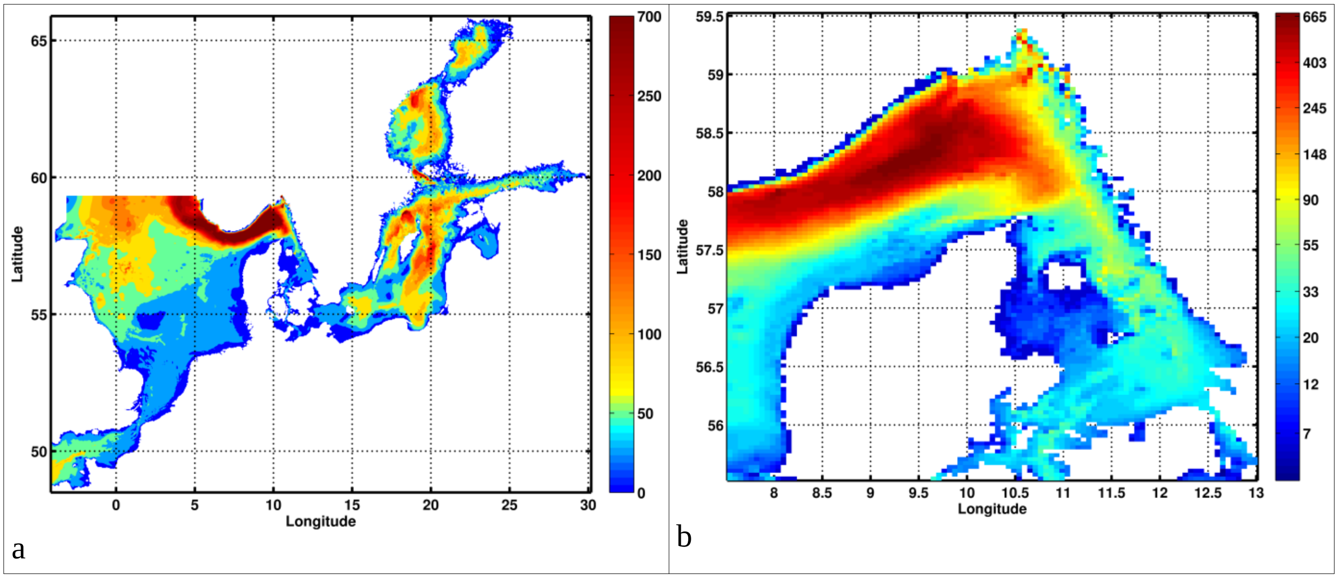

Fig. 1. Model topography. a – whole model domain, b - area of interest.

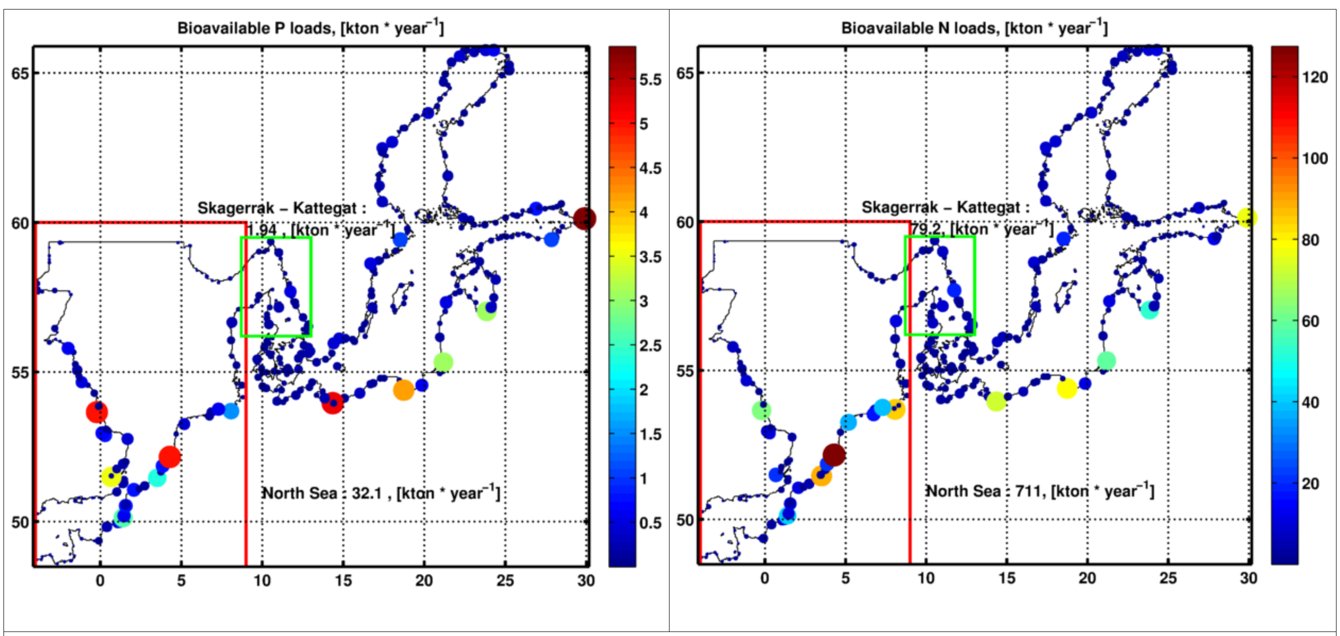

Fig. 2. Nutrient river loads to the model domain. Dots indicate model rivers. Size and color of dots show contribution of each river and follows the color scale.

2.3 Sensitivity runs

Two sensitivity runs were performed:

1. Sensitivity to reductions in load from the North Sea
   - The waterborne load to the southern North Sea was reduced by 50% for DIN and DIP.
   - The loading from Sweden and Norway to the North Sea was kept constant.
   - The loading to the Baltic Sea was kept constant.
2. Sensitivity to reductions according to the BSAP
   - BSAP was assumed to be achieved in the Baltic Proper.
   - Climatological DIN and DIP concentrations at Arkona station from the reference run were decreased to fit BSAP numbers and applied as boundary conditions.

The second experiment was done by using the same model setup as in the reference run, but with an artificial boundary in the Arkona Basin. The nutrient concentration profiles judged from the reference run were multiplied by a factor so that surface water concentrations (0-10 m) were consistent with the goal of BSAP in the Arkona Basin (i.e. winter DIN and DIP have concentrations of 2.9 mmol N / m^3 and 0.36 mmol P / m^3 respectively (HELCOM, 2013)). Other model variables were unchanged. DIP from the reference run was reduced by a factor of 0.54 while DIN was reduced only insignificantly, by a factor of 0.96.

3. Results

3.1 Validation

In appendix A1 figures are shown of modeled and observed time series (2007 – 2012) of surface (0-10 m) salinity, temperature, DIN, DIP, Si, Chl a and near bottom oxygen concentration on 7 stations located in the investigated area. Fig. 1 (in appendix A1) shows station locations. Black dots represent observed values from the SHARK database. Blue, green and red lines show model results for three simulations; reference run, reduction in NS rivers run and BSAP run, respectively. Depth of near bottom cell both from model results and from observations was chosen according to the maximum depth in the model. Since the model grid depth, representing average conditions in about 2nm x 2nm areas, may differ from the depth of specific stations, the data from observations need not necessary represent deepest measured values.

Simulation results indicate that the model has negative bias in salinity at stations Å17, Å15 and Å13 in the northern part of the study area. Central and southern parts (stations P2, Fladen, Anholt E, W Landskrona) are well represented by the model both for sea surface temperature and salinity. Low observed temperature values during the winter 2010 were well captured by the model.

The model shows higher winter surface DIN than observations at most of the stations with some exceptions (stations P2 and W Landskrona) where the model well captured winter dynamics of DIN. In contrast to DIN, simulated winter values of DIP represent observations well at all stations.

Observed near bottom oxygen was well represented by the model. An exception is deep oxygen concentrations at station Å17. Here initial concentrations of oxygen were 2 ml/l too low in the model. However, after the first 3 years of simulations the difference between observations and model became small. Modeled seasonal cycle of near bottom oxygen is in a good agreement with observations.

3.2 Maps, reference run.

In this section, an overview of the reference run results is presented. In figures 3-6 fields are shown of the mean of all years of simulation, standard deviation (STD) and coefficient of variation (CV, “=STD divided by the mean value”) for 4 selected parameters: winter (December - February) sea surface (mean value over first 10 meters of water column) DIN (Fig. 3.) and DIP (Fig. 4.), growing season (February - October) sea surface Chl-a (Fig. 5.) and summer-autumn (August – October) oxygen concentrations at sea bottom (grid cell nearest the model sea floor) (Fig. 6.). More figures from the model runs can be found in Appendix 2.

Model results show strong lateral gradients of DIN and DIP from the North West (boundary to North Sea) to the South East (entrance to the Danish Straits). High DIN in the south part of Skagerrak is mainly caused by the Jutland current. Some higher DIN and DIP concentrations, possibly due to river outflows, at the Eastern Jutland coast in the Kattegat can be seen. The impact of DIN from rivers is also seen at some spots with higher DIN on the Swedish west coast. At the same time high DIP in Kattegat is determined by the outflow from Baltic Sea through the Danish Straits, especially from the Great Belt area. Both DIP and DIN show high relative variability expressed by the CV (about 0.3) in the region influenced by the Jutland current. High DIN CV is also seen in the south and south-eastern parts of the Kattegat. Increased DIP CV is also seen north of the Sjælland Island. However, DIP does not indicate high CV in the south-eastern parts of Kattegat. The model shows highest Chl-a concentrations in the southern part of Kattegat and along the coastal line, with low values in Skagerrak. At the same time model results indicate high CV values for Chl-a in the Skagerrak area. Concentrations of modeled near bottom oxygen, followed in general the bathymetry of the region. High oxygen concentrations along the coastline are obtained by the intensive vertical mixing with saturated surface waters. The deep parts of the area show lower oxygen concentrations because of oxygen consumption due to organic matter decomposition and a limited vertical water exchange. Meanwhile highest CV, up to 0.2 for bottom oxygen, is found in the deepest part.

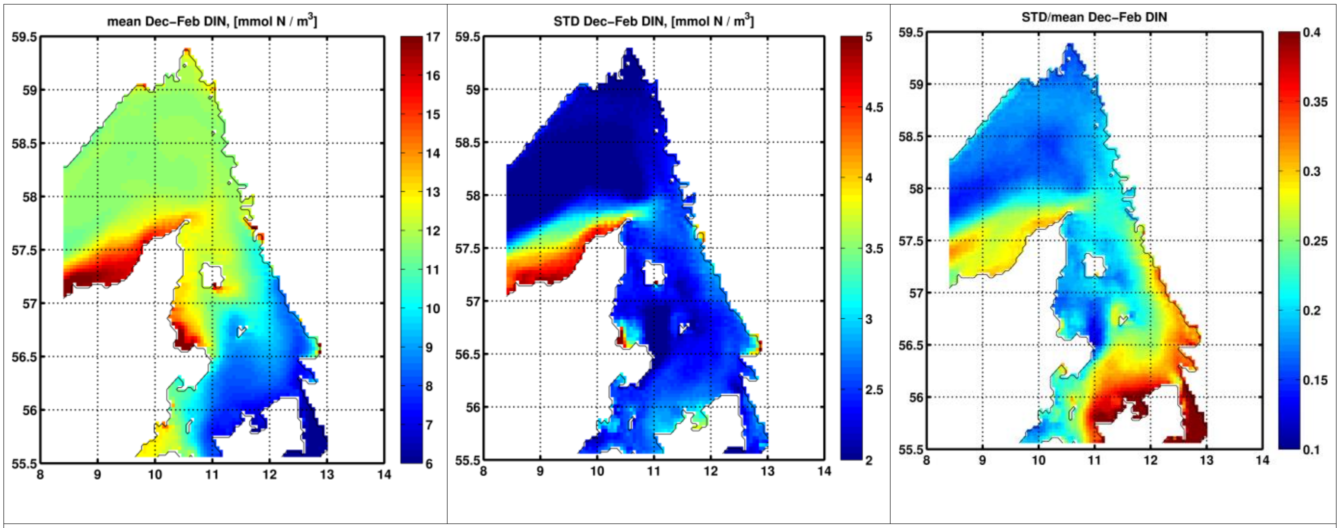

Fig. 3. Winter (DJF) sea surface (10m mean) DIN. Mean, std and std/mean (CV) for 2007–2011 years of the reference run. (CV "=STD divided by the mean value")

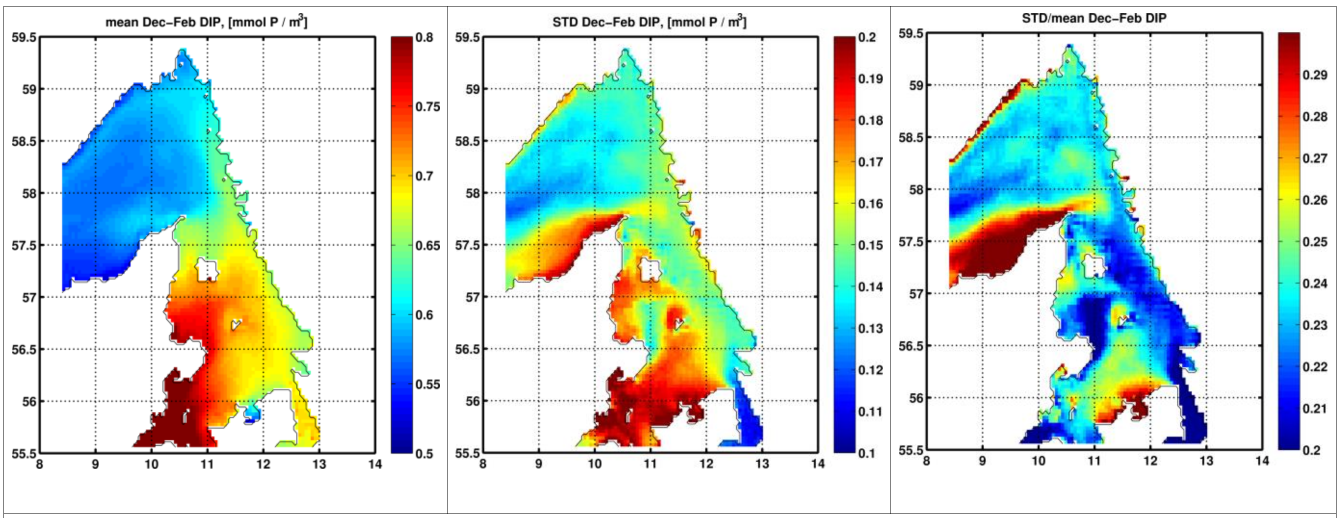

Fig. 4. Winter (DJF) sea surface (10m mean) DIP. Mean, std and std/mean for 2007–2011 years of the reference run.

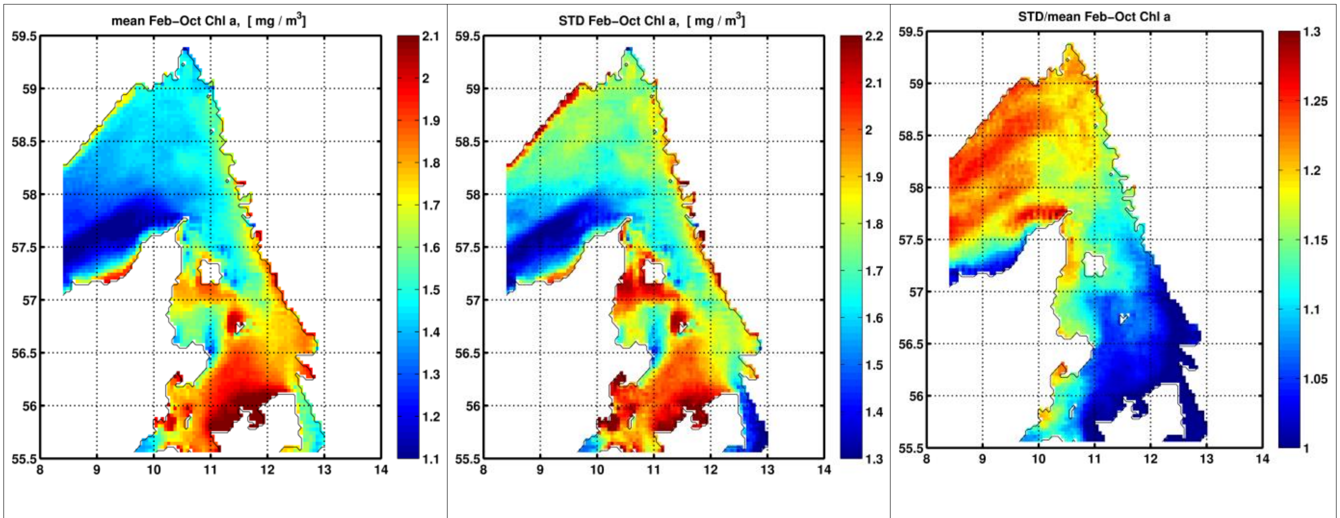

Fig. 5. Concentrations of chlorophyll-a in the growing season (February to October) at sea surface (10m mean). Mean, std and std/mean for 2007–2011 years of the reference run.

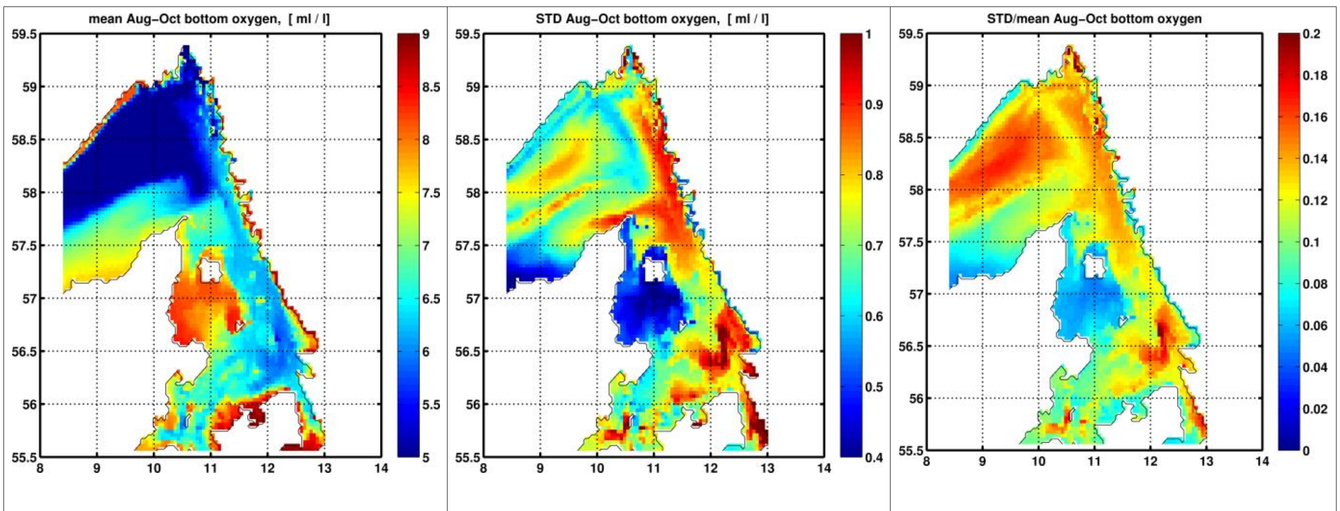

Fig. 6. Concentrations of oxygen at sea bottom (grid cell and layer nearest the sea floor) during late summer-autumn (August-October). Mean, std and std/mean for 2007–2011 years of the reference run.

3.3 Reduction in NS rivers scenario.

In this section results of the sensitivity study with river load reduction to the North Sea are presented. Fig. 7 shows changes due to reduced river loads in the mean surface layer DIN, DIP, Chl-a and bottom oxygen. The relative change shown in Fig. 7 is defined as the ratio between results from the reference run and the reduction scenario run. The ratio was first calculated separately for every day and for each model cell. Thereafter the mean values of the ratio (Fig. 7) were calculated. The main differences between the two simulations are in the DIN and DIP fields in the Skagerrak region (Fig. 7). The most significant effect is seen in the area affected by the Jutland current. Mean winter DIN decreased by up to 30% and DIP concentrations decreased by about 10%. In the rest of the Skagerrak area DIN and DIP decreased by about 17% and 6%, respectively. In the Kattegat area, DIN and DIP concentrations decreased in winter by about 10% and 3%, respectively. The strong decrease in winter DIN concentrations in Skagerrak does not entail strong decrease in Chl-a. The decrease in Chla-a is similar to DIP dynamics in the Skagerrak area with a decrease by about 6% in the area effected by the Jutland current, while the rest of the investigated area mostly remained unchanged. Simultaneous decrease in winter nutrients and Chl-a concentration during growing season does not change the bottom oxygen dynamics.

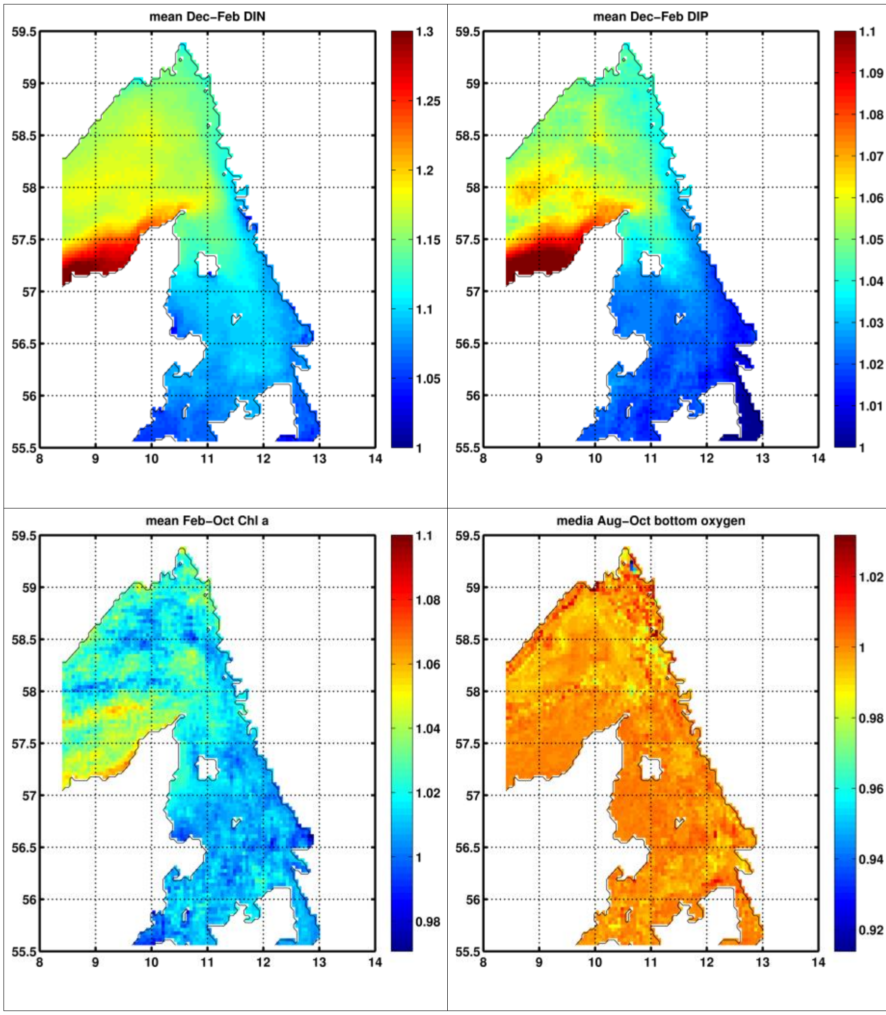

Fig. 7. Relative change in Reductions in NS river loads run (reference run / current run) in winter (DJF) sea surface (10m mean) DIN and DIP, concentrations of chlorophyll-a in the growing season (February to October) at sea surface (10m mean) and concentrations of oxygen at sea bottom (grid cell and layer nearest the sea floor) during late summer-autumn (August-October).

3.4 Maps, BSAP scenario.

In this section we describe results of the sensitivity run with artificial open boundary conditions in the Arkona basin that reproduce a BSAP scenario in the Baltic Sea. In Fig. 8, maps (similar to Fig. 7) for BSAP run are presented. Since the results of the reference run in the Arkona basin for DIN were already close to the assumed BSAP boundary conditions, there were no significant changes observed for DIN in the BSAP run. At the same time DIP concentrations were reduced by about 50%. Effect of the significant DIP reduction was seen in the Kattegat area and especially in the Danish straits were the mean winter DIP decreased by more than 40%. At the same time, due to significant changes in the N:P ratio, the mean winter DIN is increased in BSAP run in the Öresund strait by about 10%. In the rest area of interest, surface DIN does not change significantly. Similar to DIN, surface DIP does not change significantly in the Skagerrak area. However, the DIP reduction in Arkona basin resulted in a strong decrease of winter DIP in the Kattegat area with a strong gradient from south to north. The significant decrease of DIP in the Kattegat area entailed a decrease in surface Chl-a concentrations by up to 10% compared to the reference run. Similar to the scenario with river load reduction in the North Sea, the BSAP scenario does not show any significant changes in bottom oxygen concentrations.

.

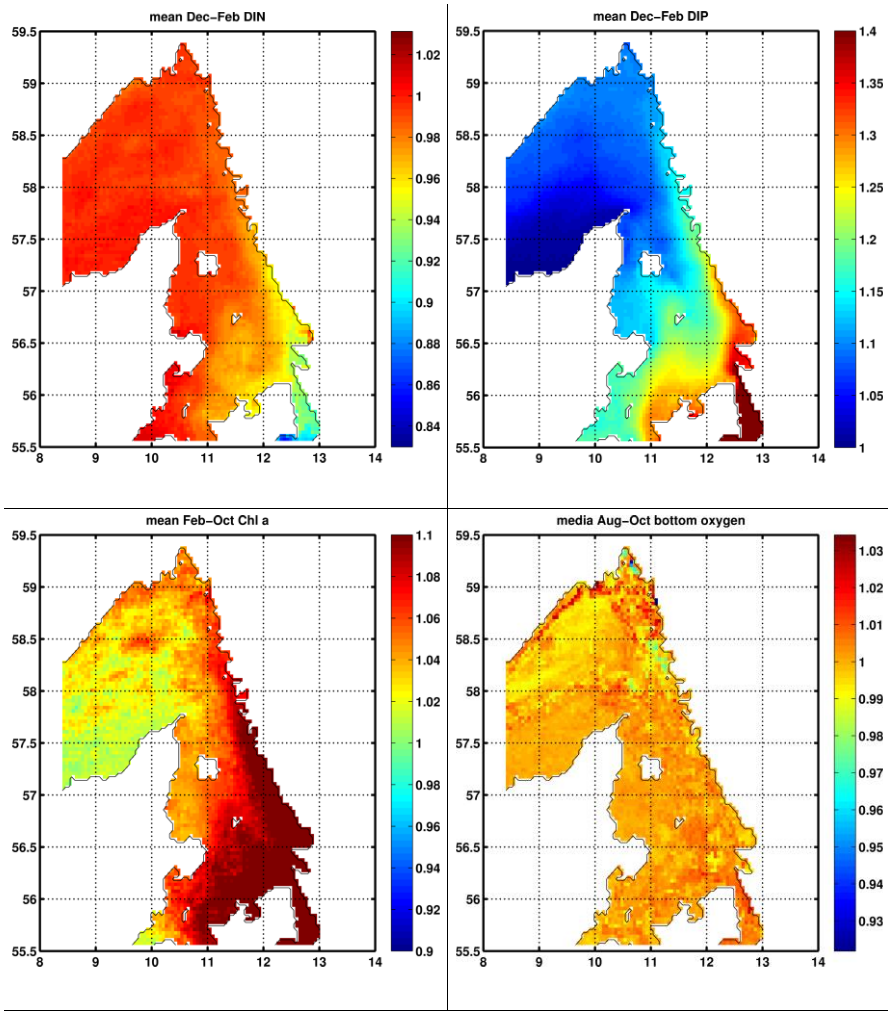

Fig. 8. Relative change in BSAP run (reference run / current run) in winter (DJF) sea surface (10m mean) DIN and DIP, concentrations of chlorophyll-a in the growing season (February to October) at sea surface (10m mean) and concentrations of oxygen at sea bottom (grid cell and layer nearest the sea floor) during late summer-autumn (August-October).

4. Discussion and Conclusions.

High DIN concentrations in the modeled Skagerrak area are caused by the influence of the Jutland current. Model DIN bias in in the Wadden Sea (in south-eastern part of the North Sea) causes a significant effect on the dynamics of DIN in Skagerrak. At the same time the seasonal cycles are well captured by the model for DIN and DIP. In contrast to DIN and DIP, the model is not good at reproducing the seasonal cycle of Si in the Skagerrak – Kattegat area, while dynamics of Si in the North Sea were well captured by the model. Less variability of Si in the model could be due to a systematic error in spring bloom phytoplankton dynamics for Si. To solve a similar problem in the coupled North Sea-Baltic Sea ecosystem model Maar et al. (2011) included a function describing the increased silicate uptake by diatoms with increasing SiO_2:DIN ratios to match the observations. In the current investigation it would not be possible to use such an approach since mass conservation is important for the investigation of possible scenarios to answer main question for changes in sinks and sources.

The model in its present state shows good enough results for current investigation. To bypass the effect of bias in DIN, we use the coefficient of variation (the ratio of the standard deviation to the mean) that gives a better approximation of surface winter variability than the absolute value given by the standard deviation.

Model results indicate that one of the significant sources of DIN in the investigated area is the open boundary to the North Sea. High concentration of DIN in the Jutland current produces high DIN concentrations in Skagerrak. Together with the low DIN in outflow from the Arkona basin this produces a surface DIN gradient in the Skagerrak-Kattegat area (with higher DIN in the North). As opposed to DIN, the gradient of surface DIP has an opposite sign, defined by high surface DIP in the outflow from the Baltic Sea. Analyses of the variability of modeled winter surface DIN and DIP shows high CV values, up to 30%, mainly in the Skagerrak in the area affected by the Jutland current and in the southern Kattegat. Also, model results indicate high CV values of DIN along the Swedish west coast, but not for DIP. According to model results highest Chl-a concentrations were found in the south part of Kattegat and along the coast. Unlike nutrients, Chl-a CV values are higher in the regions not affected by the Jutland current and the Baltic Sea outflow. On the other hand, Chl-a CV values varied between 1 and 1.3 which means much stronger variability than winter nutrients (up to 0.3). As it was mentioned before, near bottom oxygen fields follow the bathymetry of the area with lower oxygen concentrations in the deep parts of the area. At the same time there is no significant correlation between Chl-a fields and the near bottom oxygen fields.

Both sensitivity studies (reduced N and P river loads in the North Sea (NS run) and BSAP in Baltic Sea (BS run)) show significant changes in surface DIN and DIP. At the same time each scenario indicates changes that are mainly regional, in one area in Skagerrak for the NS run and in another area in the Kattegat for the BS run. Applying a reduction scenario in the North Sea rivers resulted in decreasing winter DIN and DIP in Skagerrak, but not in the Kattegat. Opposed to that, the BS run resulted in a decrease of DIP in Kattegat and an insignificant effect in the Skagerrak. It should be mentioned again that in case of the BS run, mainly the DIP concentration was significantly reduced to achieve the BSAP values in the Arkona basin. Reduction of DIP and the following relaxing of DIN caused slight increases in DIN concentrations in the Kattegat. In contrast to winter nutrient concentrations, Chl-a concentrations changed insignificantly, although following the nutrient changes. A comparison of the CV for Chl-a from the reference run with results from the sensitivity studies indicated minor alterations. Changes in surface DIN and DIP and minor changes in Chl-a in both sensitivity studies do not change the distribution of oxygen in study area. All changes in near bottom oxygen concentrations are insignificant compared to the variability in the reference run.

5. Acknowledgement

The work presented in this study was funded by the Swedish Agency for Marine and Water management HaV, and partly by the Integrated management of Agriculture, Fishery, Environment and Economy project (IMAGE) from the Danish Agency for Science, Technology and Innovation (# 09-067259/DSF). The development and set-up of the NEMO-Nordic-SCOBI model was funded by the Swedish Research Council for Environment, Agricultural Sciences and Spatial Planning (FORMAS) within the project "Impact of changing climate on circulation and biogeochemical cycles of the integrated North Sea and Baltic Sea system" (grant no. 214-2009-577). Model simulations were performed on the super computer Krypton at the National Supercomputing Centre, Linköping University, Sweden. The authors wish to thank all the people who have contributed to the development of the NEMO-Nordic stand-alone, operational and coupled configurations inside and outside SMHI.

References

Almroth, E., and M.D. Skogen, 2010. A North Sea and Baltic Sea model ensemble eutrophication assessment. Ambio, 39(1), 59-69.

Almroth-Rosell, E., Eilola, K., Hordoir, R., Meier, H.E.M., Hall, P., 2011. Transport of fresh and resuspended particulate organic material in the Baltic Sea — a model study. J. Mar. Sys. 87, 1–12.

Almroth-Rosell, E., K. Eilola, I. Kuznetsov, P. Hall, and H. E. M. Meier, 2015. A new approach to model oxygen dependent benthic phosphate fluxes in the Baltic Sea. J. Mar. Syst. 144: 127–141. DOI:10.1016/j.jmarsys.2014.11.007.

Dieterich, C., Schimanke, S., Wang, S., Vli, G., Liu, Y., Hordoir, R., Axell, L., Höglund, A. and H.E.M. Meier. 2013. Evaluation of the SMHI coupled atmosphere-ice-ocean model RCA4-NEMO. Report Oceanography, SMHI.

Donnelly, C., Andersson J. C.M. and Arheimer, B., 2015. Using flow signatures and catchment similarities to evaluate the E-HYPE multi-basin model across Europe. Hydrological Sciences Journal, 61, pp. 255 – 273. DOI: 10.1080/02626667.2015.1027710.

Eilola, K., Almroth, E., J. Naustvoll, P. Andersen and B. Karlson, 2006. Modelling the dynamics of harmful blooms of Chattonella sp. in the Skagerrak and the Kattegat. ICES CM 2006/E12, ICES Annual Science conference.

Eilola, K. and J. Sahlberg, 2006: Model assessment of the predicted environmental consequences for OSPAR problem areas following nutrient reductions. Rapport Oceanografi No. 83. SMHI Norrköping Sweden.

Eilola, K., H.E.M. Meier and E. Almroth, 2009. On the dynamics of oxygen, phosphorus and cyanobacteria in the Baltic Sea; A model study. J. Mar. Sys., 75, pp. 163-184.

Eilola, K., B. G. Gustafson, I. Kuznetsov, H. E. M. Meier, T. Neumann and O. P. Savchuk, 2011: Evaluation of biogeochemical cycles in an ensemble of three state-of-the-art numerical models of the Baltic Sea. J. Mar. Sys., 88, pp. 267-284.

Eilola, K., E. Almroth Rosell, C. Dieterich, F. Fransner, A. Höglund and H. E. M. Meier, 2012: Modeling nutrient transports and exchanges of nutrients between shallow regions and the open Baltic Sea in present and future climate. AMBIO, Vol. 41, Issue 6, 574-585, DOI: 10.1007/s13280-012-0319-9.

Eilola, K., S. Mårtensson, and H. E. M. Meier, 2013: Modeling the impact of reduced sea ice cover in future climate on the Baltic Sea biogeochemistry. Geophys. Res. Lett., Vol. 40, 1-6, doi:10.1029/2012GL054375.

Eilola, K., E. Almroth Rosell, and H. E. M. Meier, 2014: Impact of saltwater inflows on phosphorus cycling and eutrophication in the Baltic Sea. A 3D model study. Tellus A, 66, 23985, http://dx.doi.org/10.3402/tellusa.v66.23985.

HELCOM, 2013a. Eutrophication status of the Baltic Sea 2007-2011. A concise thematic assessment. HELCOM Thematic assessment.

Hordoir, R., Haapala, J. B., Dieterich, C., Schimanke, S., Höglund, A. and Meier, H. 2013a. A 3D Ocean Modelling Configuration for Baltic & North Sea Exchange Analysis. Report Oceanography, SMHI.

Hordoir, R., Dieterich, C., Basu, C., Dietze, H. and Meier, H. 2013b. Freshwater outflow of the Baltic Sea and transport in the Norwegian current: A statistical correlation analysis based on a numerical experiment. Continental Shelf Research, 64, pp. 1 – 9.

Hordoir, R., L. Axell, U. Löptien, H. Dietze, and I. Kuznetsov, 2015. Influence of sea level rise on the dynamics of salt inflows in the Baltic Sea. Journal of Geophysical Research: Oceans, 120 (10), 6653-6668.

ICES. ICES Dataset on Ocean Hydrography. The International Council for the Exploration of the Sea,

Copenhagen, 2009.
Leppäranta, M. and Myrberg, K., 2009. Physical Oceanography of the Baltic Sea. Praxis Publishing, Chichester, UK. ISBN: 978-3-540-79702-9.
Maar, M., E. Friis Møller, J.Larsen, K. Skovgaard Madsen, Z.Wan, J. She, L.Jonasson, T.Neumann, 2011. Ecosystem modelling across a salinity gradient from the North Sea to the Baltic Sea, Ecol. Modelling 222, 1696–1711. doi:10.1016/j.ecolmodel.2011.03.006.
Marmefelt, E., Arheimer, B., Langner, J., 1999. An integrated biochemical model system for the Baltic Sea. Hydrobiologia 393, 45-56.
Meier, H.E.M., Andersson, H. C., Arheimer, B., Blenckner, T., Chubarenko, B., Donnelly, C., Eilola, K., Gustafsson, B. G., Hansson, A., Havenhand, J., Höglund, A., Kuznetsov, I., MacKenzie, B. R., Müller-Karulis, B., Neumann, T., Niiranen, S., Piwowarczyk, J., Raudsepp, U., Reckermann, M., Ruoho-Airola, T., Savchuk, O. P., Schenk, F., Schimanke, S., Väli, G., Weslawski, J.-M., and Zorita, E., 2012: Comparing reconstructed past variations and future projections of the Baltic Sea ecosystem—first results from multi-model ensemble simulations. Environ. Res. Lett. 7 034005, doi:10.1088/1748-9326/7/3/034005.
PARCOM, 1988, Recommendation 88/2 of 17 June 1988 on the reduction in inputs of nutrients to the Paris Convention area.
Rodhe J, Tett P, Wulff F., 2006. The Baltic and North Seas: a regional review of some important physical-chemicalbiological interaction processes. In: Robinson AR, Brink KH (eds) The sea, Vol 14B. Harvard University Press, Cambridge, MA, p 1033−1075.
Savchuk, O. P., Eilola, K., Gustafsson, B. G., Medina, M. R. and Ruoho-Airola, T. 2012. Long-term reconstruction of nutrient loads to the Baltic Sea, 1850-2006. Baltic Nest Institute Technical Report Series.
Sahlberg, J., 2009. The Coastal Zone Model. SMHI Report series Oceanography. No. 98. http://www.smhi.se/sgn0106/if/biblioteket/rapporter_pdf/Oceanografi_98.pdf
Skogen, M.D., K. Eilola, J.L.S. Hansen, H.E.M. Meier, M.S. Molchanov, and V.A. Ryabchenko, 2014. Eutrophication Status of the North Sea, Skagerrak, Kattegat and the Baltic Sea in present and future climates: A model study. Journal of Marine Systems, 132, 174-184.
Wang, S., Dieterich, C., Döscher, R., Höglund, A., Hordoir, R., Meier, H., Samuelsson, P., & Schimanke, S. 2015. Development and evaluation of a new regional coupled atmosphere-ocean model in the North Sea and Baltic Sea. Tellus A.

Appendix A2. Stations.

List of Figures

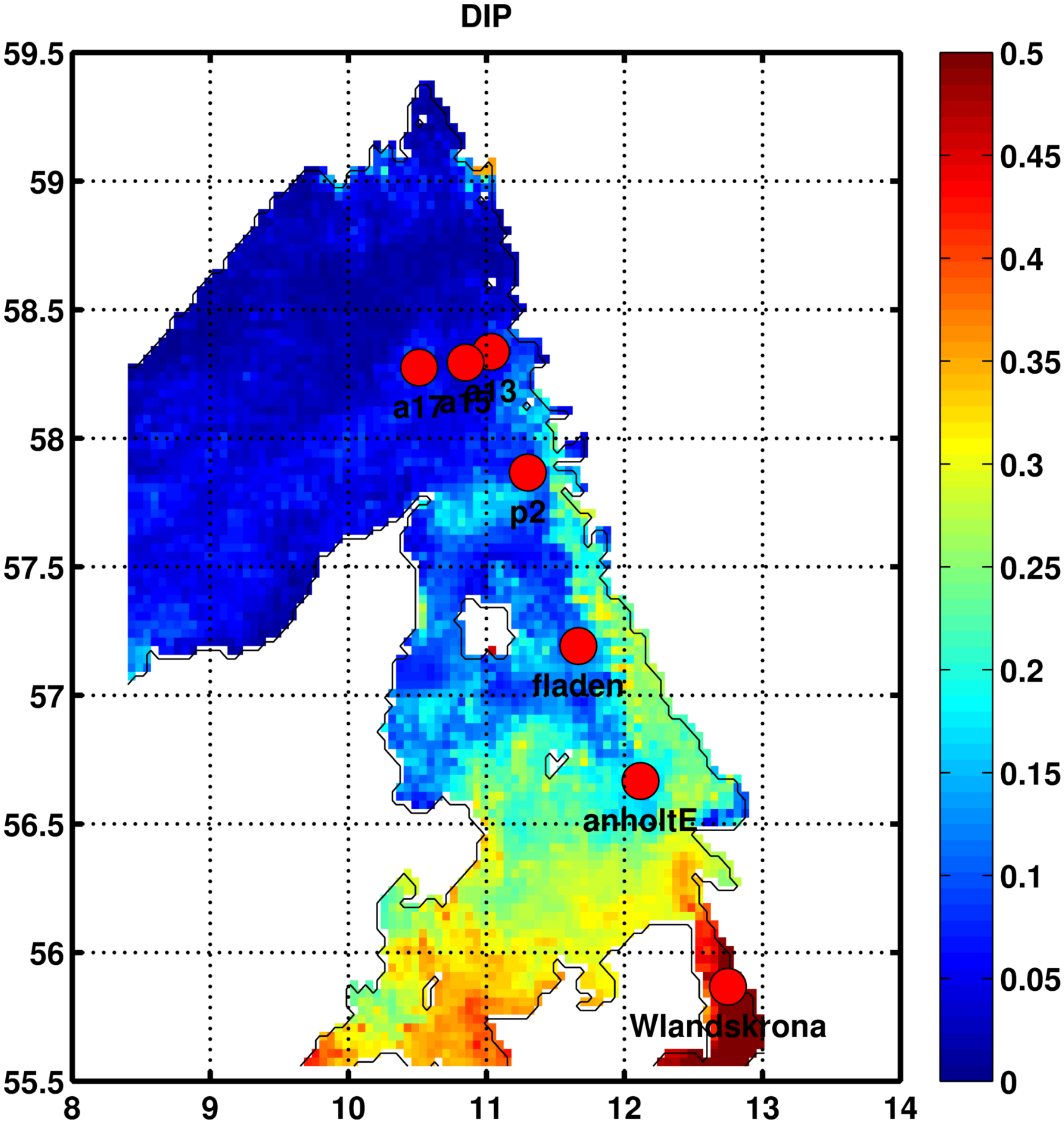

Figure 1: Stations map.

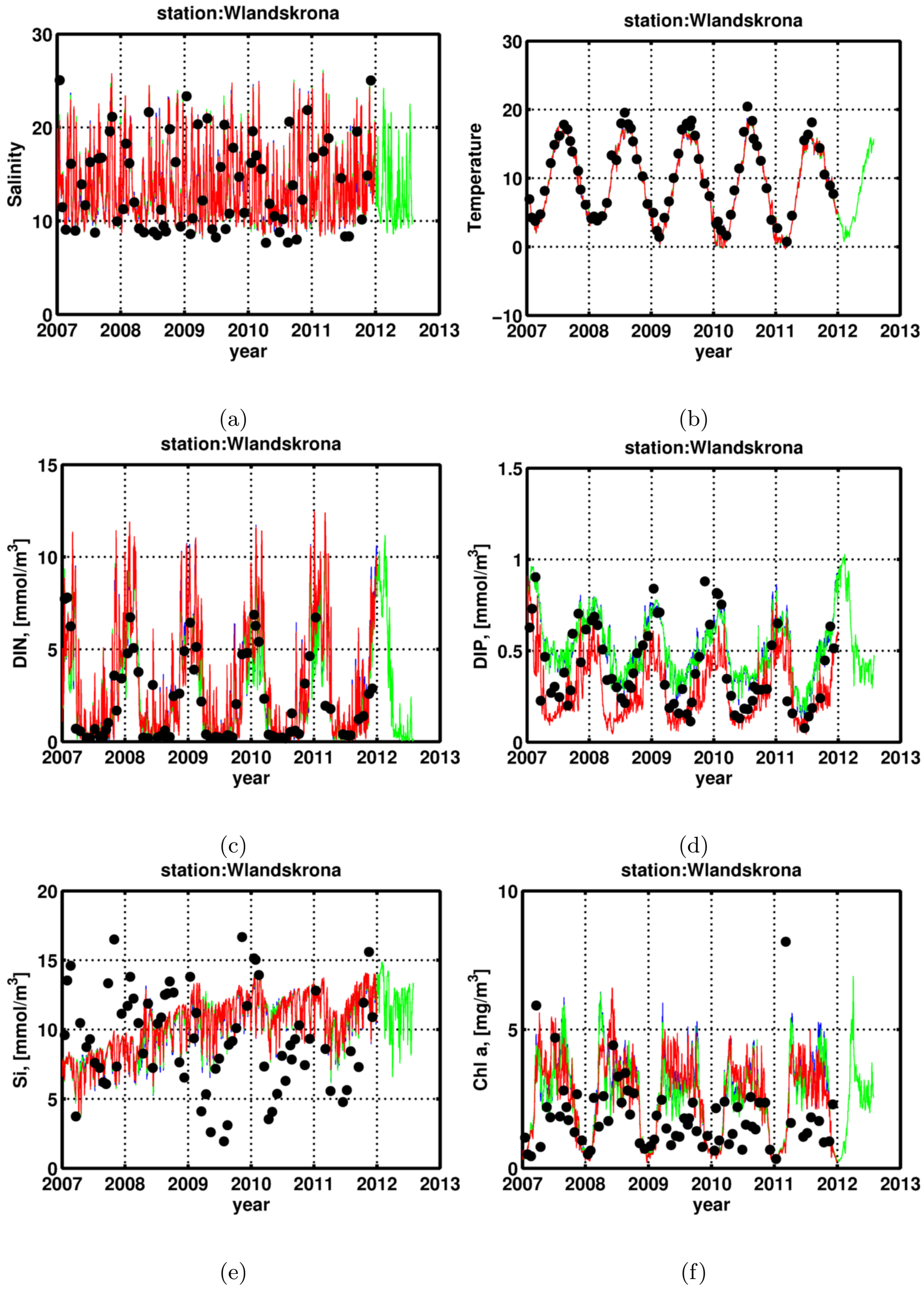

Figure 2: Station Wlandskrona: Reference – blue, Reductions in NS river loads – green, BSAP – red run.

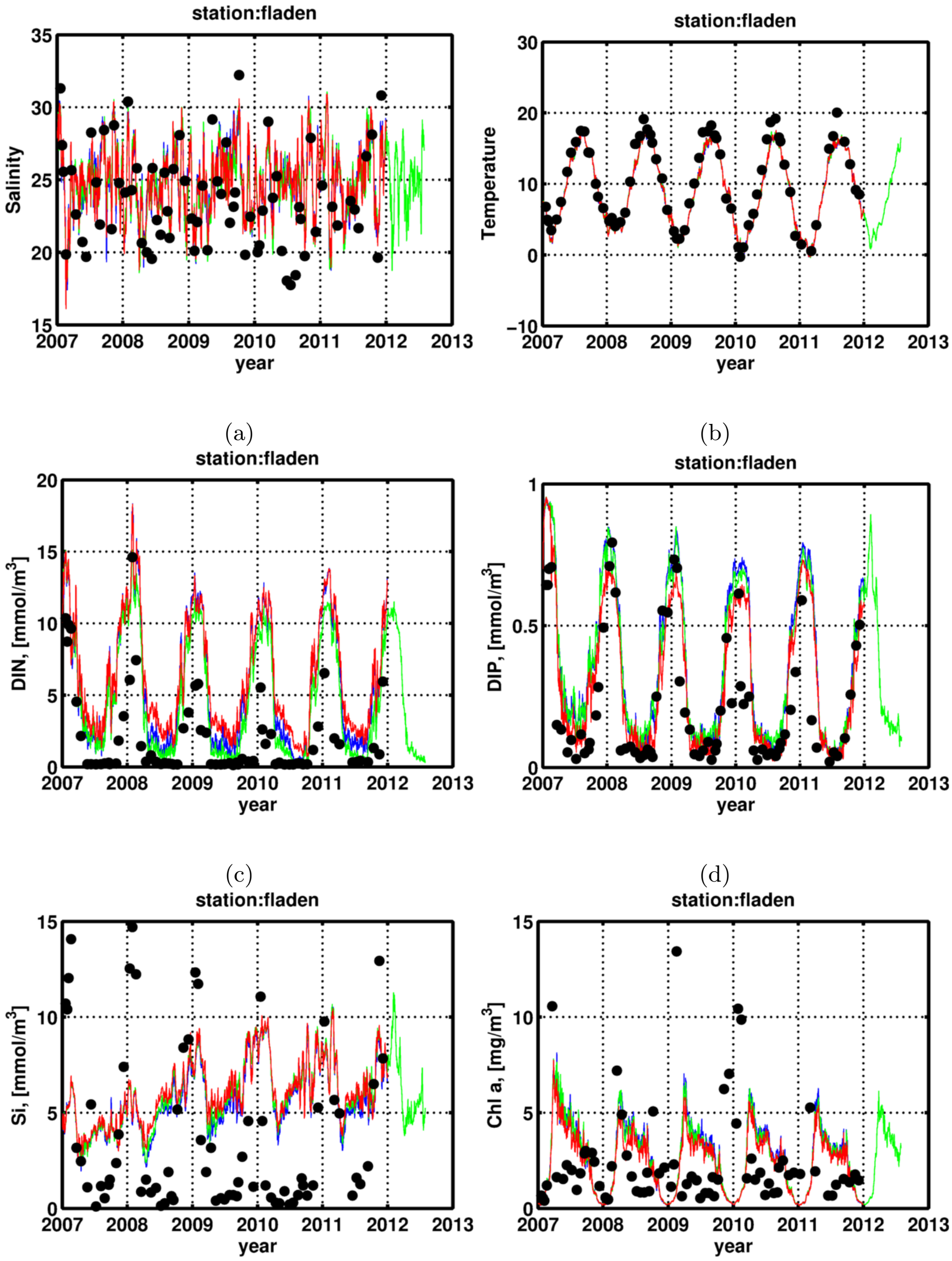

(a) (b) (c) (d) (e) (f)

Figure 3: Station fladen: Reference – blue, Reductions in NS river loads – green, BSAP – red run.

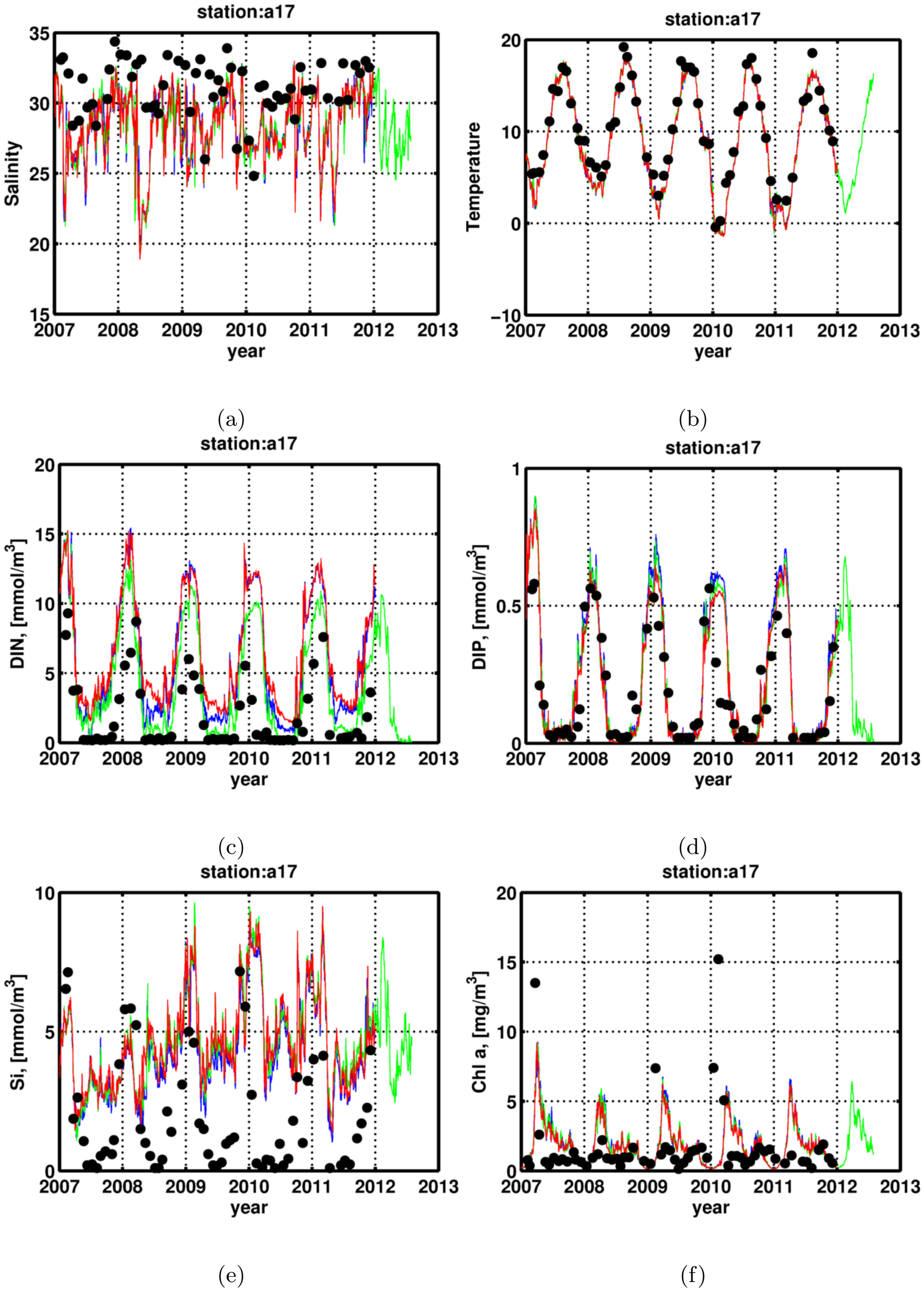

Figure 4: Station a17: Reference – blue, Reductions in NS river loads – green, BSAP – red run.

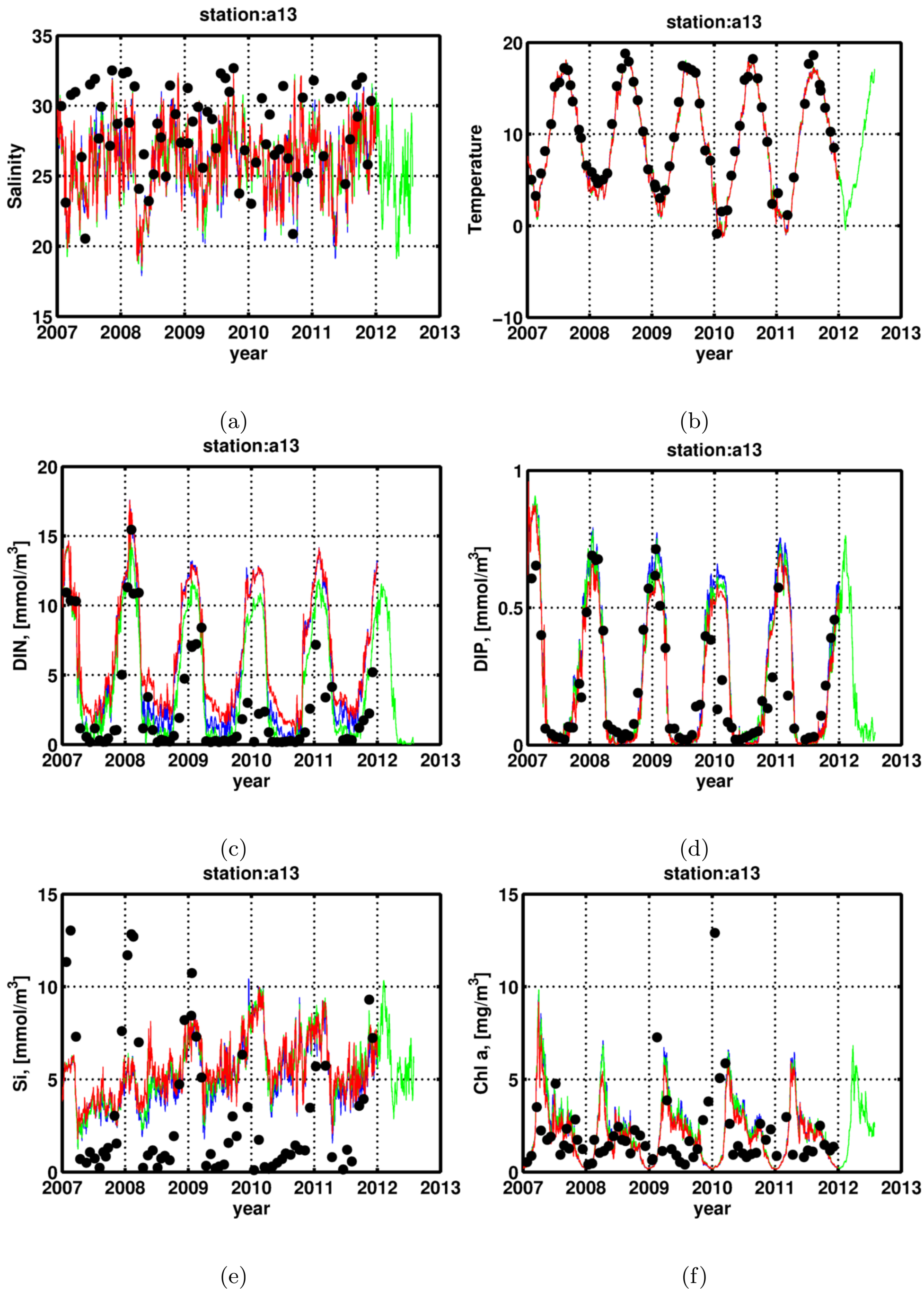

Figure 5: Station a13: Reference – blue, Reductions in NS river loads – green, BSAP – red run.

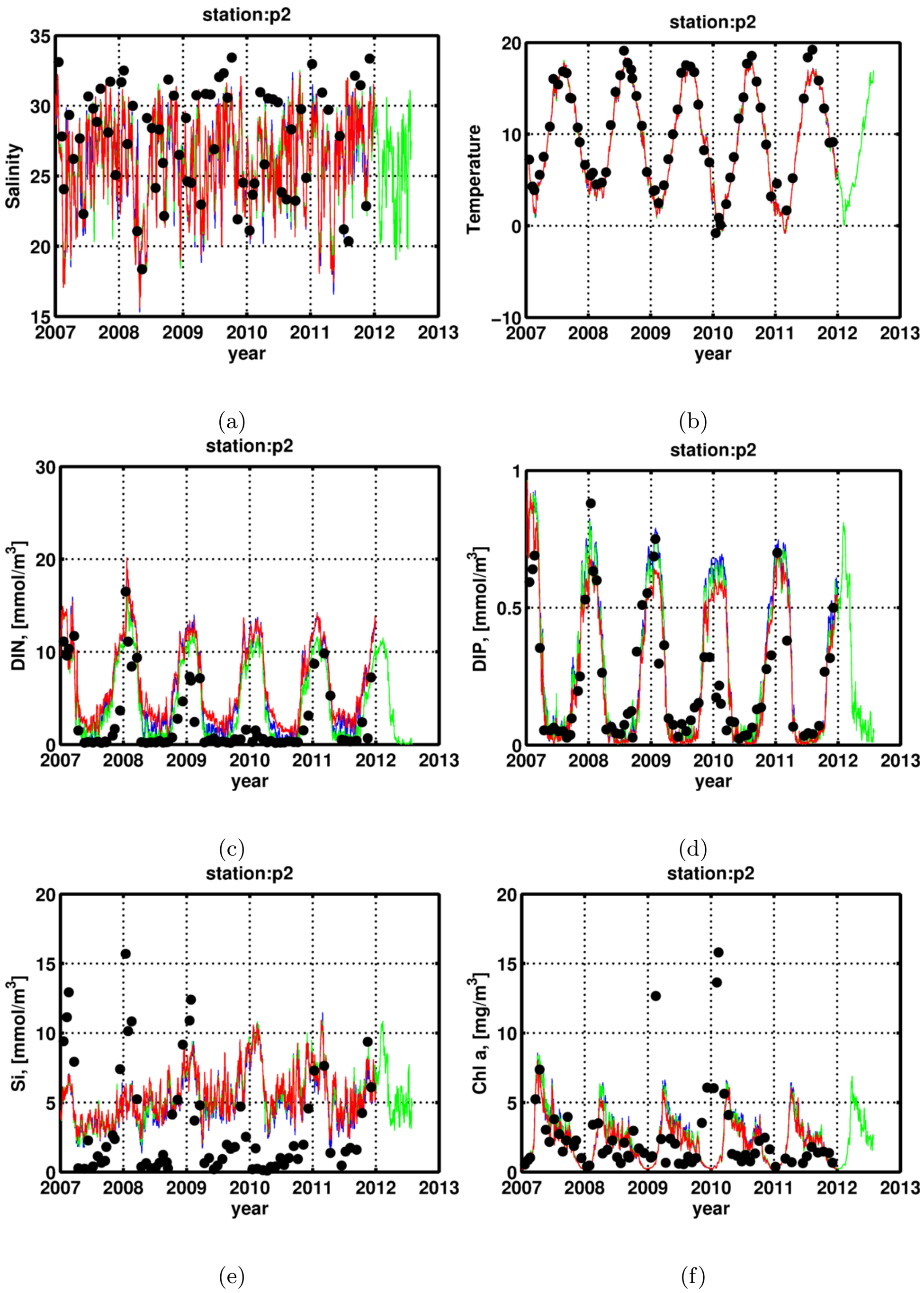

Figure 6: Station p2: Reference – blue, Reductions in NS river loads – green, BSAP – red run.

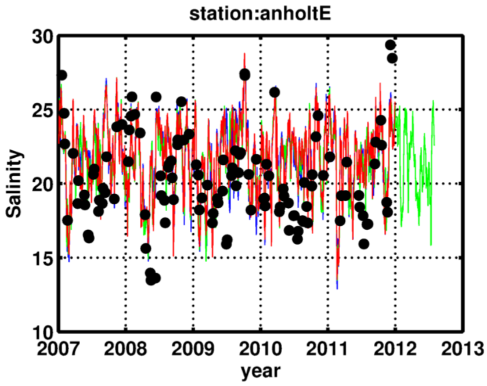

(a)

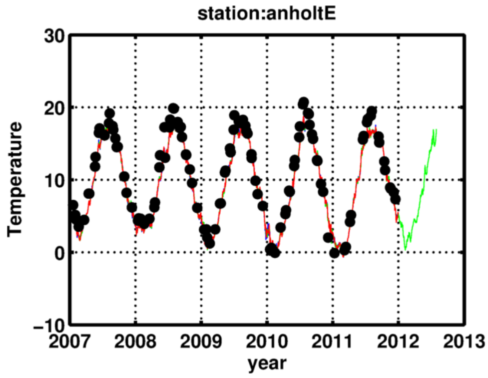

(b)

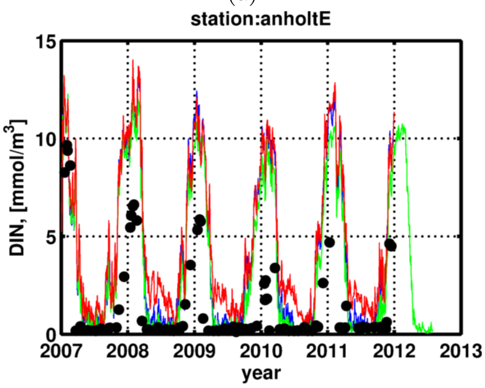

(c)

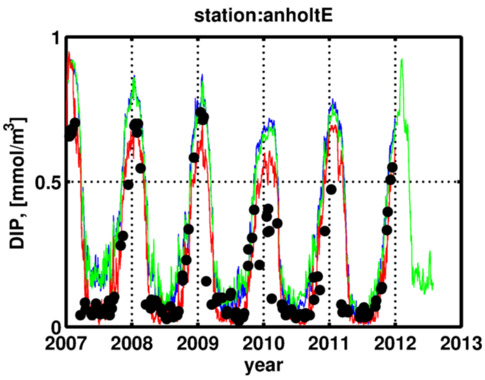

(d)

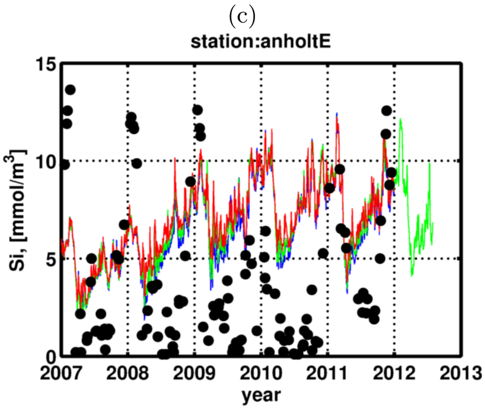

(e)

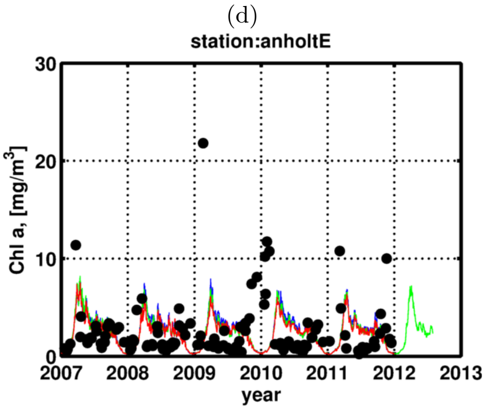

(f)

Figure 7: Station anholtE: Reference – blue, Reductions in NS river loads – green, BSAP – red run.

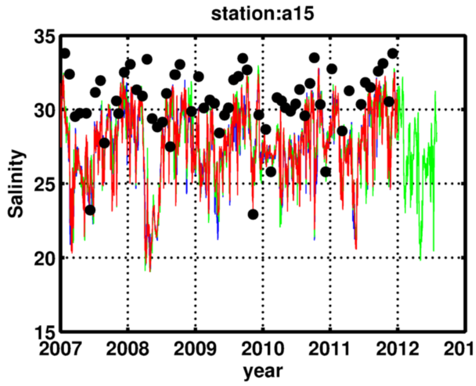

(a)

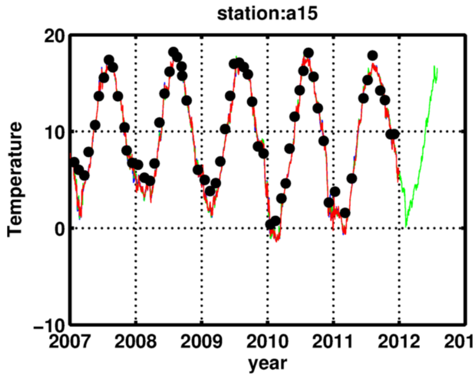

(b)

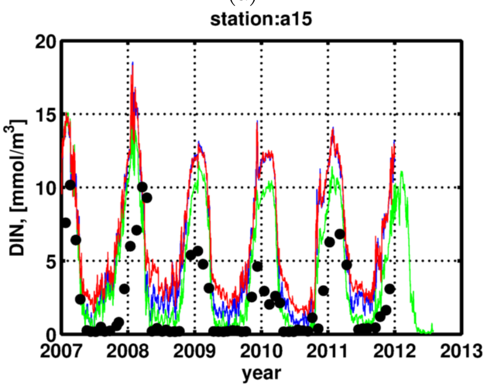

(c)

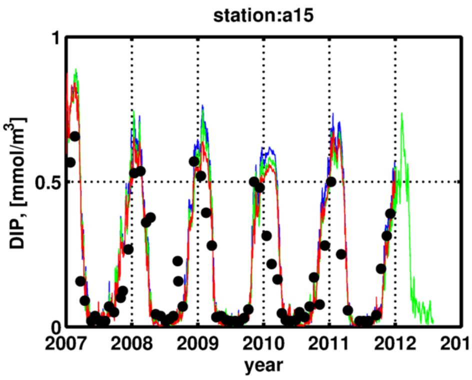

(d)

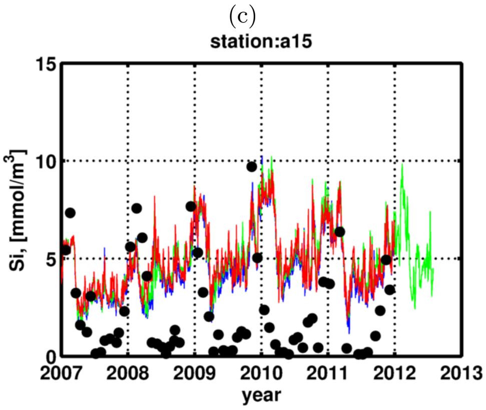

(e)

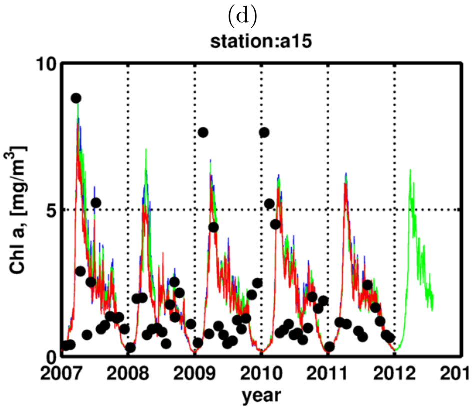

(f)

Figure 8: Station a15: Reference – blue, Reductions in NS river loads – green, BSAP – red run.

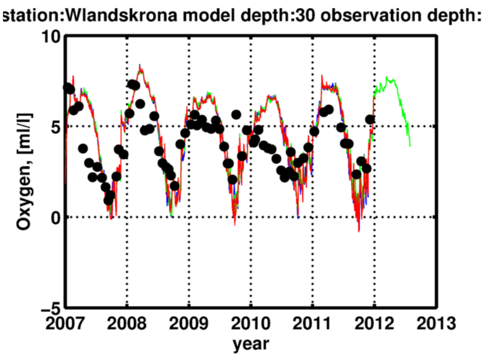

(a)

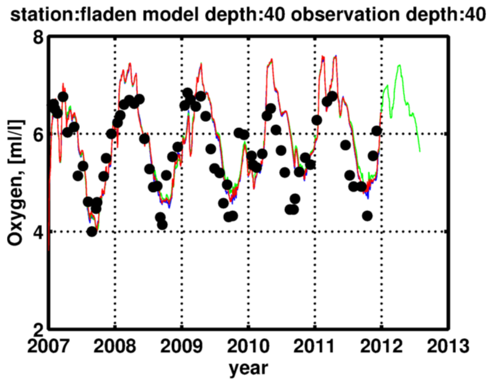

(b)

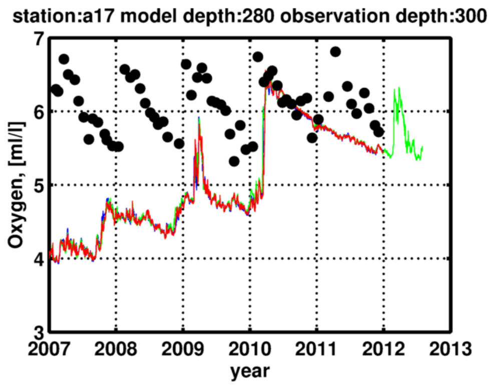

(c)

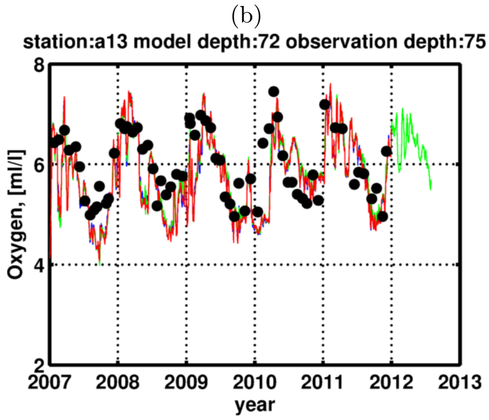

(d)

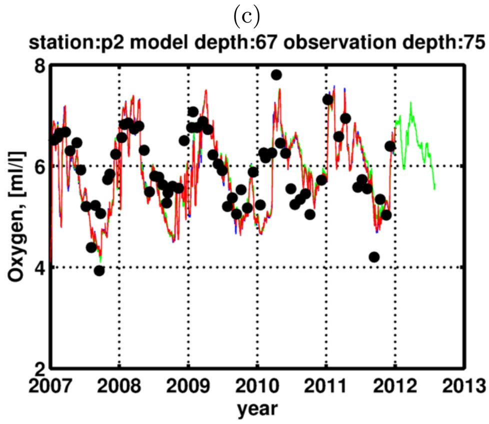

(e)

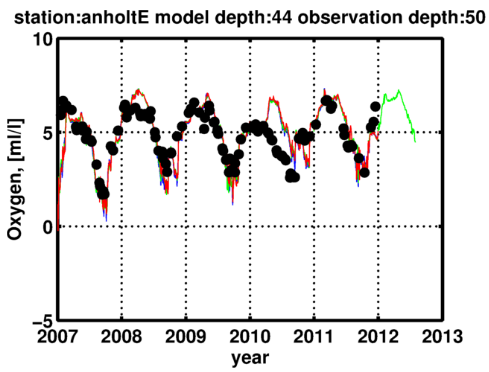

(f)

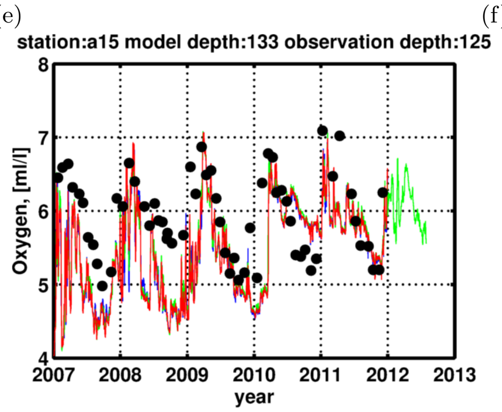

(g)

Figure 9: Oxygen concentration close to the bottom, Reference – blue, Reductions in NS river loads – green, BSAP – red run.

Appendix A2. Maps

List of Figures

0.1 Reference run

Maps of mean, median, STD, CV, minimum and maximum values : figures 1 – 8

0.2 Reductions in NS river loads run

Maps of mean, median, STD, CV, minimum and maximum values : figures 9 – 16.

Changes between reference and reductions in NS river loads runs (reference run - current run): figures 17 – 24

Relative change in reductions in NS river loads run (reference run / current run): figures 25 – 32

0.3 BSAP run

Maps of mean, median, STD, CV, minimum and maximum values : figures 33 – 40

Changes between reference and BSAP runs (reference run - current run): figures 41 – 48

Relative change in BSAP run (reference run / current run): figures 49 – 56

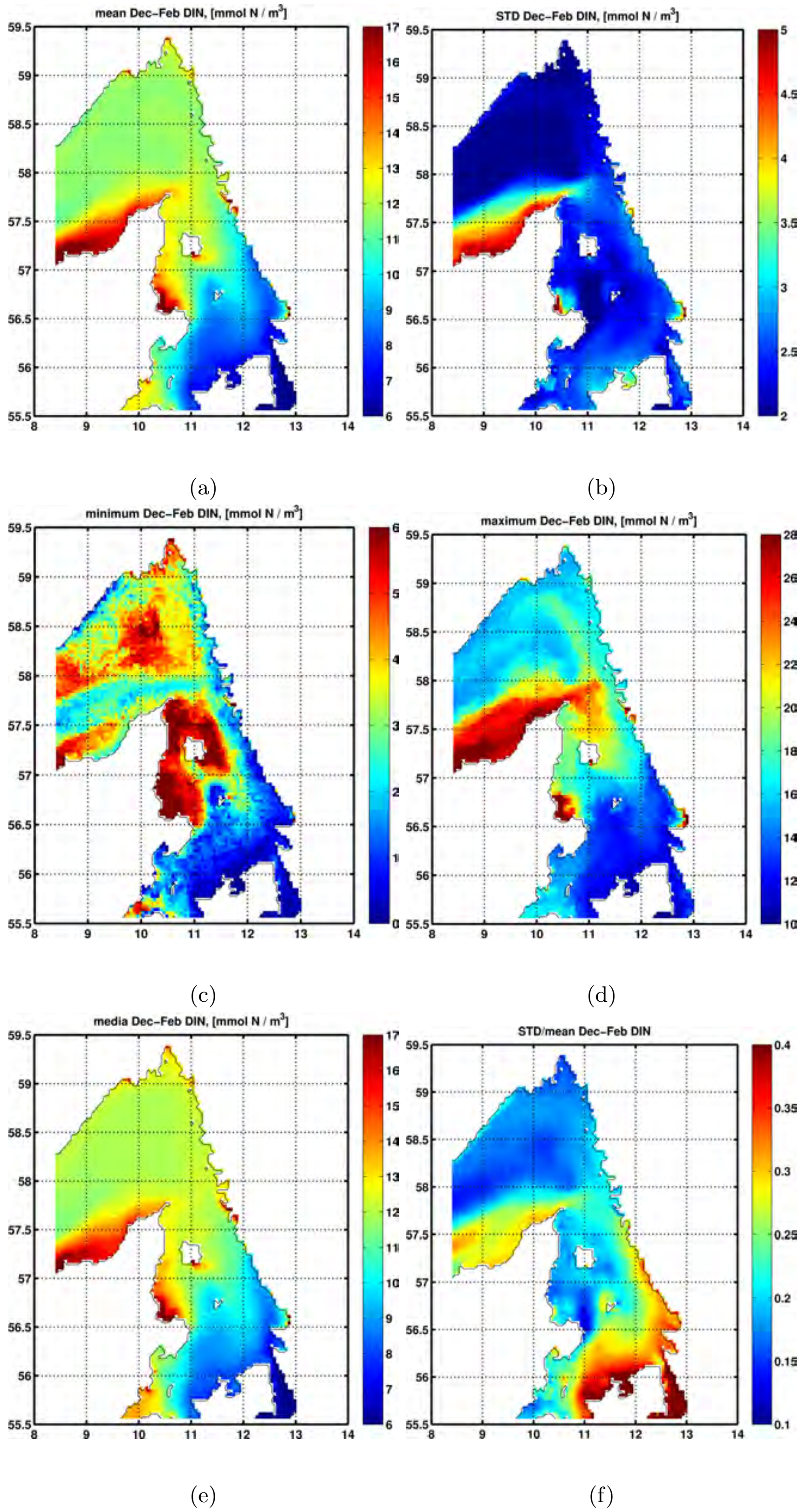

Figure 1: Winter (DJF) sea surface (10m mean) DIN. Mean, std, minimum, maximum, median and std/mean for 2007–2011 years of Reference run.

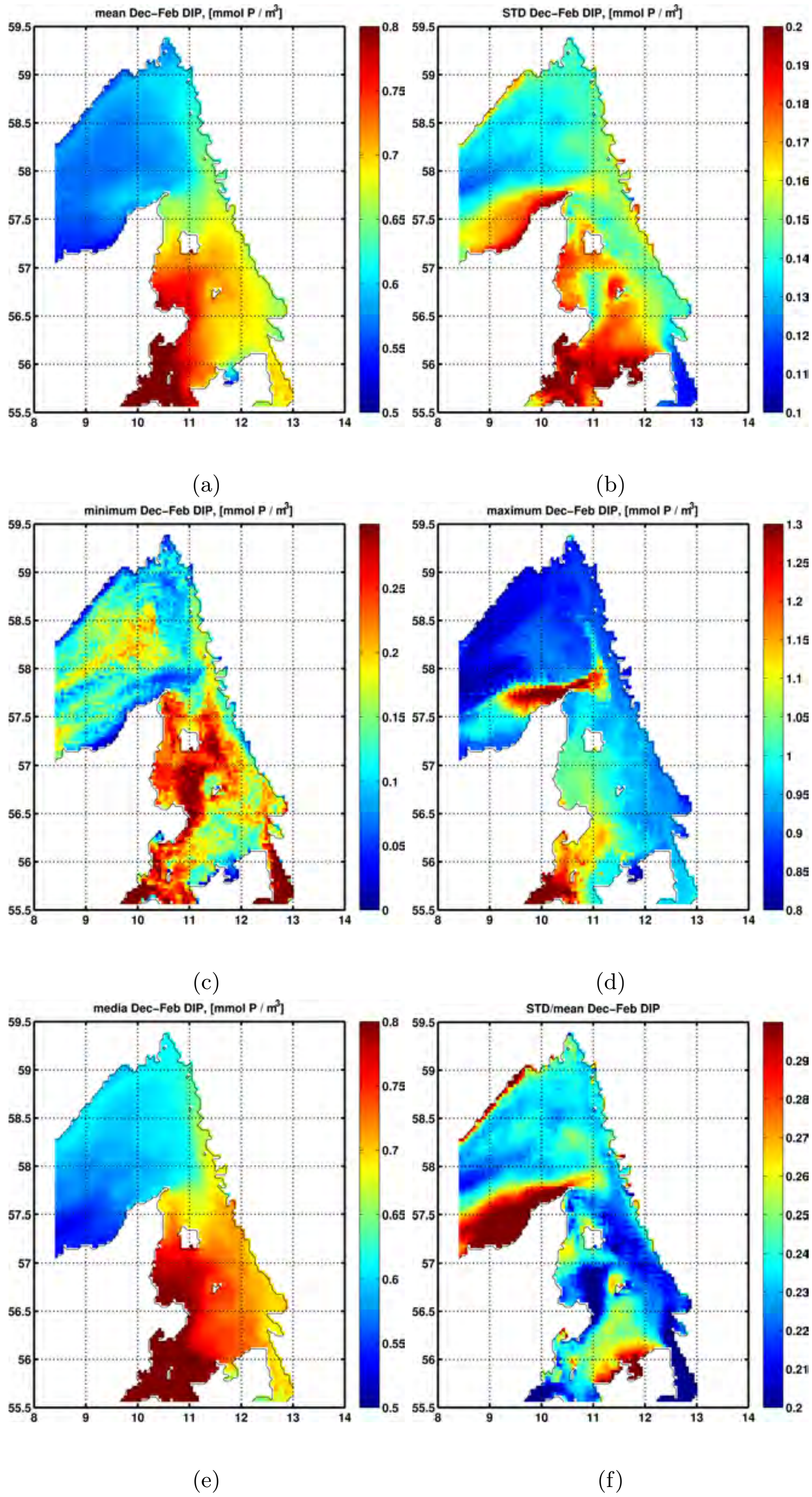

Figure 2: Winter (DJF) sea surface (10m mean) DIP. Mean, std, minimum, maximum, median and std/mean for 2007–2011 years of Reference run.

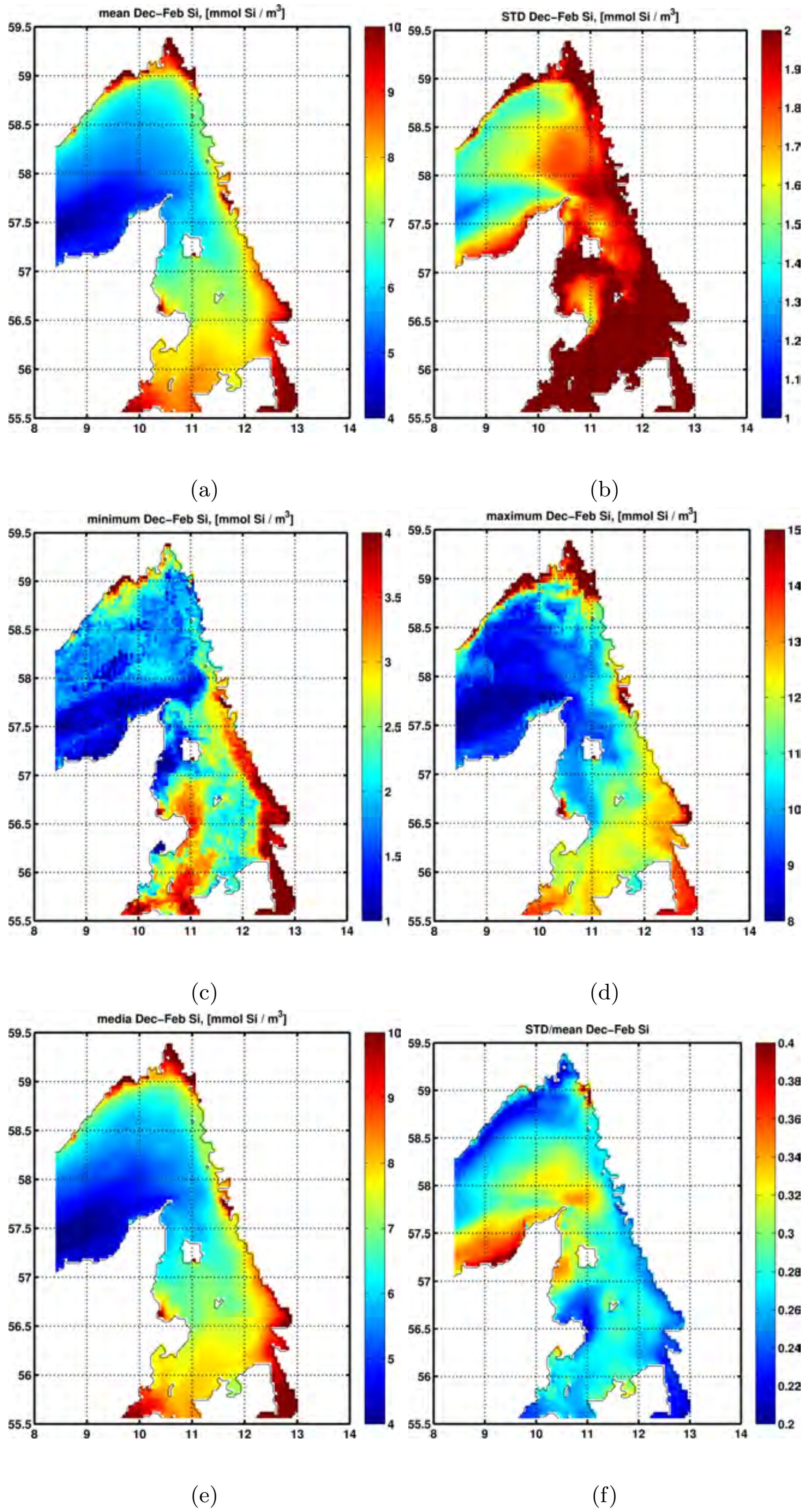

Figure 3: Winter (DJF) sea surface (10m mean) Si. Mean, std, minimum, maximum, median and std/mean for 2007–2011 years of Reference run.

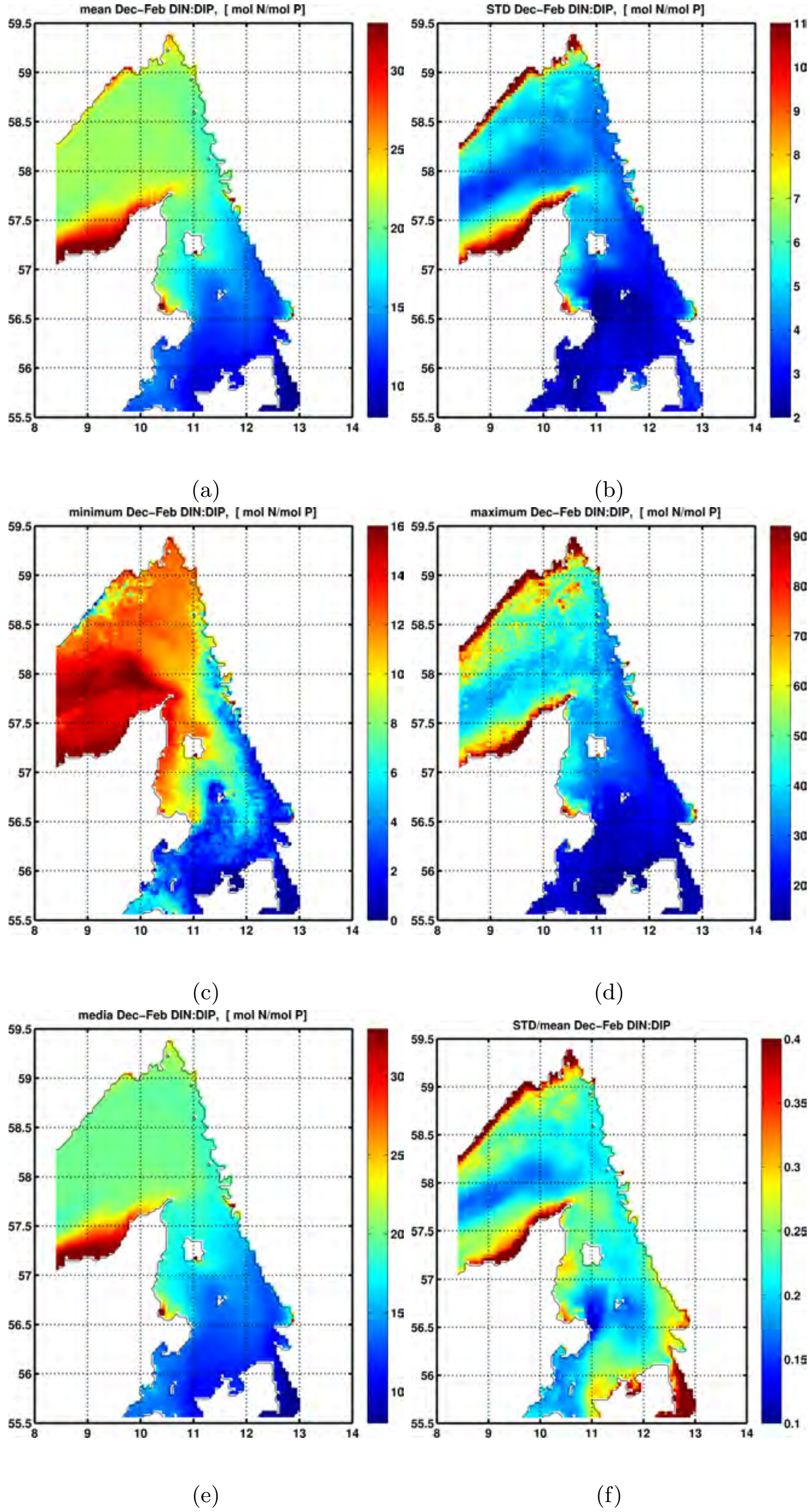

Figure 4: Winter (DJF) sea surface (10m mean) DIN:DIP. Mean, std, minimum, maximum, median and std/mean for 2007–2011 years of Reference run.

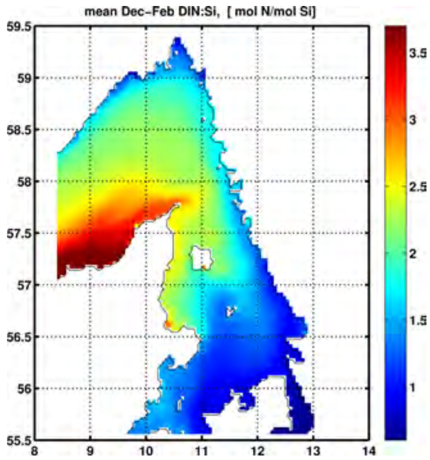

(a)

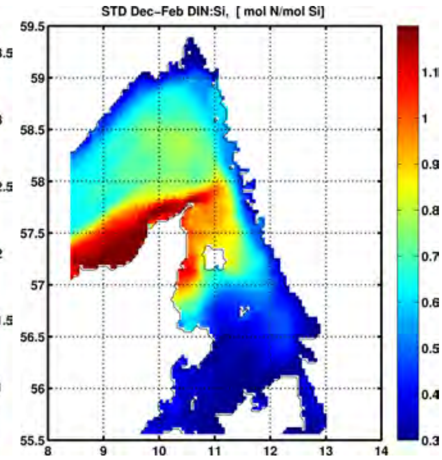

(b)

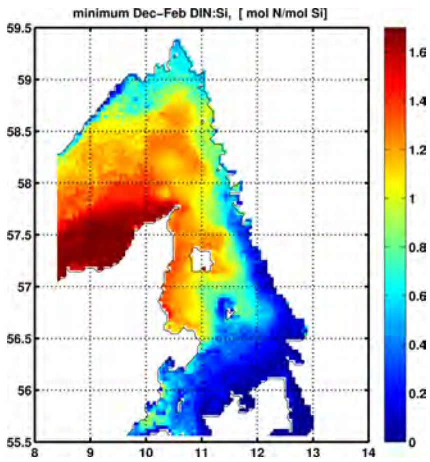

(c)

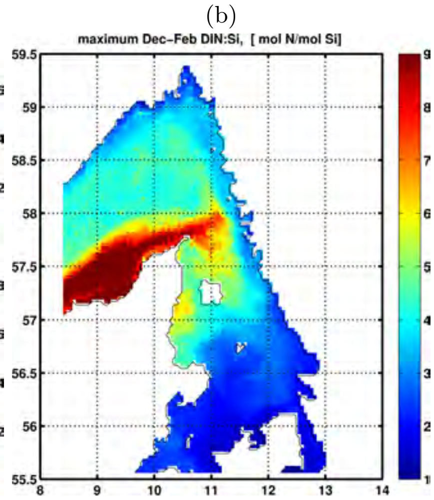

(d)

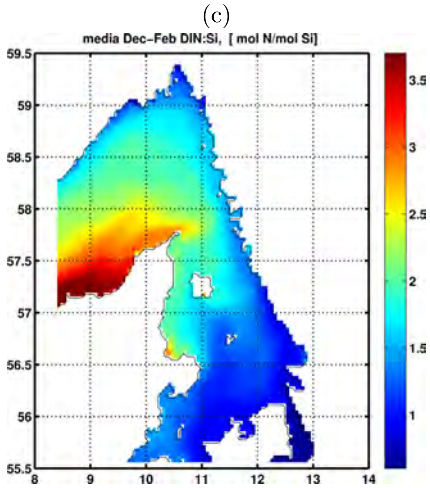

(e)

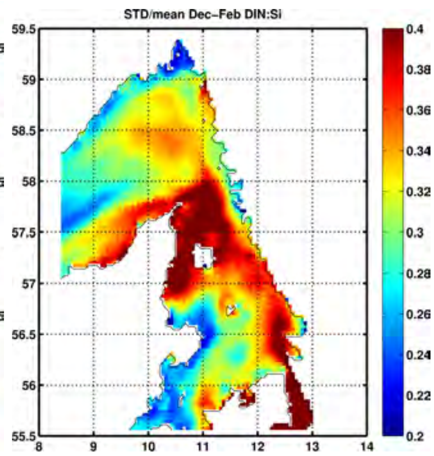

(f)

Figure 5: Winter (DJF) sea surface (10m mean) DIN:Si. Mean, std, minimum, maximum, median and std/mean for 2007–2011 years of Reference run.

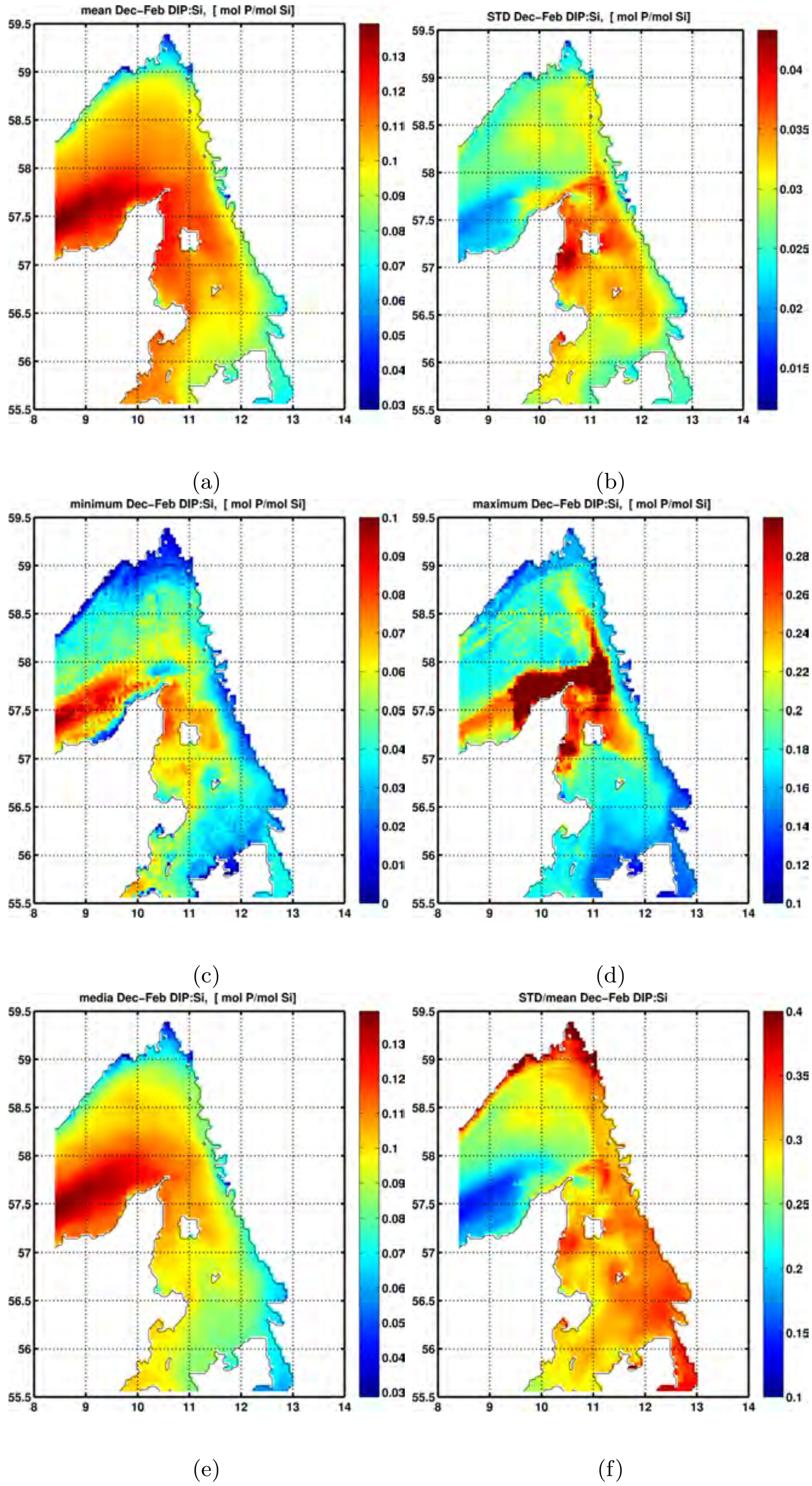

Figure 6: Winter (DJF) sea surface (10m mean) DIP:Si. Mean, std, minimum, maximum, median and std/mean for 2007–2011 years of Reference run.

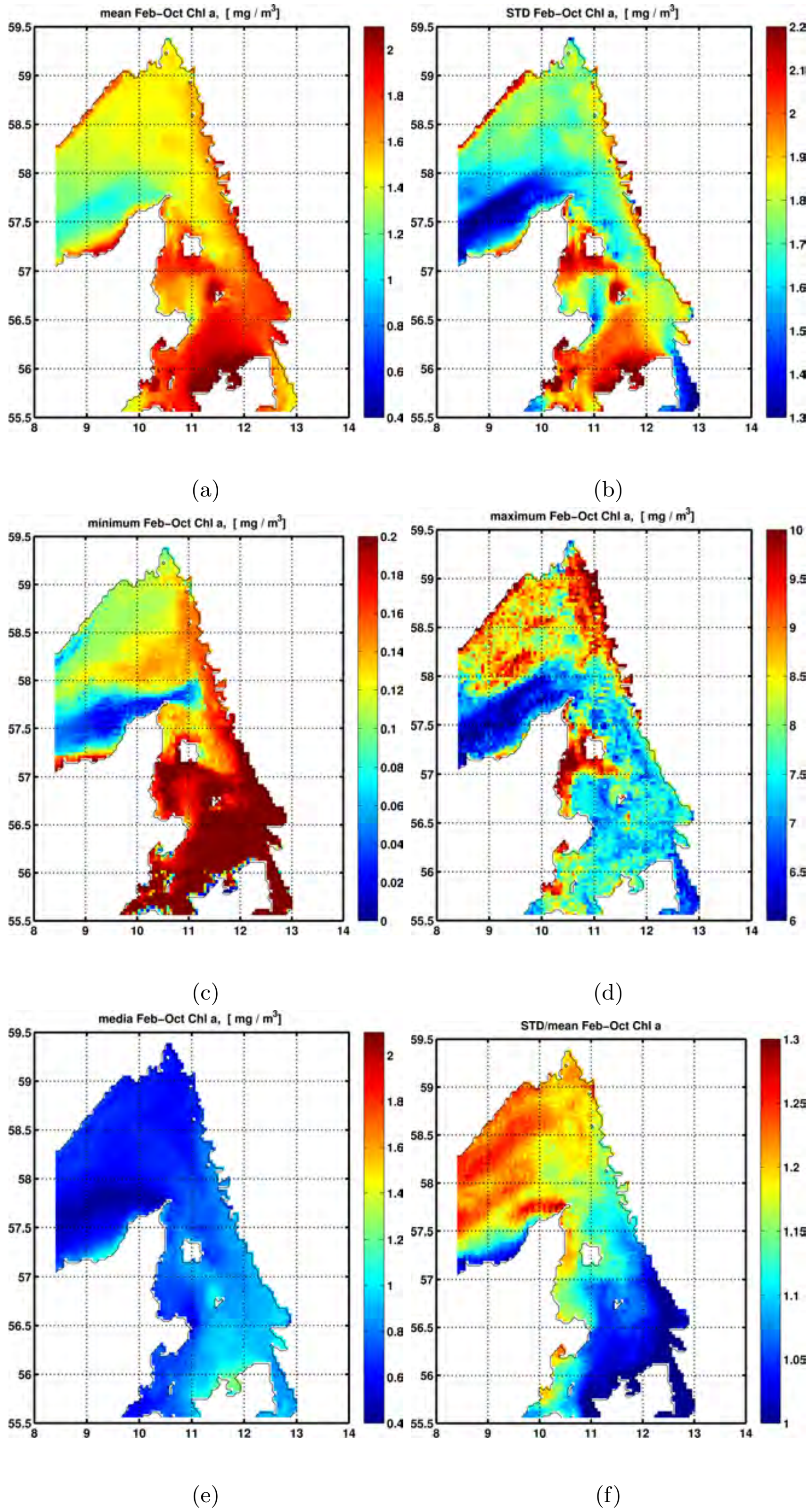

Figure 7: Concentrations of chlorophyll-a in the growing season (February to October) at sea surface (10m mean) Mean, std, minimum, maximum, median and std/mean for 2007–2011 years of Reference run.

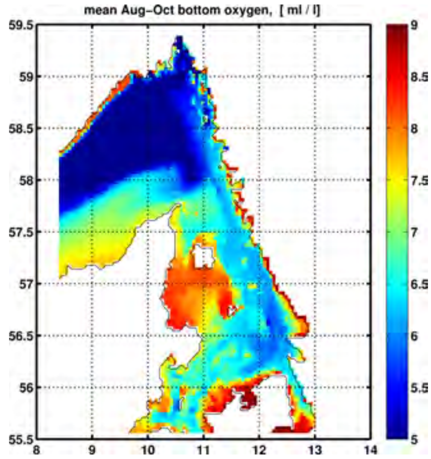

(a)

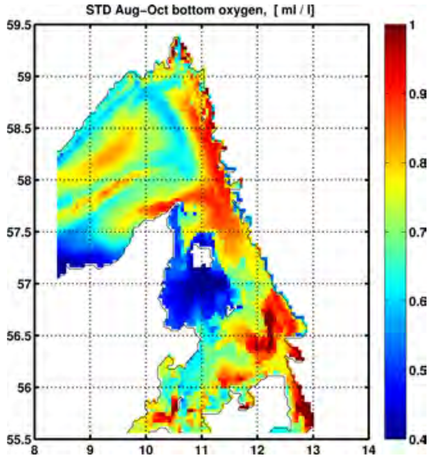

(b)

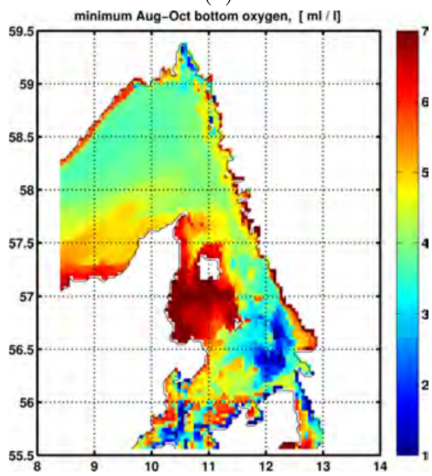

(c)

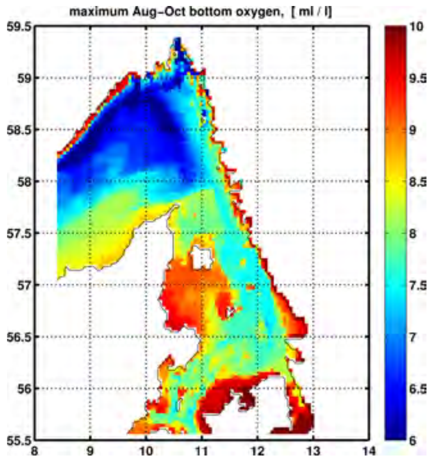

(d)

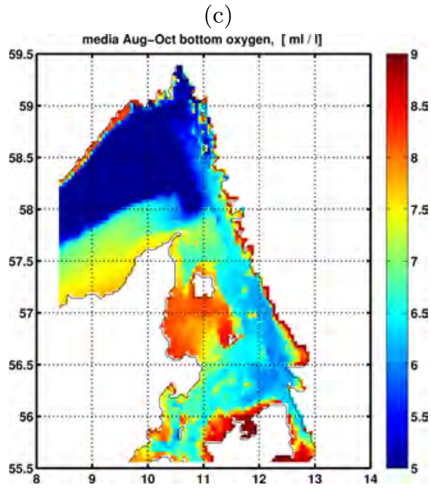

(e)

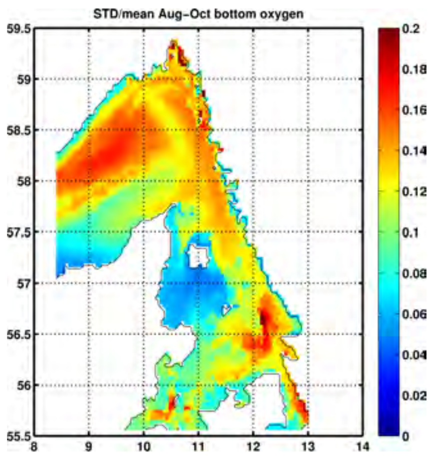

(f)

Figure 8: Concentrations of oxygen at sea bottom (grid cell and layer nearest the sea floor) during late summer-autumn (August-October). Mean, std, minimum, maximum, median and std/mean for 2007–2011 years of Reference run.

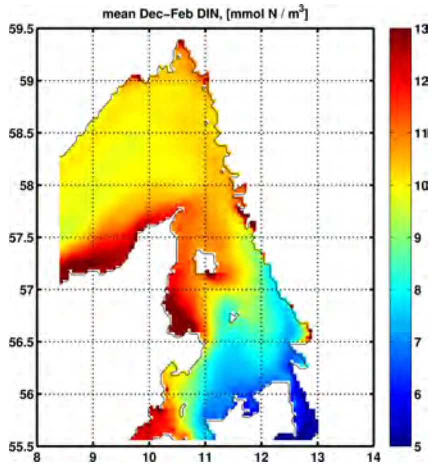

(a)

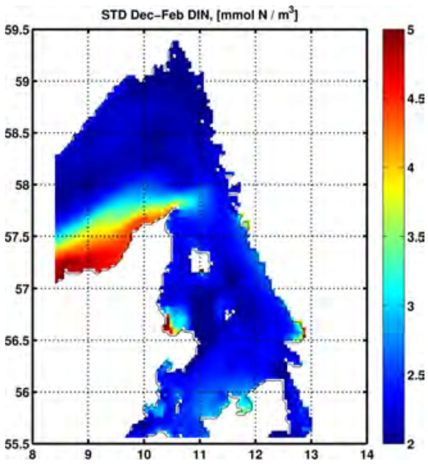

(b)

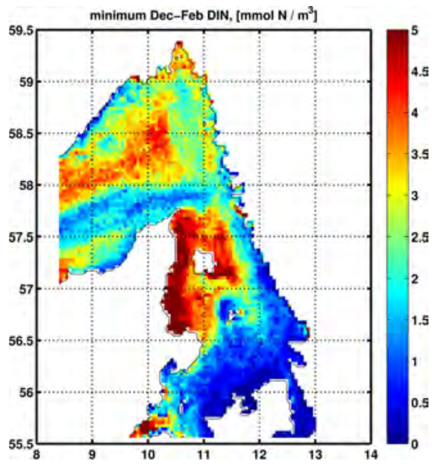

(c)

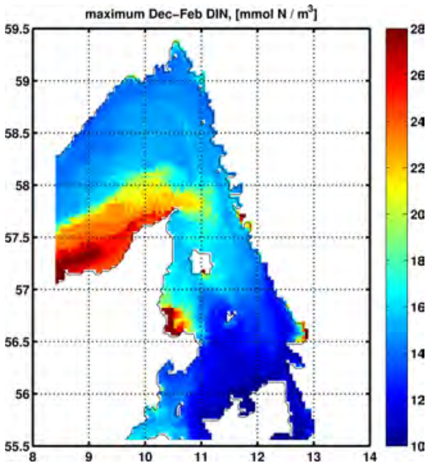

(d)

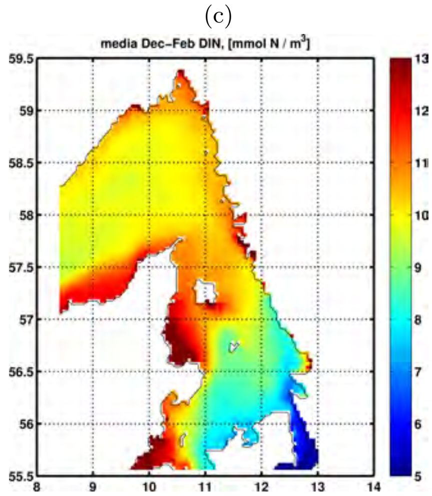

(e)

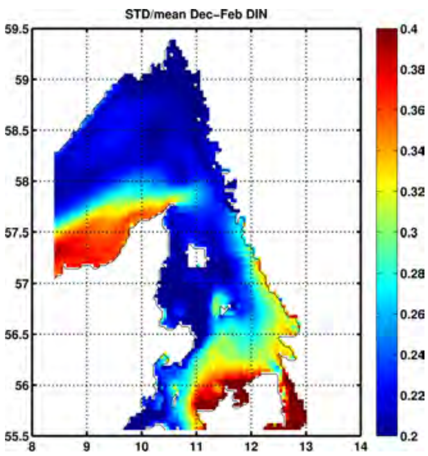

(f)

Figure 9: Winter (DJF) sea surface (10m mean) DIN. Mean, std, minimum, maximum, median and std/mean for 2007–2011 years of Reductions in NS river loads run.

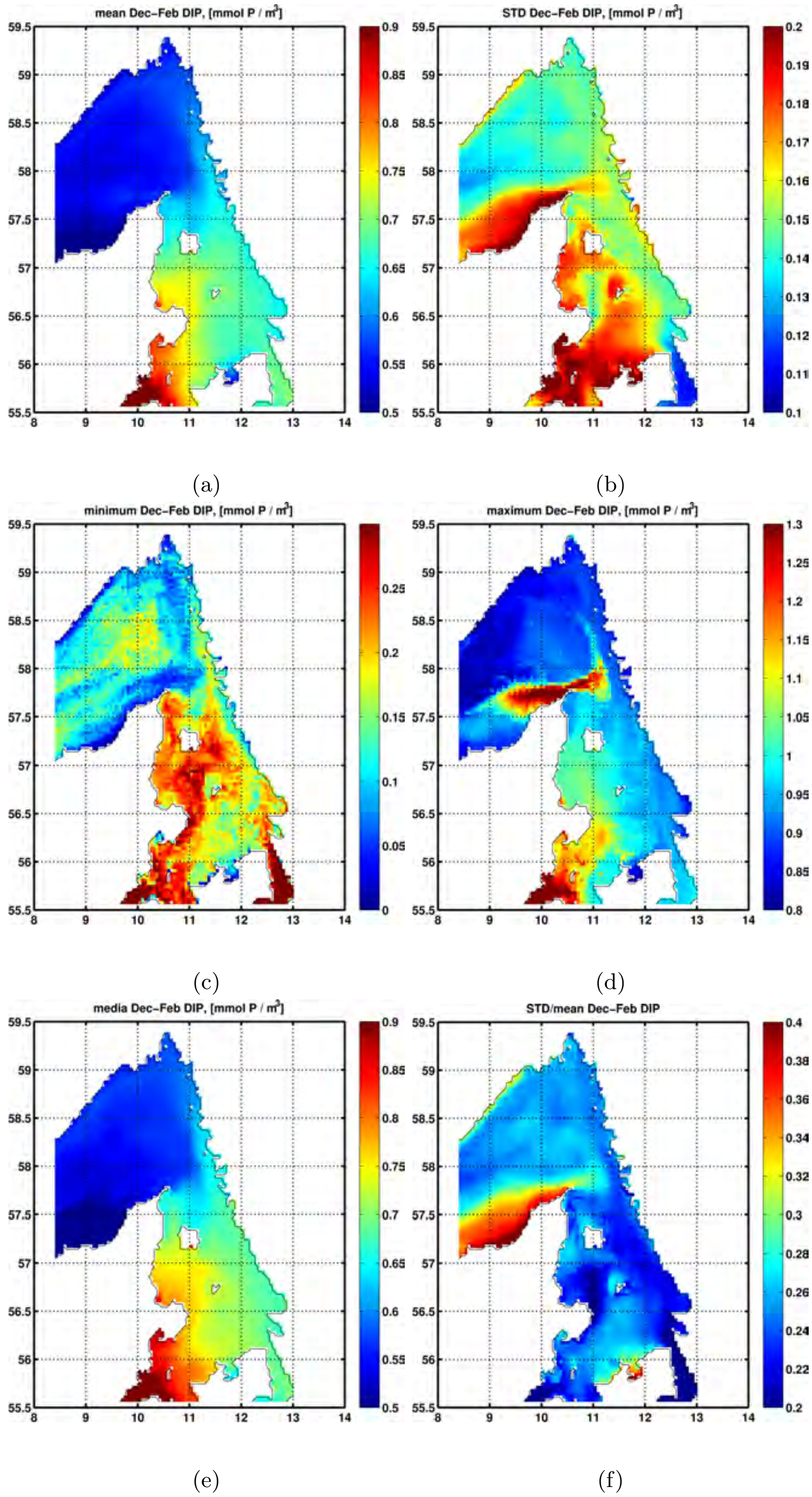

Figure 10: Winter (DJF) sea surface (10m mean) DIP. Mean, std, minimum, maximum, median and std/mean for 2007–2011 years of Reductions in NS river loads run.

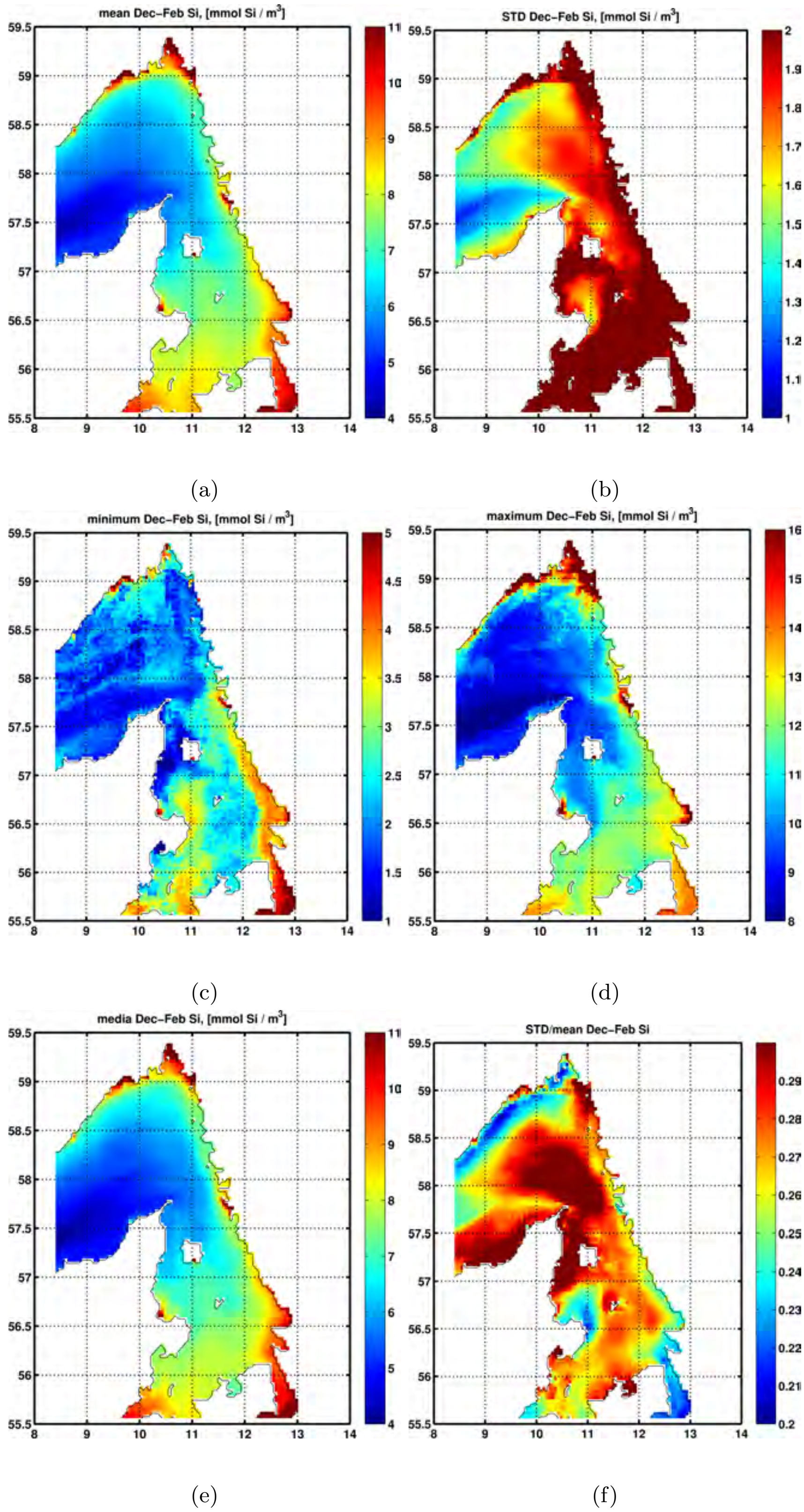

Figure 11: Winter (DJF) sea surface (10m mean) Si. Mean, std, minimum, maximum, median and std/mean for 2007–2011 years of Reductions in NS river loads run.

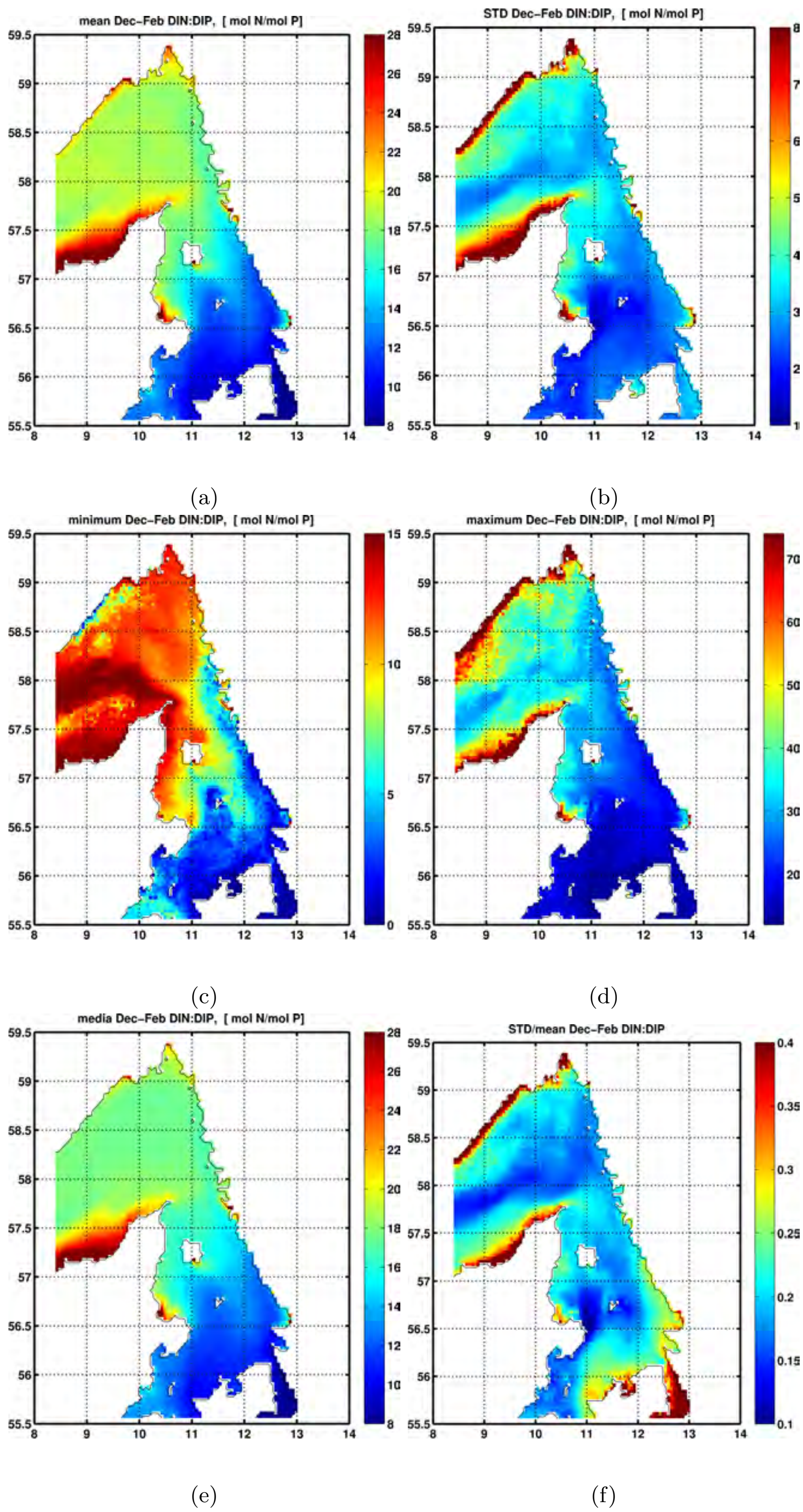

Figure 12: Winter (DJF) sea surface (10m mean) DIN:DIP. Mean, std, minimum, maximum, median and std/mean for 2007–2011 years of Reductions in NS river loads run.

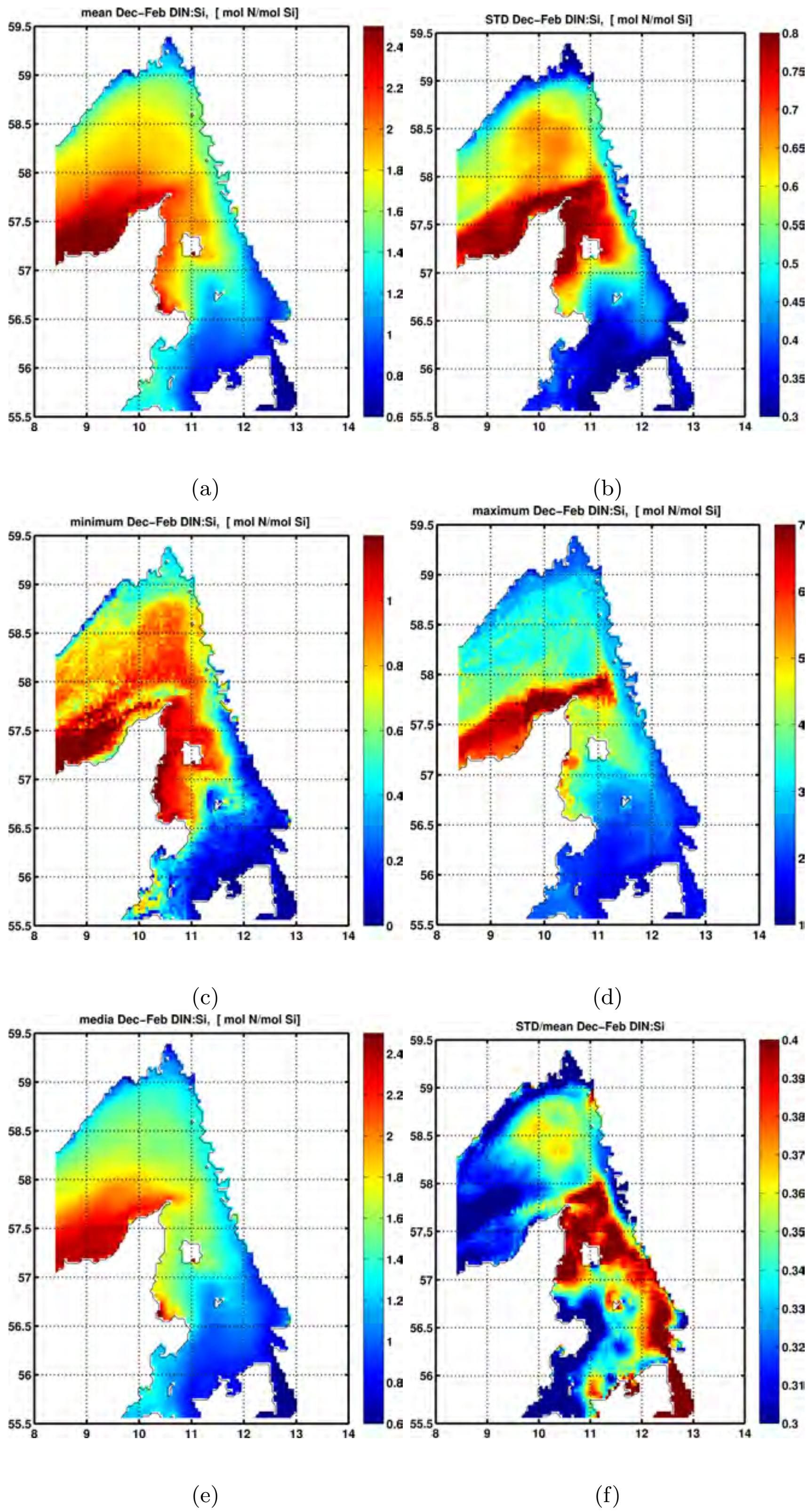

Figure 13: Winter (DJF) sea surface (10m mean) DIN:Si. Mean, std, minimum, maximum, median and std/mean for 2007–2011 years of Reductions in NS river loads run.

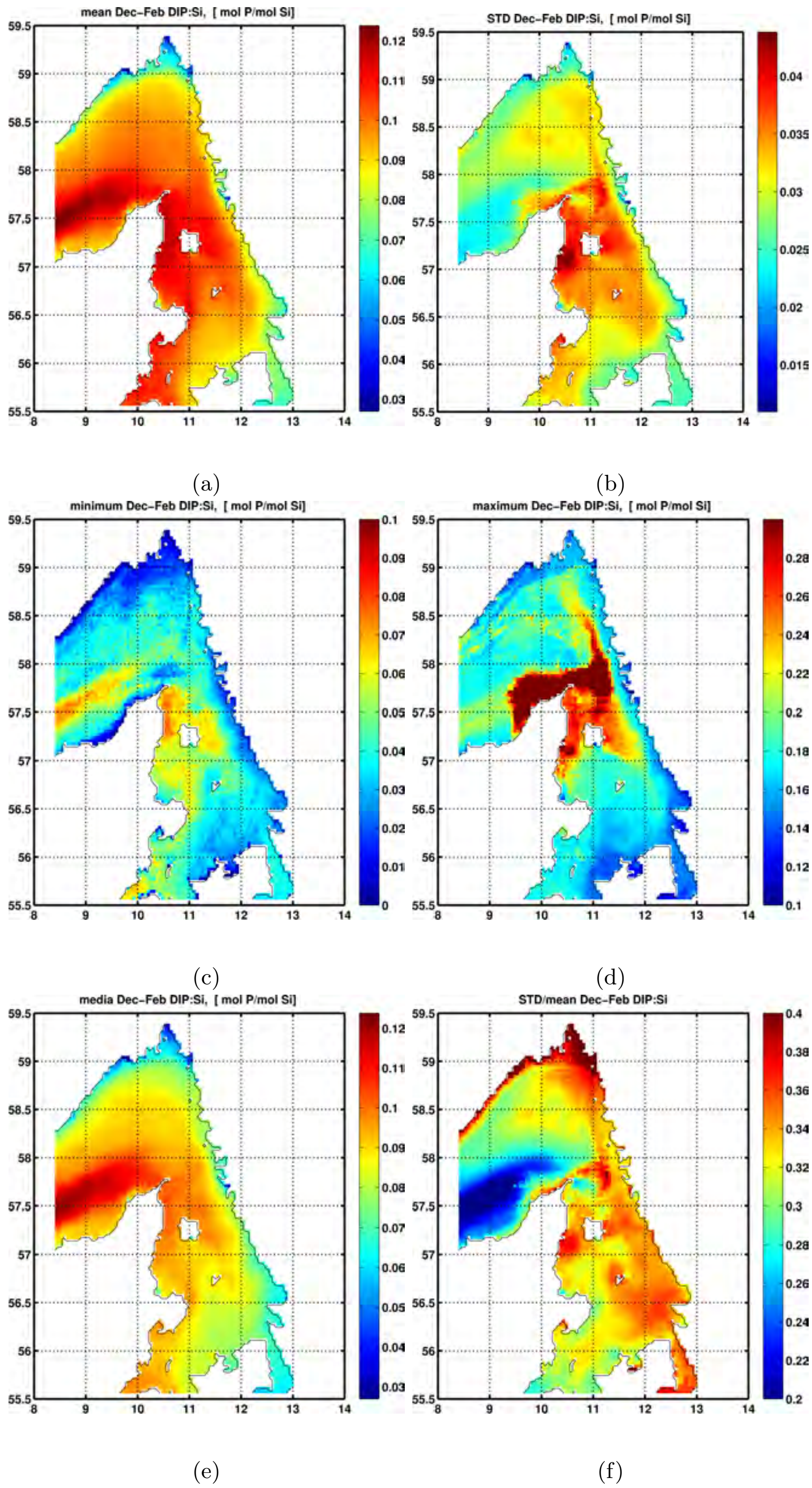

Figure 14: Winter (DJF) sea surface (10m mean) DIP:Si. Mean, std, minimum, maximum, median and std/mean for 2007–2011 years of Reductions in NS river loads run.

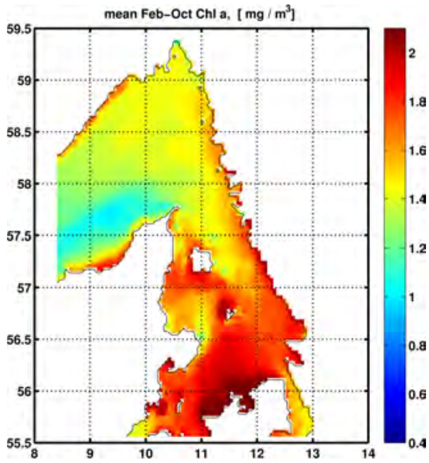

(a)

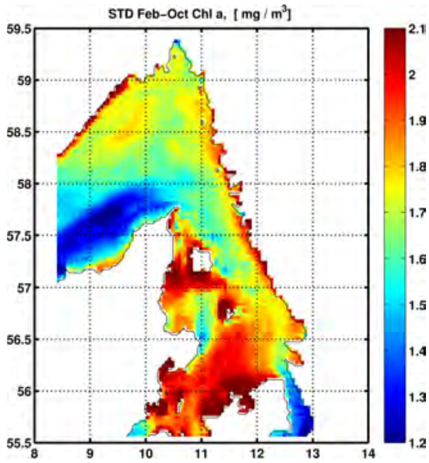

(b)

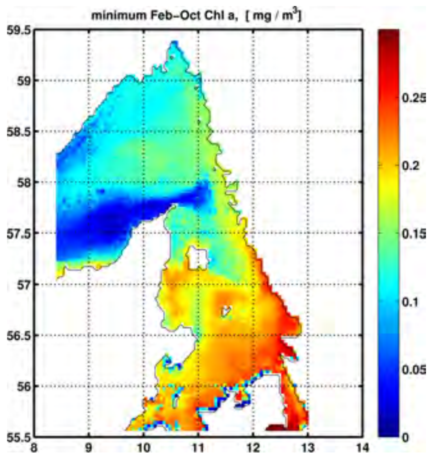

(c)

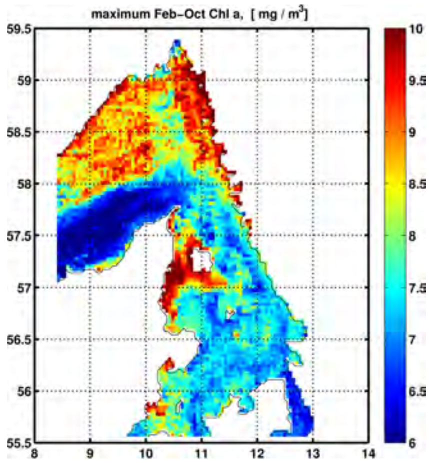

(d)

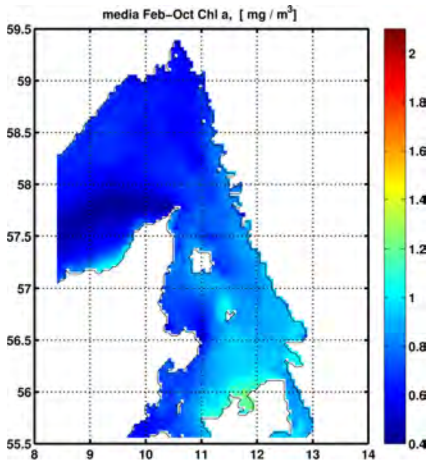

(e)

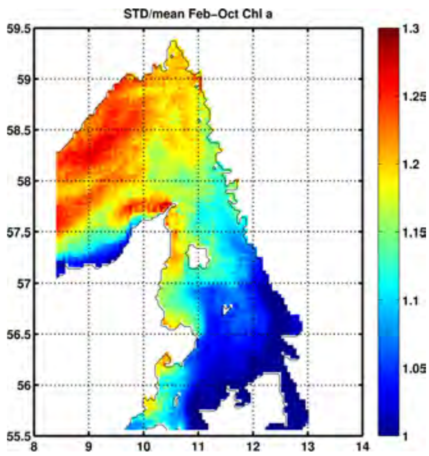

(f)

Figure 15: Concentrations of chlorophyll-a in the growing season (February to October) at sea surface (10m mean) Mean, std, minimum, maximum, median and std/mean for 2007–2011 years of Reductions in NS river loads run.

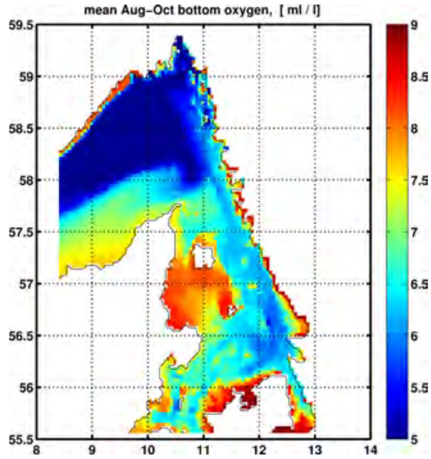

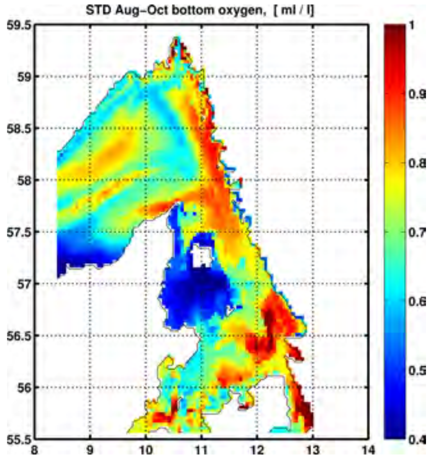

(a) (b)

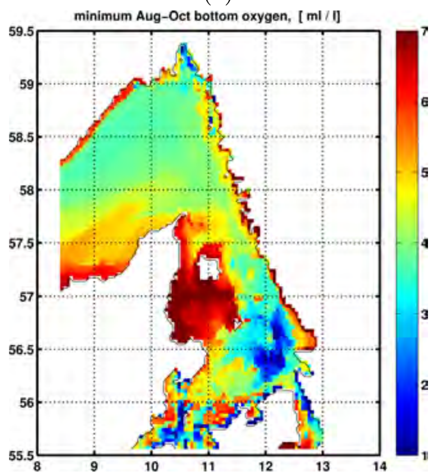

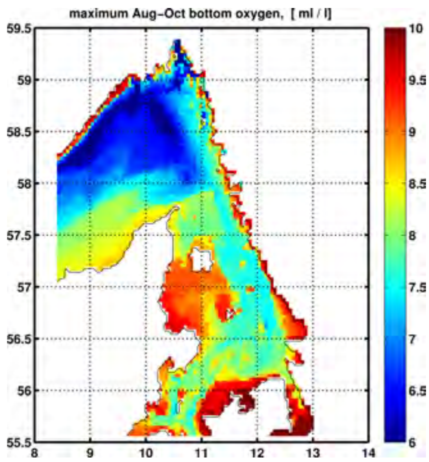

(c) (d)

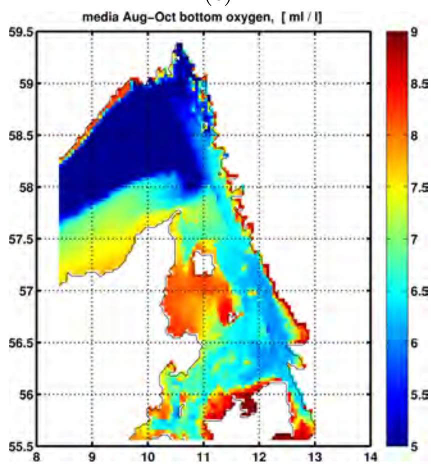

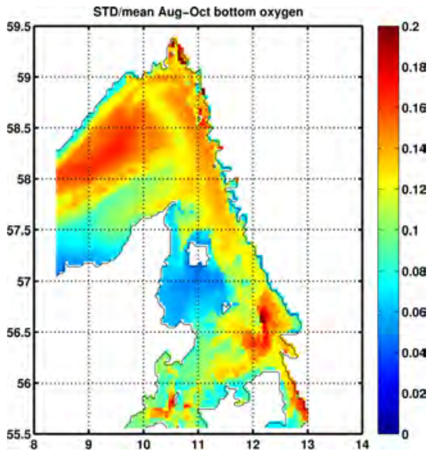

(e) (f)

Figure 16: Concentrations of oxygen at sea bottom (grid cell and layer nearest the sea floor) during late summer-autumn (August-October). Mean, std, minimum, maximum, median and std/mean for 2007–2011 years of Reductions in NS river loads run.

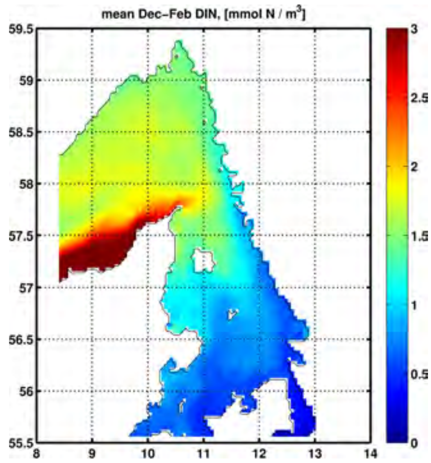

(a)

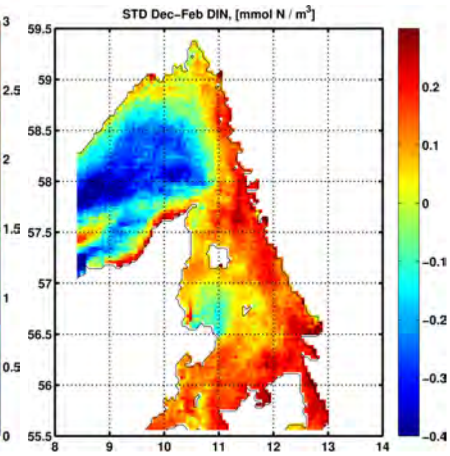

(b)

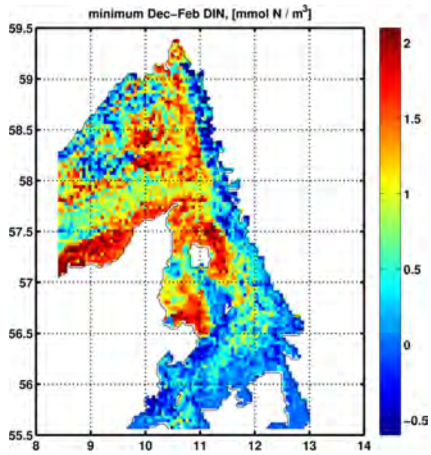

(c)

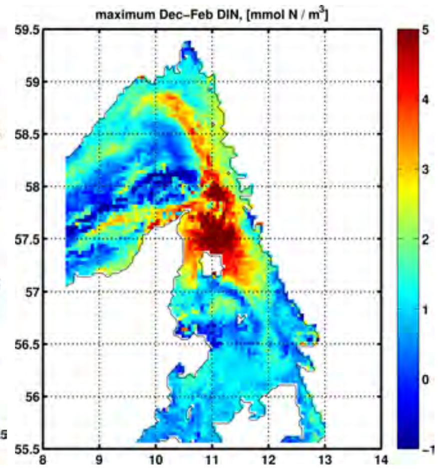

(d)

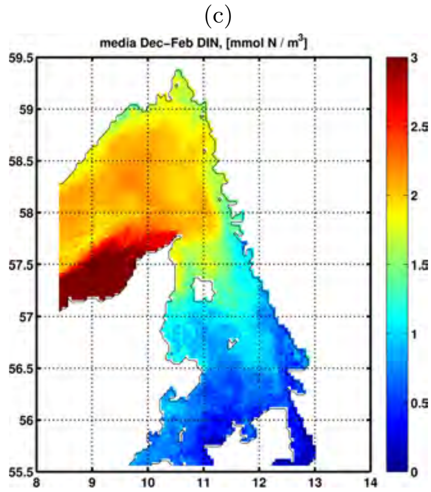

(e)

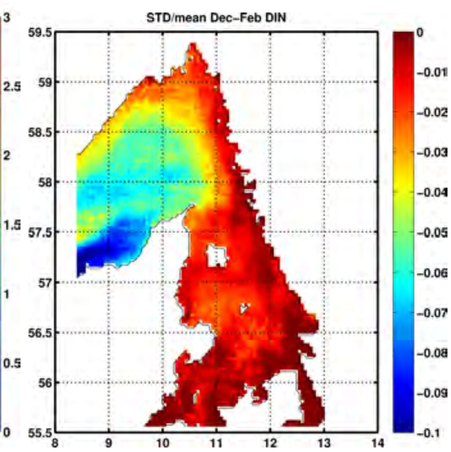

(f)

Figure 17: Changes between reference and Reductions in NS river loads runs (reference run - current run) in winter (DJF) sea surface (10m mean) DIN. Mean - (a), std - (b), minimum - (c), maximum - (d), median - (e) and std/mean - (f) for 2007–2011 years of Reductions in NS river loads run.

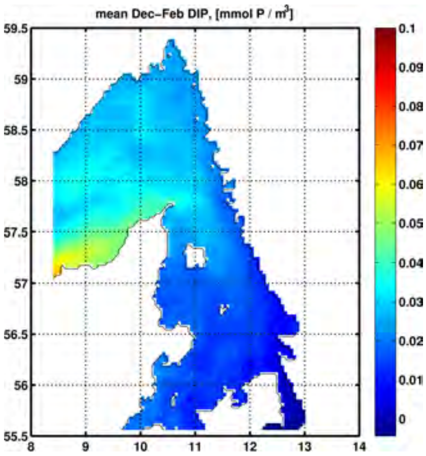

(a)

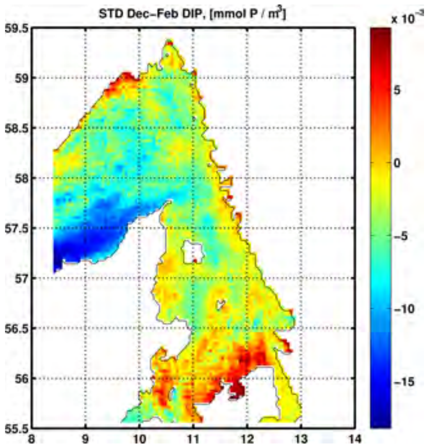

(b)

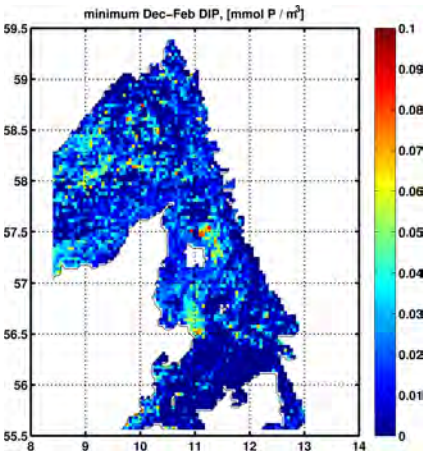

(c)

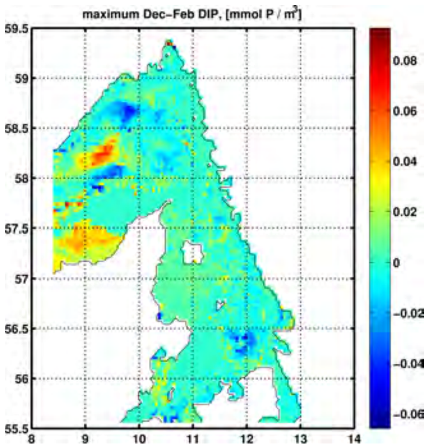

(d)

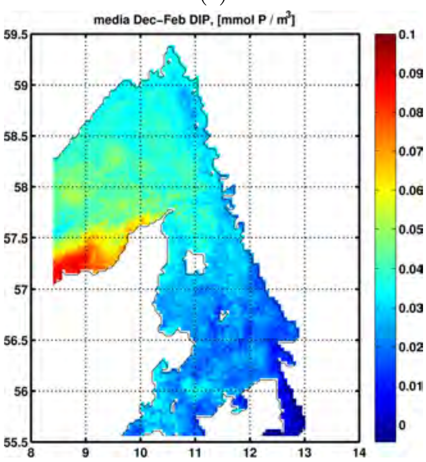

(e)

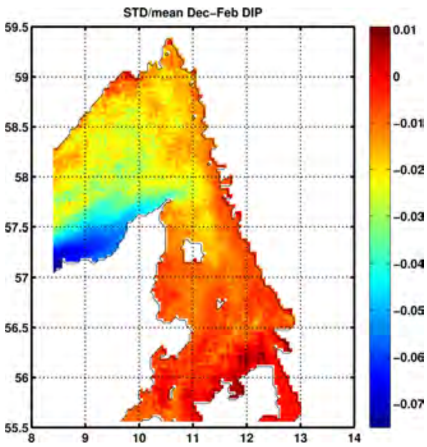

(f)

Figure 18: Changes between reference and Reductions in NS river loads runs (reference run - current run) in winter (DJF) sea surface (10m mean) DIP. Mean - (a), std - (b), minimum - (c), maximum - (d), median - (e) and std/mean - (f) for 2007–2011 years of Reductions in NS river loads run.

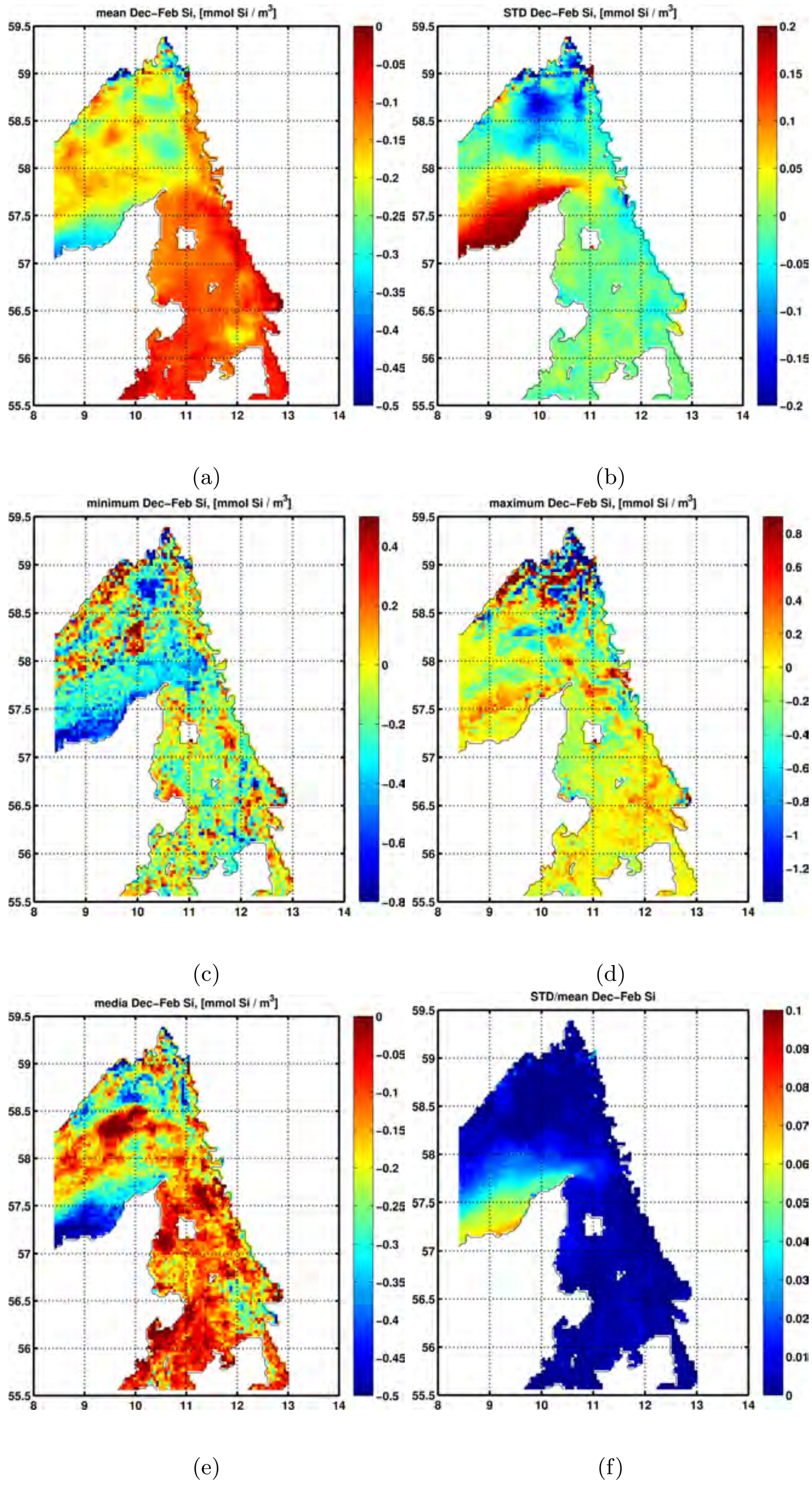

Figure 19: Changes between reference and Reductions in NS river loads runs (reference run - current run) in winter (DJF) sea surface (10m mean) Si. Mean - (a), std - (b), minimum - (c), maximum - (d), median - (e) and std/mean - (f) for 2007–2011 years of Reductions in NS river loads run.

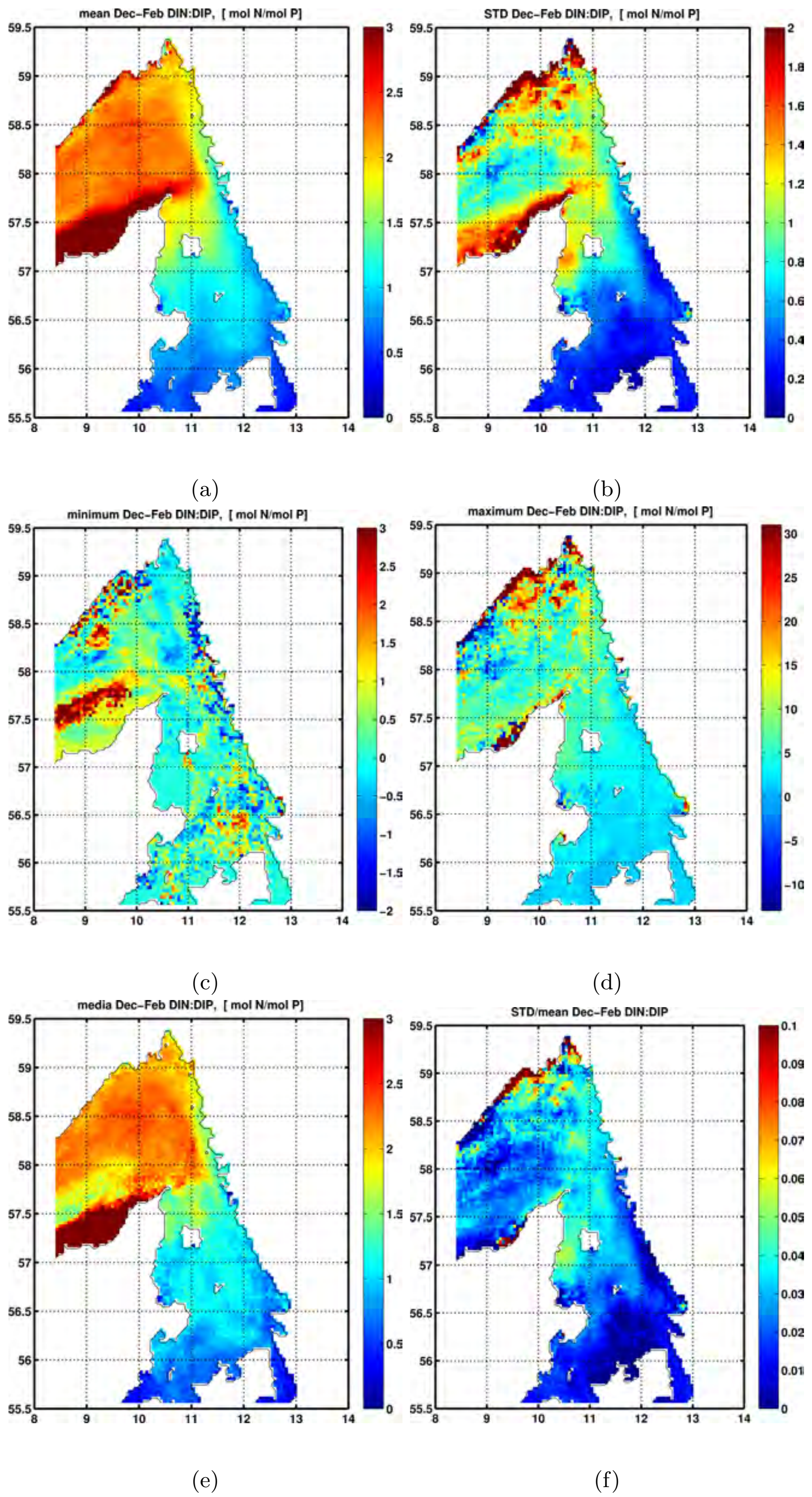

Figure 20: Changes between reference and Reductions in NS river loads runs (reference run - current run) in winter (DJF) sea surface (10m mean) DIN:DIP. Mean - (a), std - (b), minimum - (c), maximum - (d), median - (e) and std/mean - (f) for 2007–2011 years of Reductions in NS river loads run.

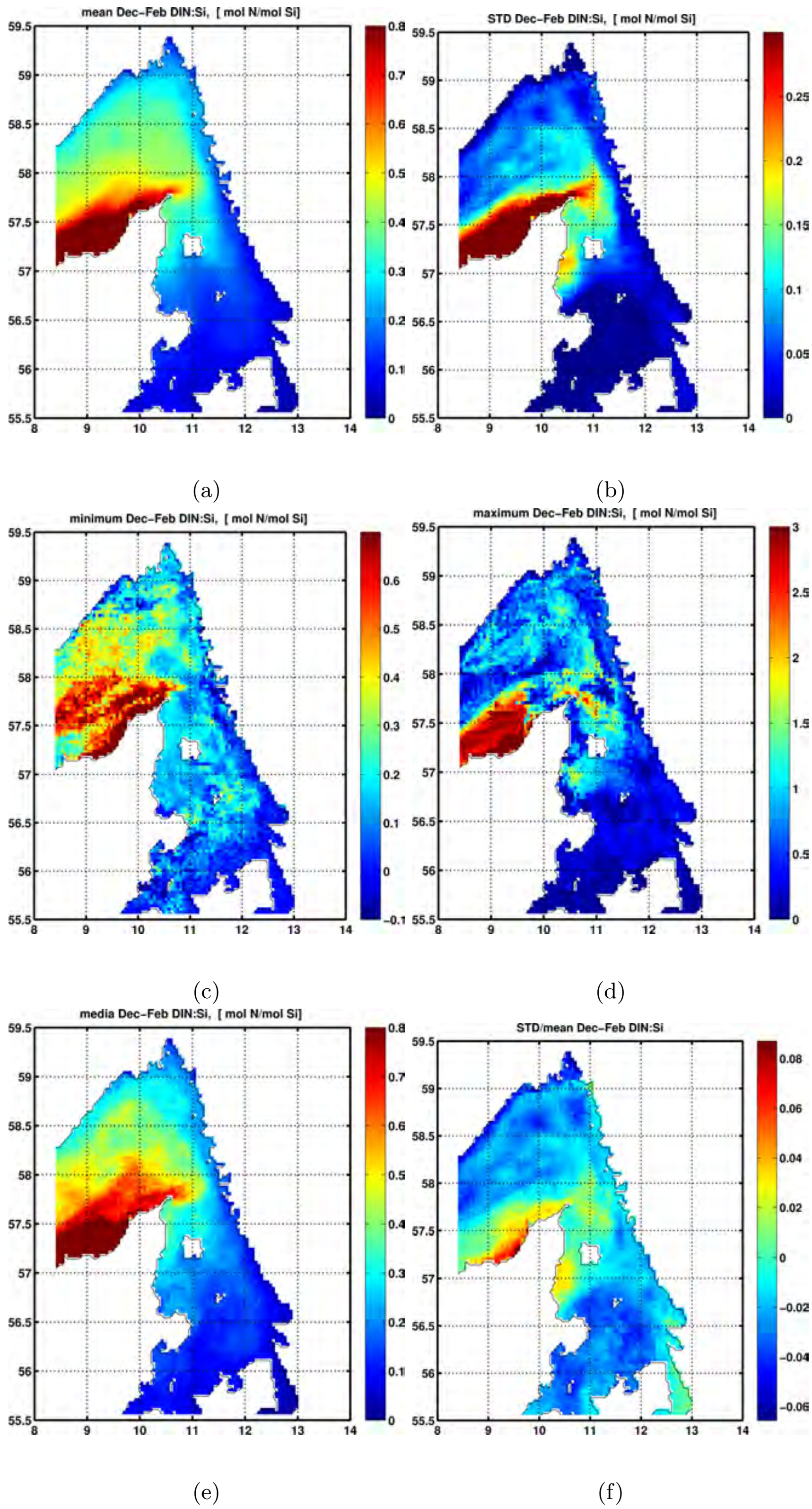

Figure 21: Changes between reference and Reductions in NS river loads runs (reference run - current run) in winter (DJF) sea surface (10m mean) DIN:Si. Mean - (a), std - (b), minimum - (c), maximum - (d), median - (e) and std/mean - (f) for 2007–2011 years of Reductions in NS river loads run.

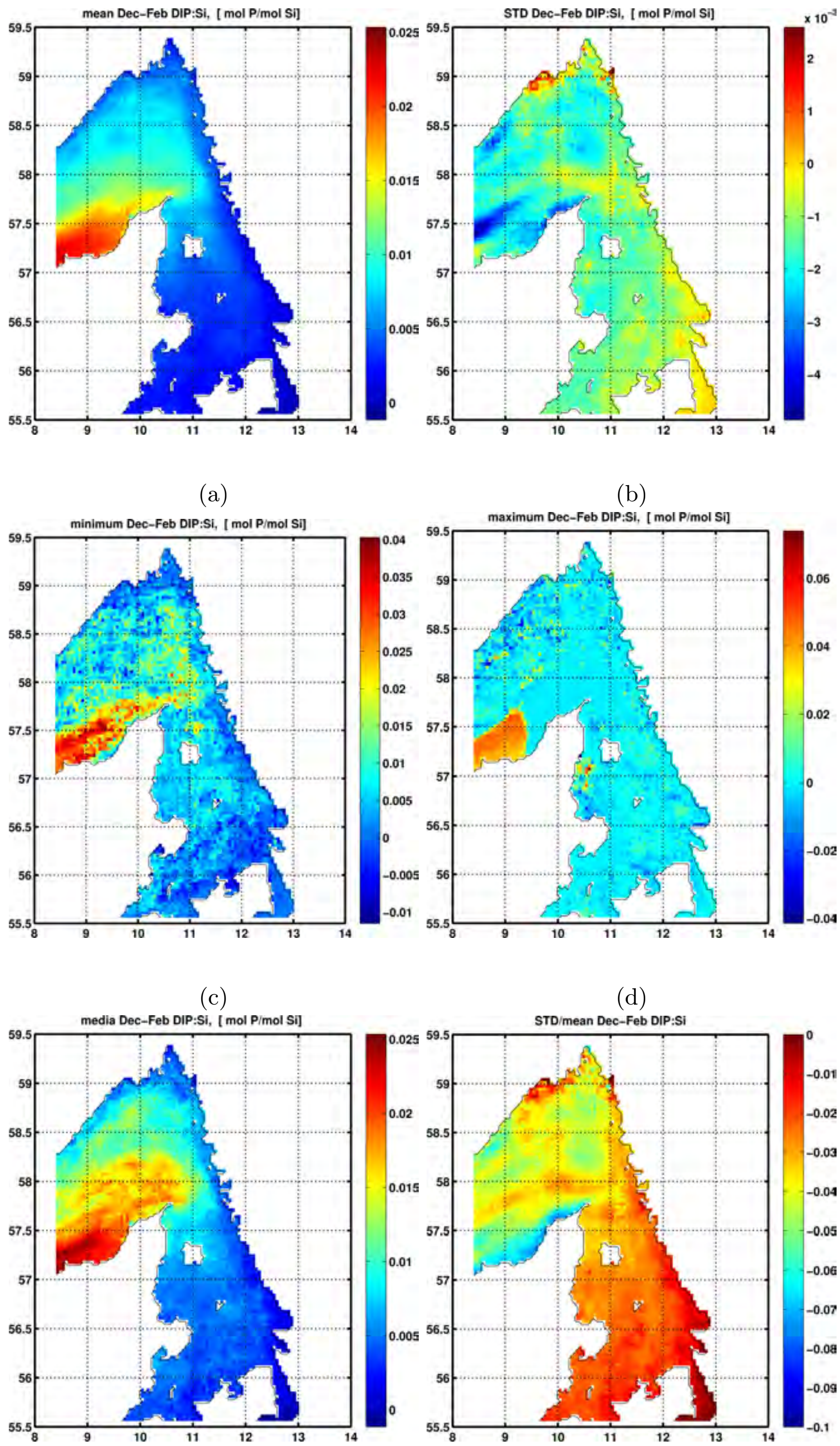

(e) (f)

Figure 22: Changes between reference and Reductions in NS river loads runs (reference run - current run) in winter (DJF) sea surface (10m mean) DIP:Si. Mean - (a), std - (b), minimum - (c), maximum - (d), median - (e) and std/mean - (f) for 2007–2011 years of Reductions in NS river loads run.

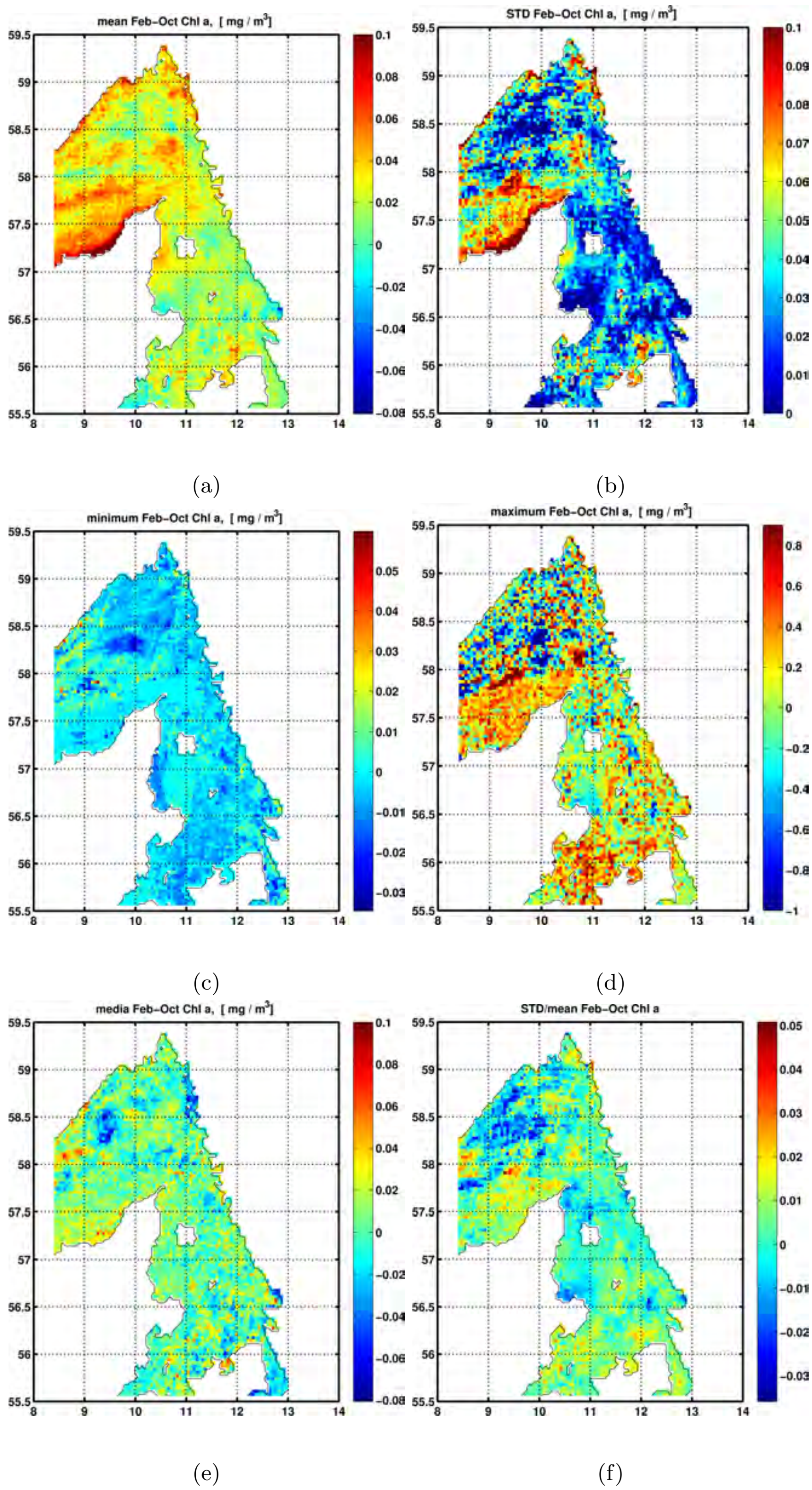

Figure 23: Changes between reference and Reductions in NS river loads runs (reference run - current run) in concentrations of chlorophyll-a in the growing season (February to October) at sea surface (10m mean) Mean - (a), std - (b), minimum - (c), maximum - (d), median - (e) and std/mean - (f) for 2007–2011 years of Reductions in NS river loads run.

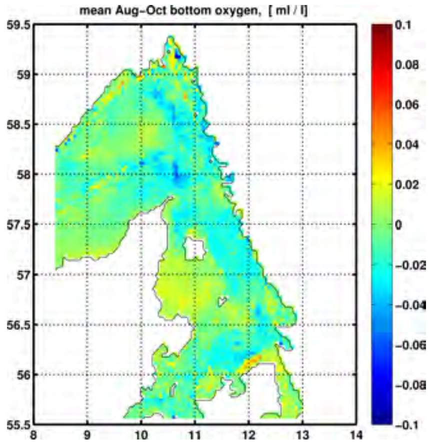

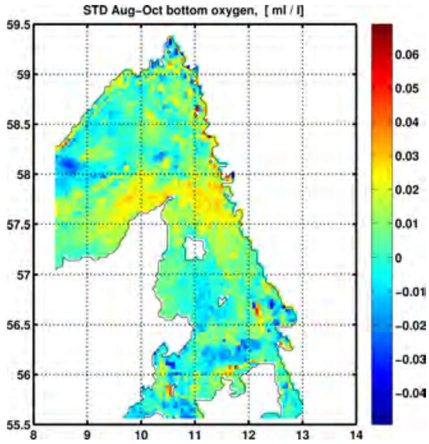

(a) (b)

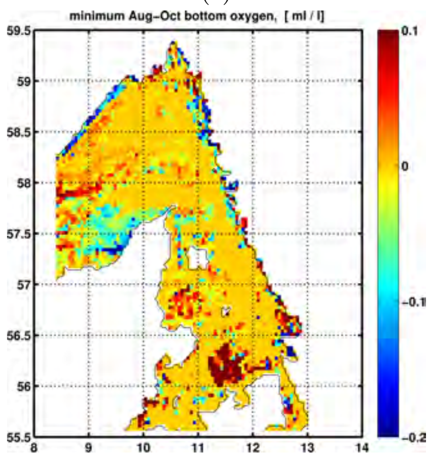

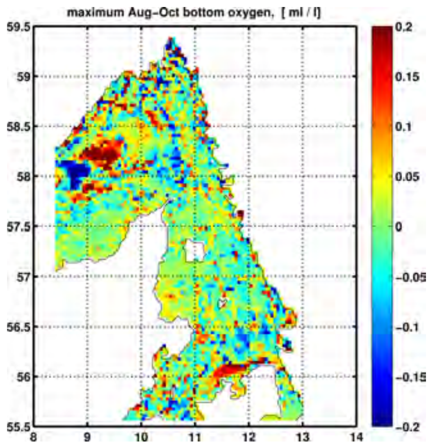

(c) (d)

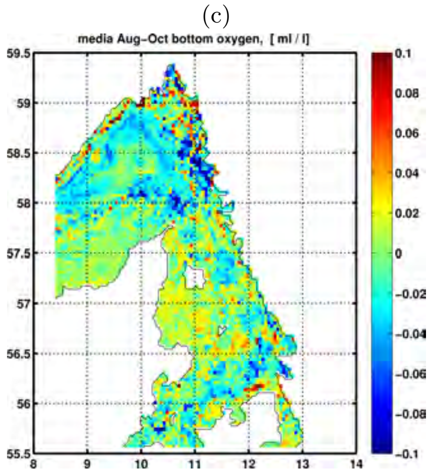

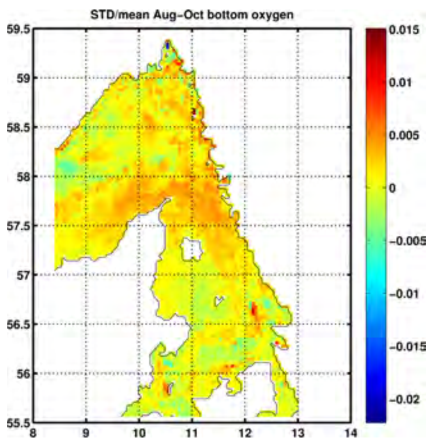

(e) (f)

Figure 24: Changes between reference and Reductions in NS river loads runs (reference run - current run) in concentrations of oxygen at sea bottom (grid cell and layer nearest the sea floor) during late summer-autumn (August-October). Mean - (a), std - (b), minimum - (c), maximum - (d), median - (e) and std/mean - (f) for 2007–2011 years of Reductions in NS river loads run.

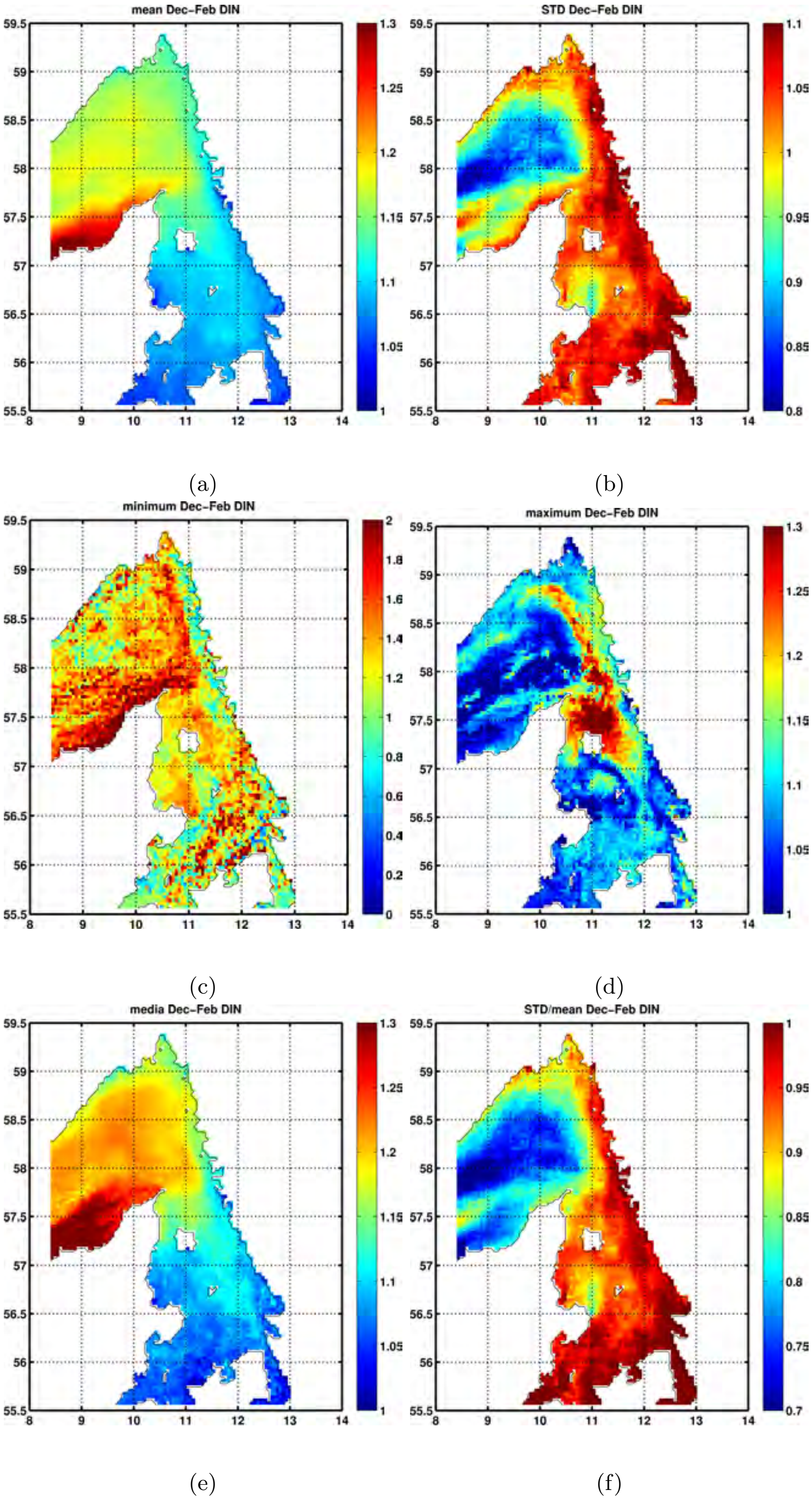

Figure 25: Relative change in Reductions in NS river loads run (reference run / current run) in winter (DJF) sea surface (10m mean) DIN. Mean - (a), std - (b), minimum - (c), maximum - (d), median - (e) and std/mean - (f) for 2007–2011 years of Reductions in NS river loads run.

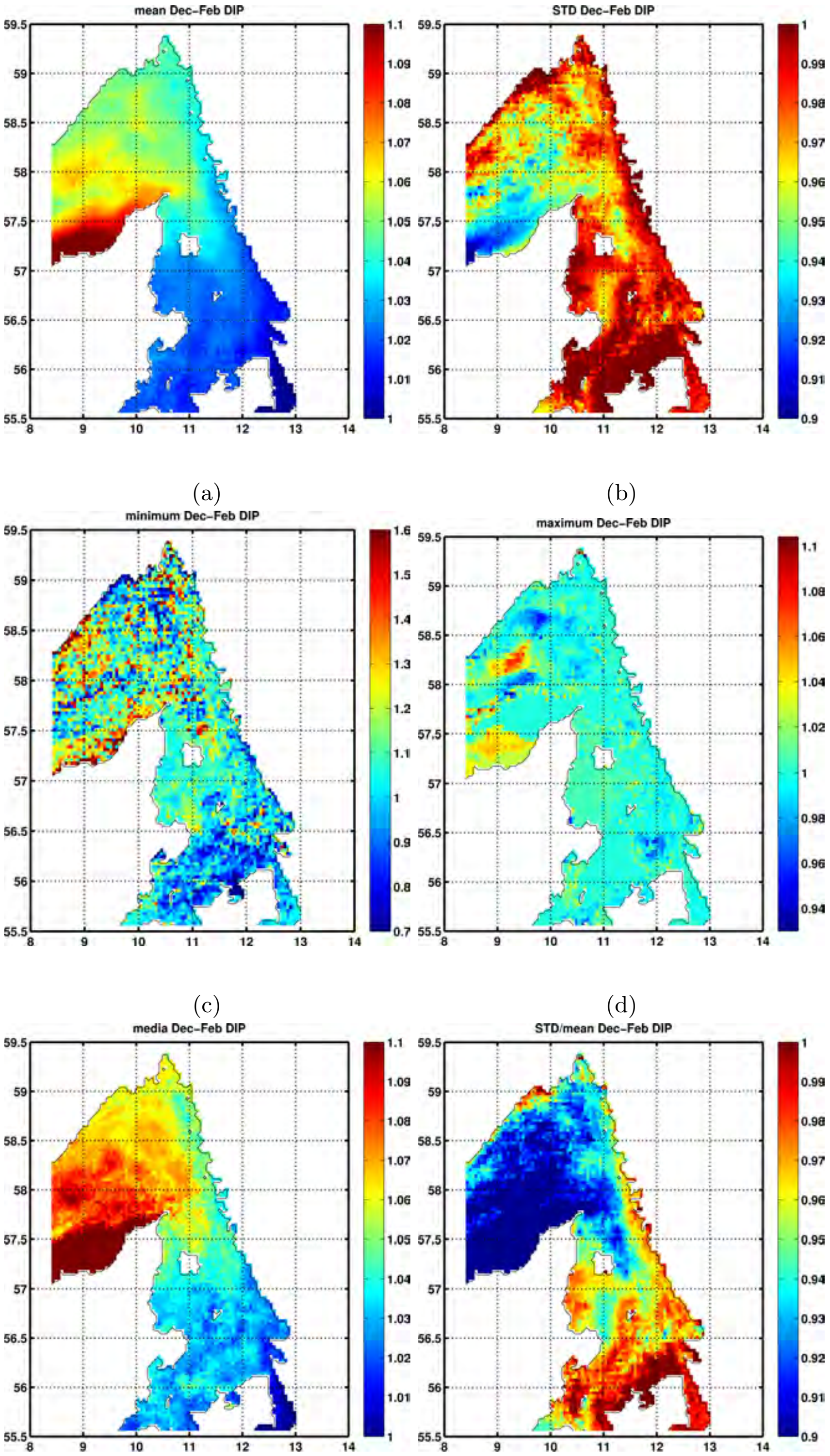

(a) (b)

(c) (d)

(e) (f)

Figure 26: Relative change in Reductions in NS river loads run (reference run / current run) in winter (DJF) sea surface (10m mean) DIP. Mean - (a), std - (b), minimum - (c), maximum - (d), median - (e) and std/mean - (f) for 2007–2011 years of Reductions in NS river loads run.

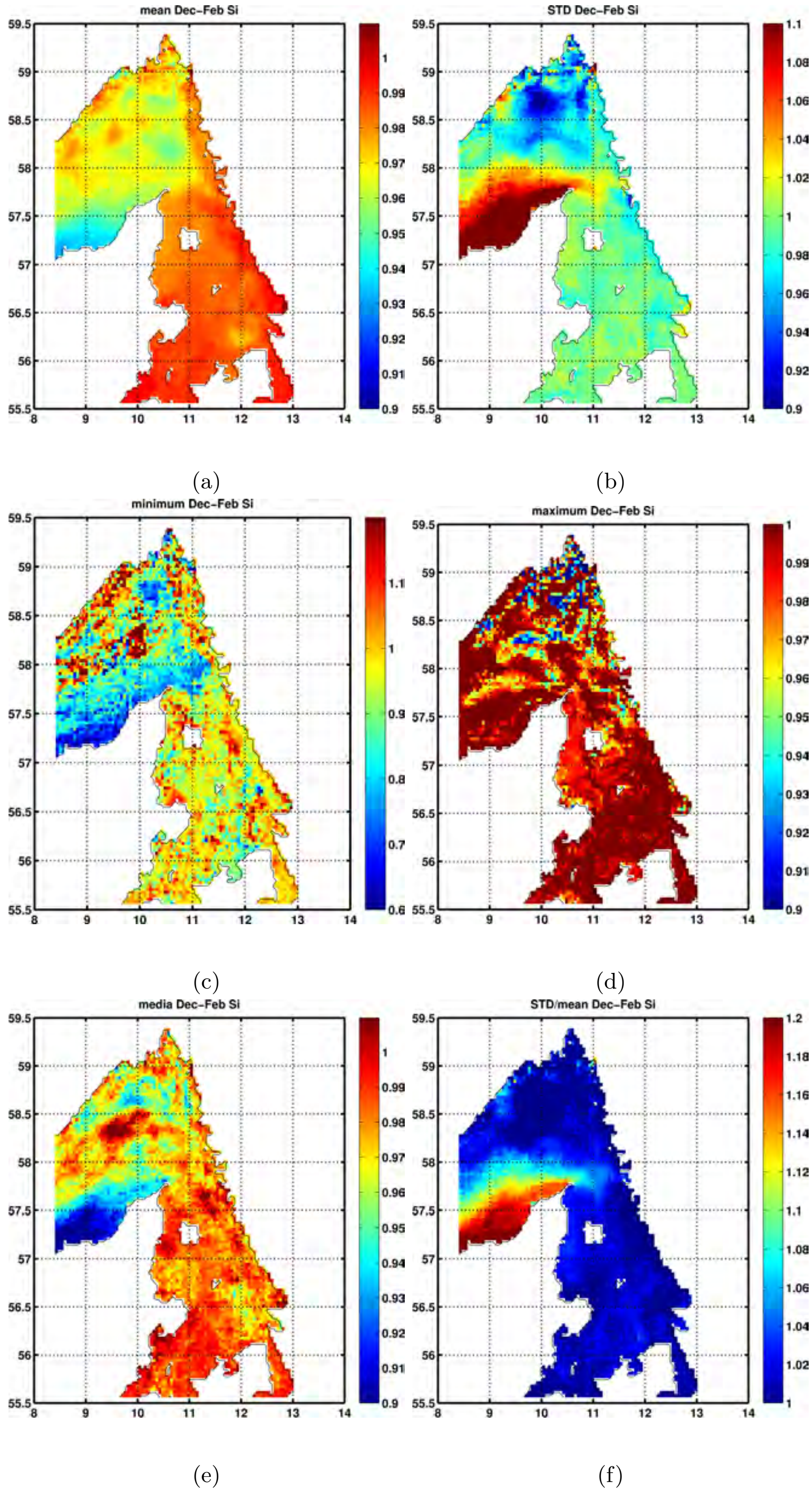

Figure 27: Relative change in Reductions in NS river loads run (reference run / current run) in winter (DJF) sea surface (10m mean) Si. Mean - (a), std - (b), minimum - (c), maximum - (d), median - (e) and std/mean - (f) for 2007–2011 years of Reductions in NS river loads run.

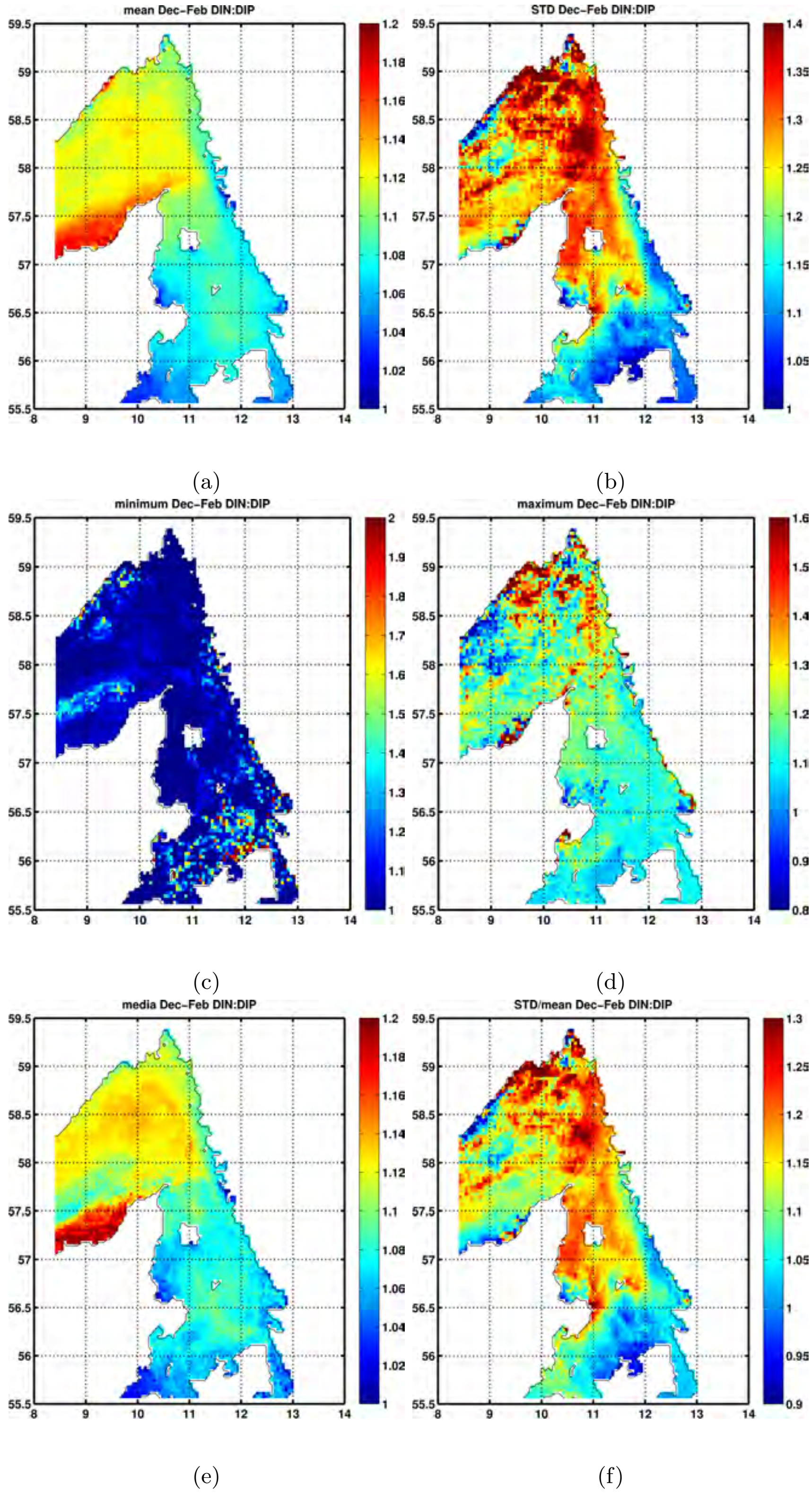

Figure 28: Relative change in Reductions in NS river loads run (reference run / current run) in winter (DJF) sea surface (10m mean) DIN:DIP. Mean - (a), std - (b), minimum - (c), maximum - (d), median - (e) and std/mean - (f) for 2007–2011 years of Reductions in NS river loads run.

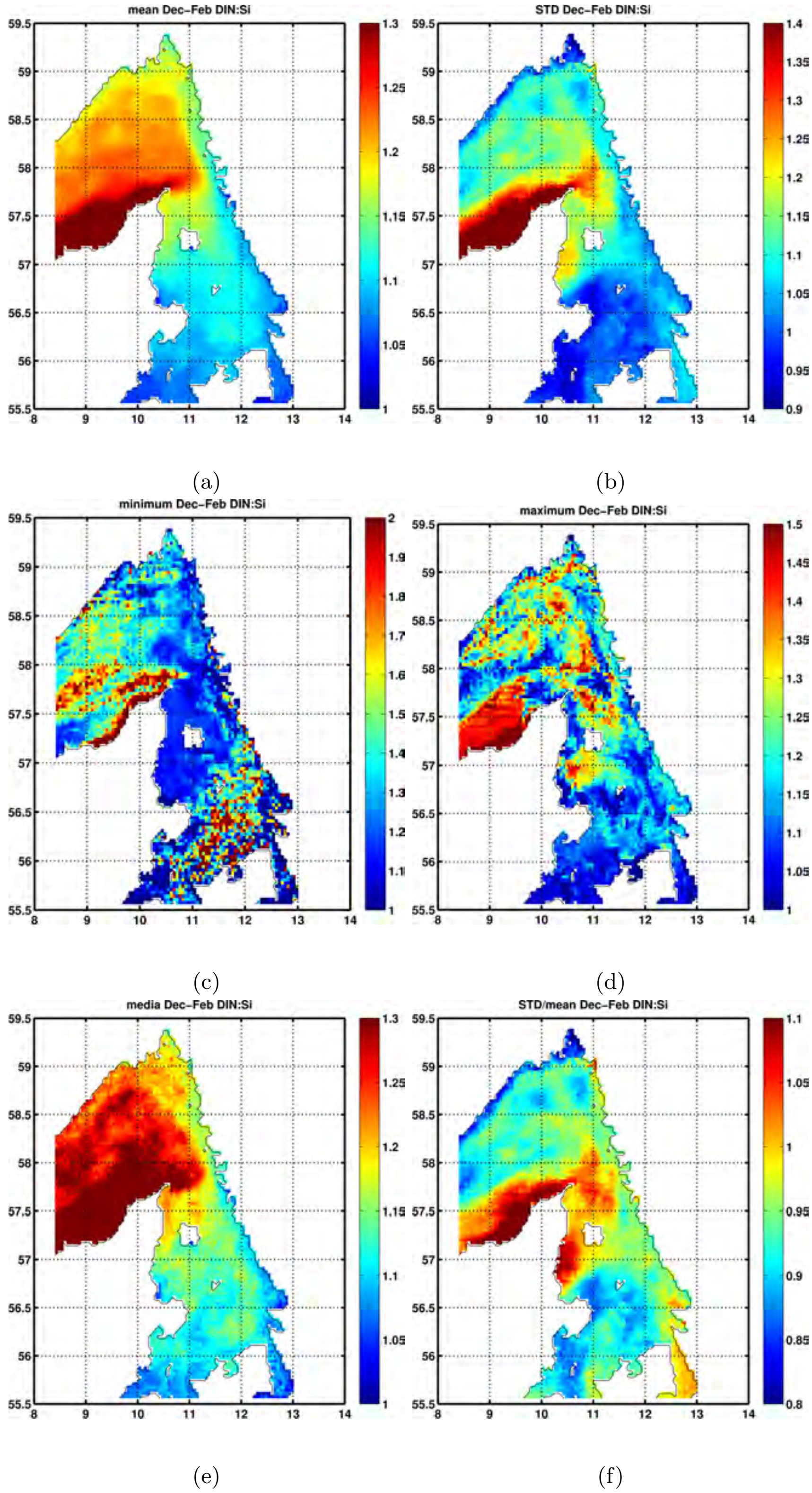

Figure 29: Relative change in Reductions in NS river loads run (reference run / current run) in winter (DJF) sea surface (10m mean) DIN:Si. Mean - (a), std - (b), minimum - (c), maximum - (d), median - (e) and std/mean - (f) for 2007–2011 years of Reductions in NS river loads run.

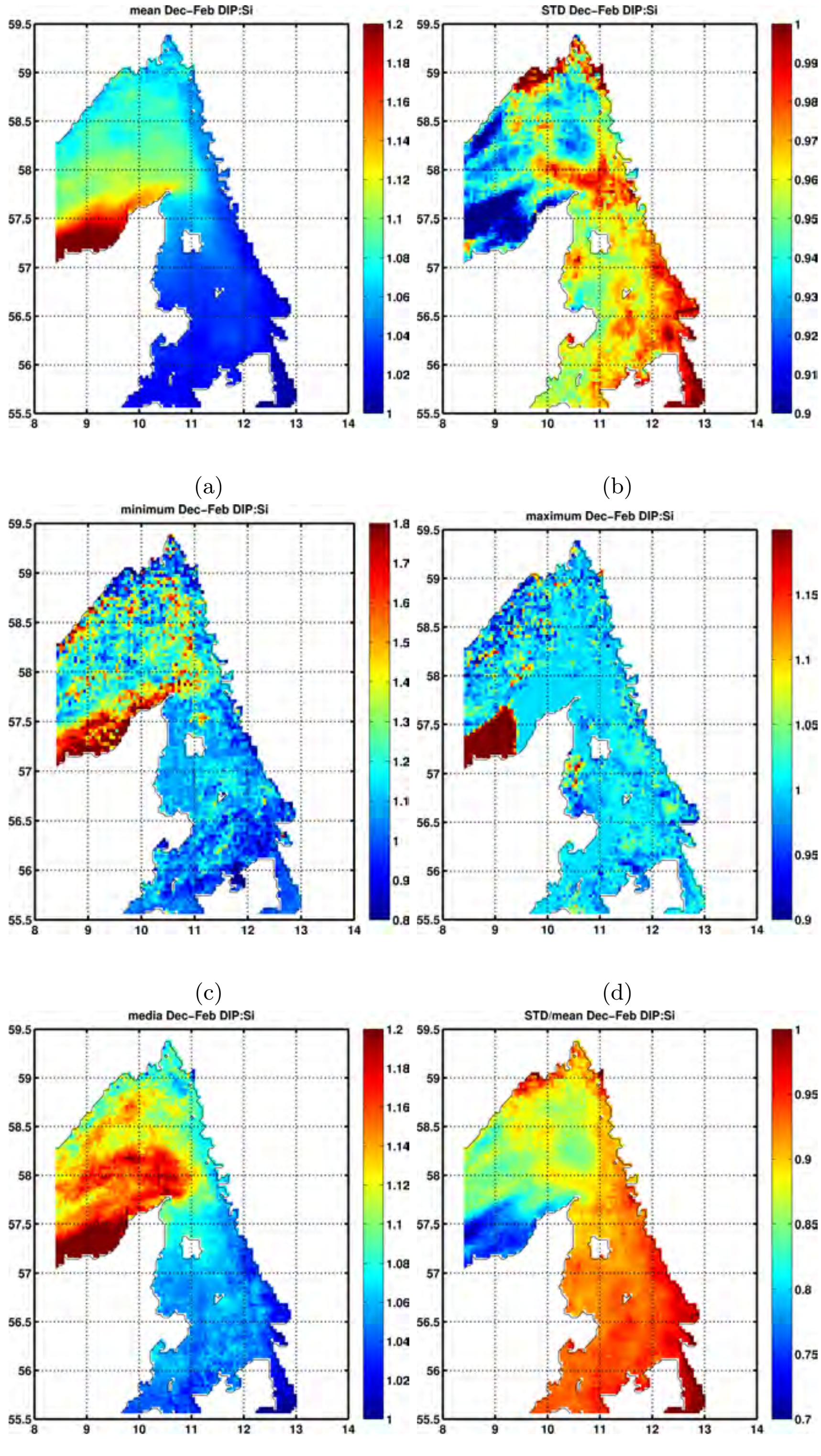

(a) (b)

(c) (d)

(e) (f)

Figure 30: Relative change in Reductions in NS river loads run (reference run / current run) in winter (DJF) sea surface (10m mean) DIP:Si. Mean - (a), std - (b), minimum - (c), maximum - (d), median - (e) and std/mean - (f) for 2007–2011 years of Reductions in NS river loads run.

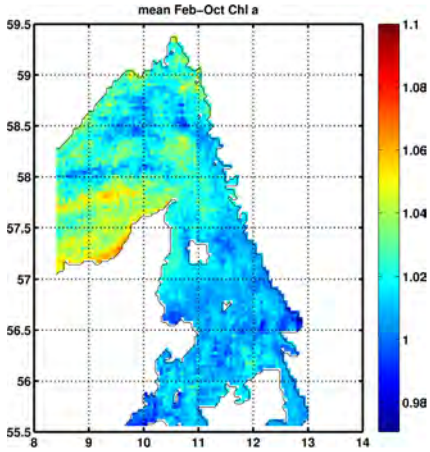

(a)

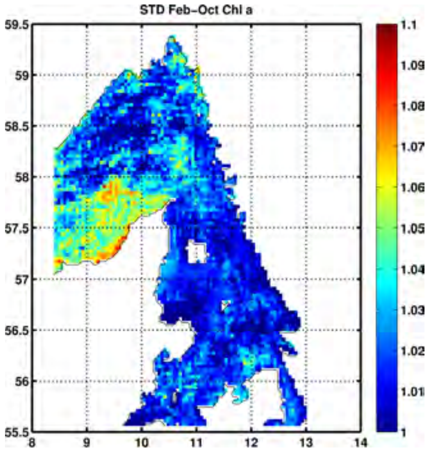

(b)

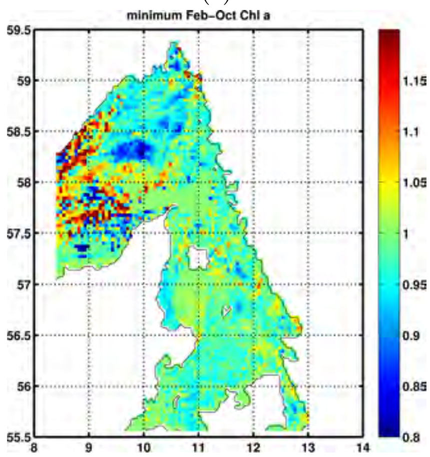

(c)

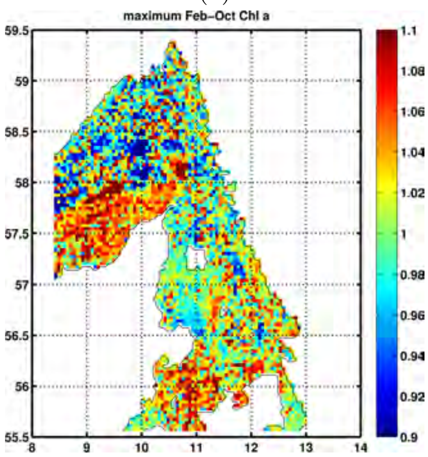

(d)

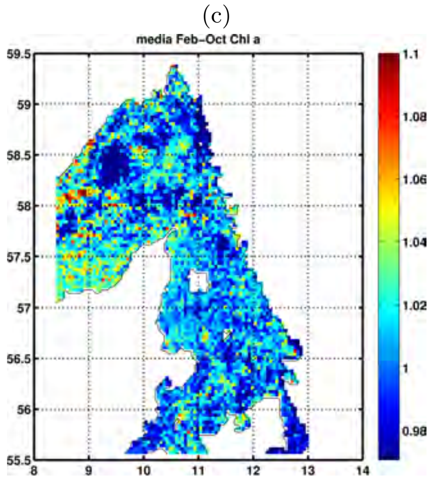

(e)

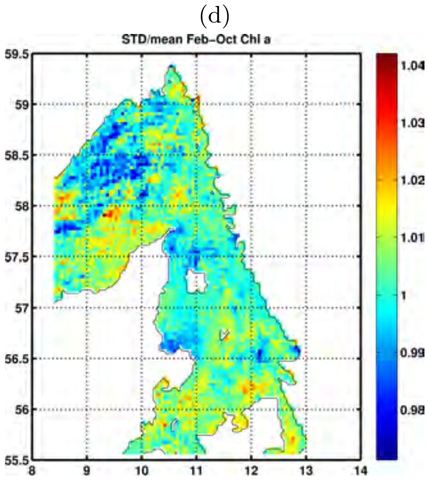

(f)

Figure 31: Relative change in Reductions in NS river loads run (reference run / current run) in concentrations of chlorophyll-a in the growing season (February to October) at sea surface (10m mean) Mean - (a), std - (b), minimum - (c), maximum - (d), median - (e) and std/mean - (f) for 2007–2011 years of Reductions in NS river loads run.

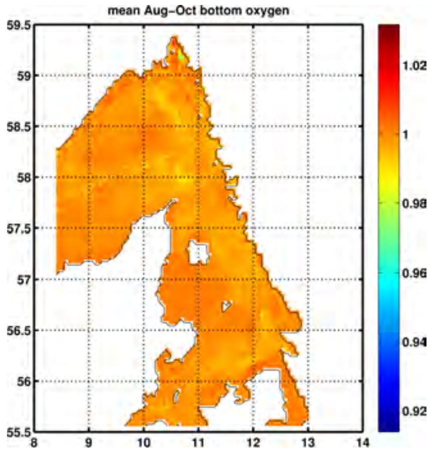

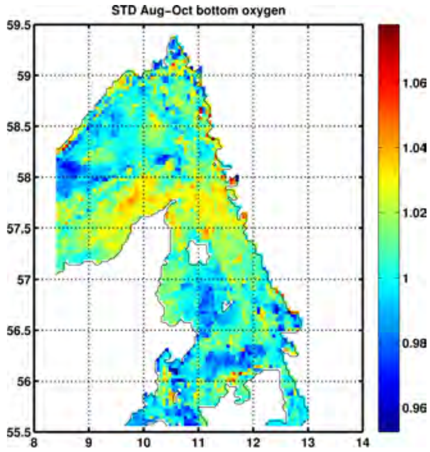

(a) (b)

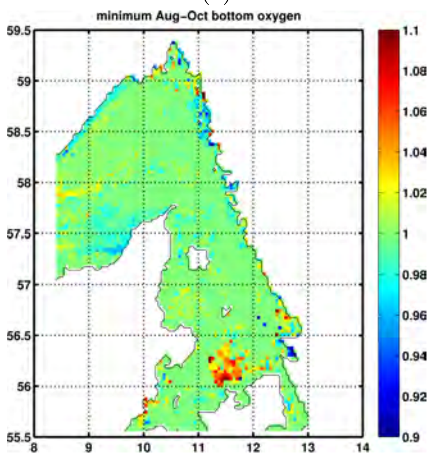

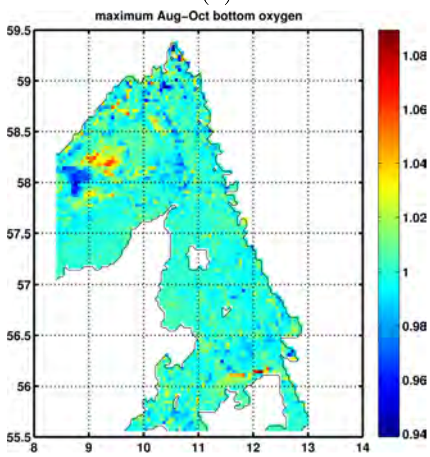

(c) (d)

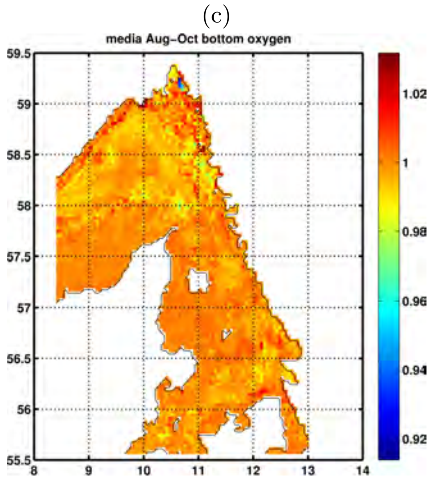

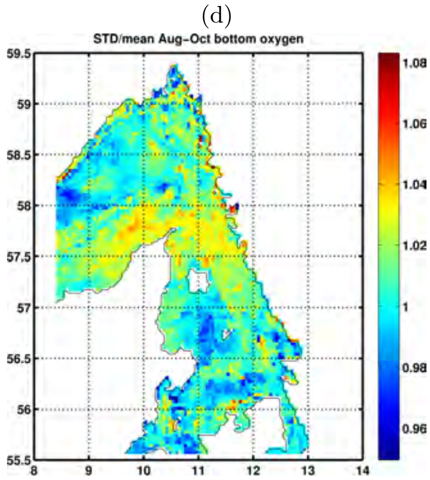

(e) (f)

Figure 32: Relative change in Reductions in NS river loads run (reference run / current run) in concentrations of oxygen at sea bottom (grid cell and layer nearest the sea floor) during late summer-autumn (August-October). Mean - (a), std - (b), minimum - (c), maximum - (d), median - (e) and std/mean - (f) for 2007–2011 years of Reductions in NS river loads run.

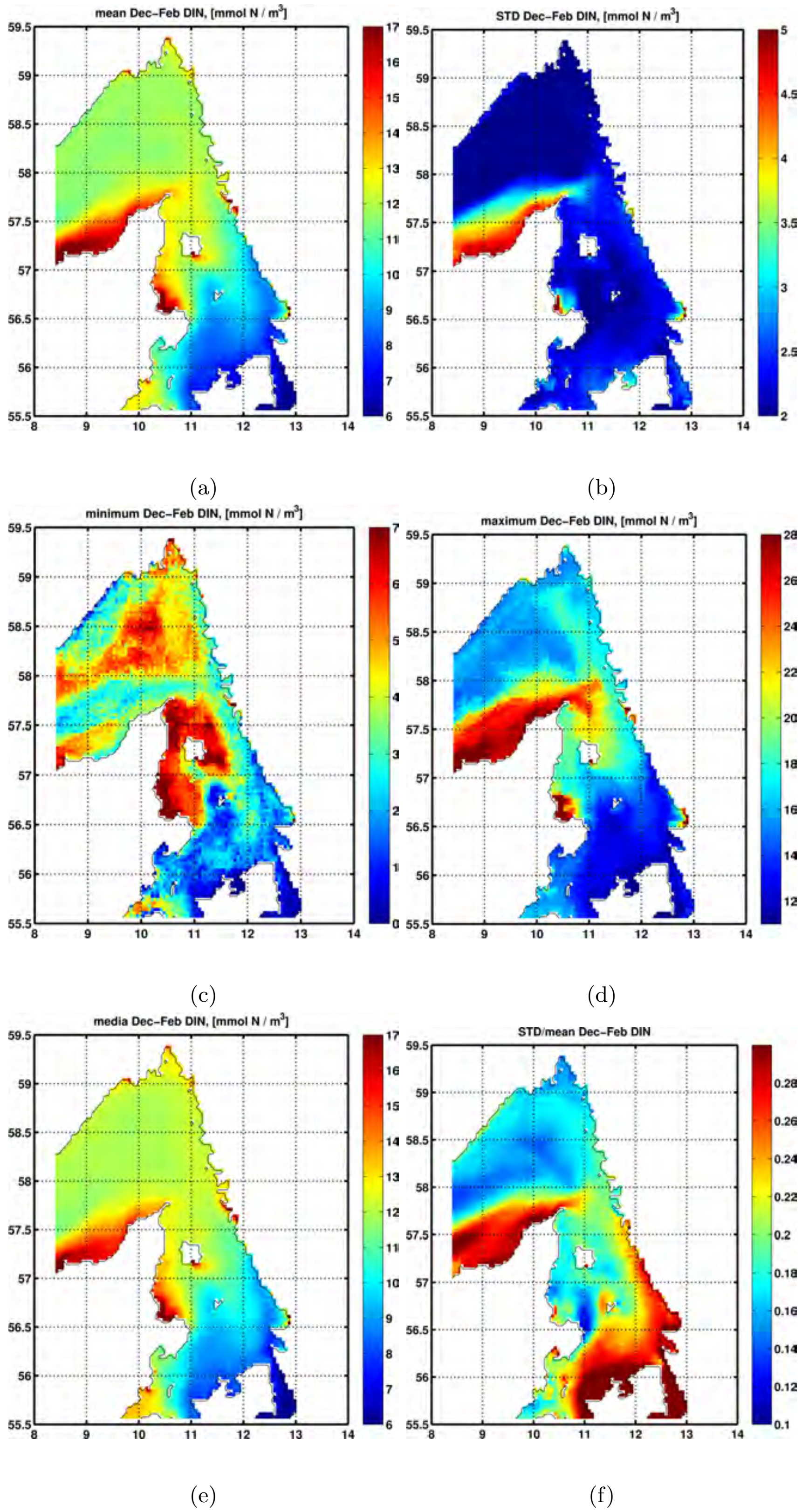

Figure 33: Winter (DJF) sea surface (10m mean) DIN. Mean, std, minimum, maximum, median and std/mean for 2007–2011 years of BSAP run.

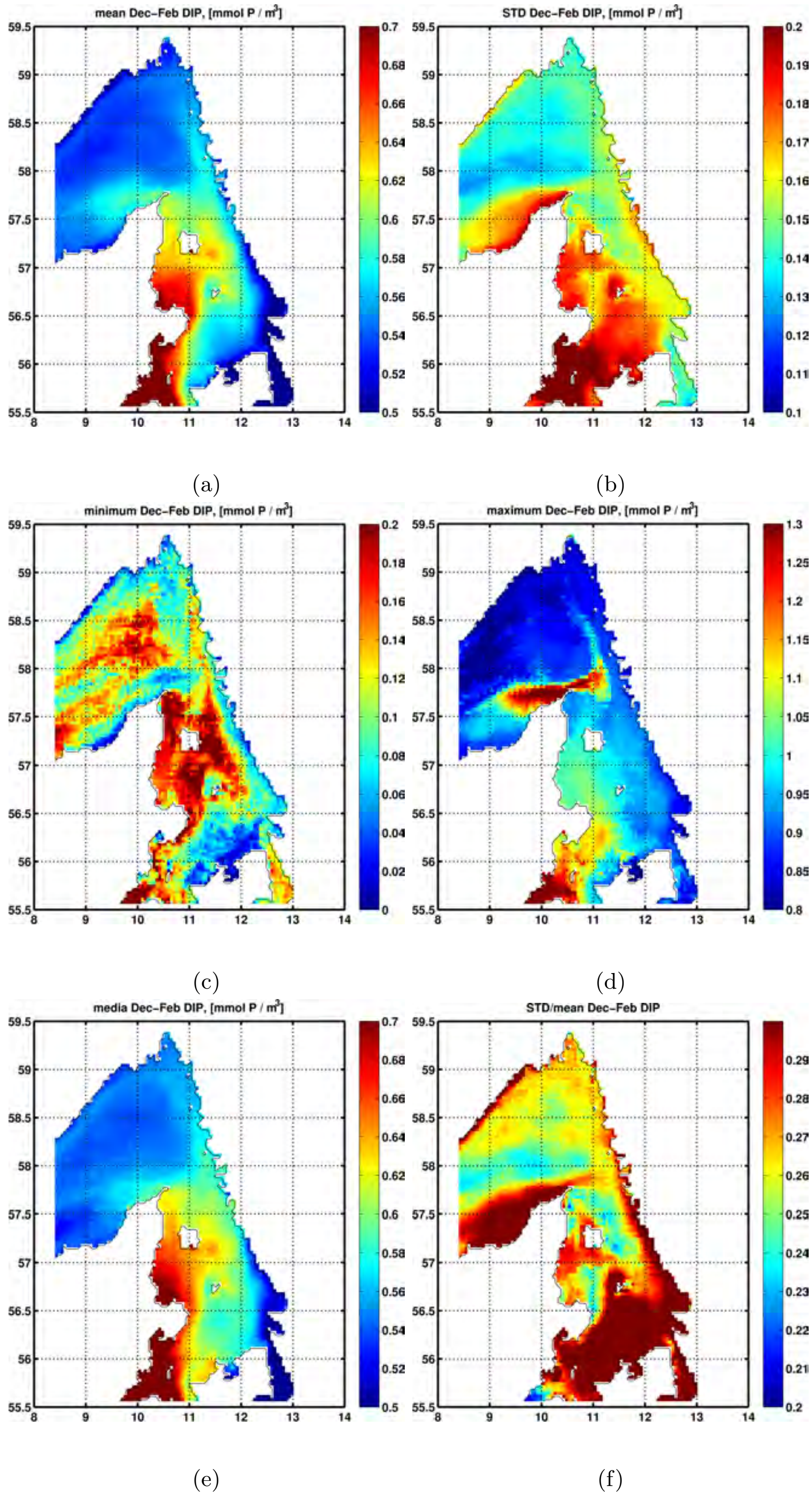

Figure 34: Winter (DJF) sea surface (10m mean) DIP. Mean, std, minimum, maximum, median and std/mean for 2007–2011 years of BSAP run.

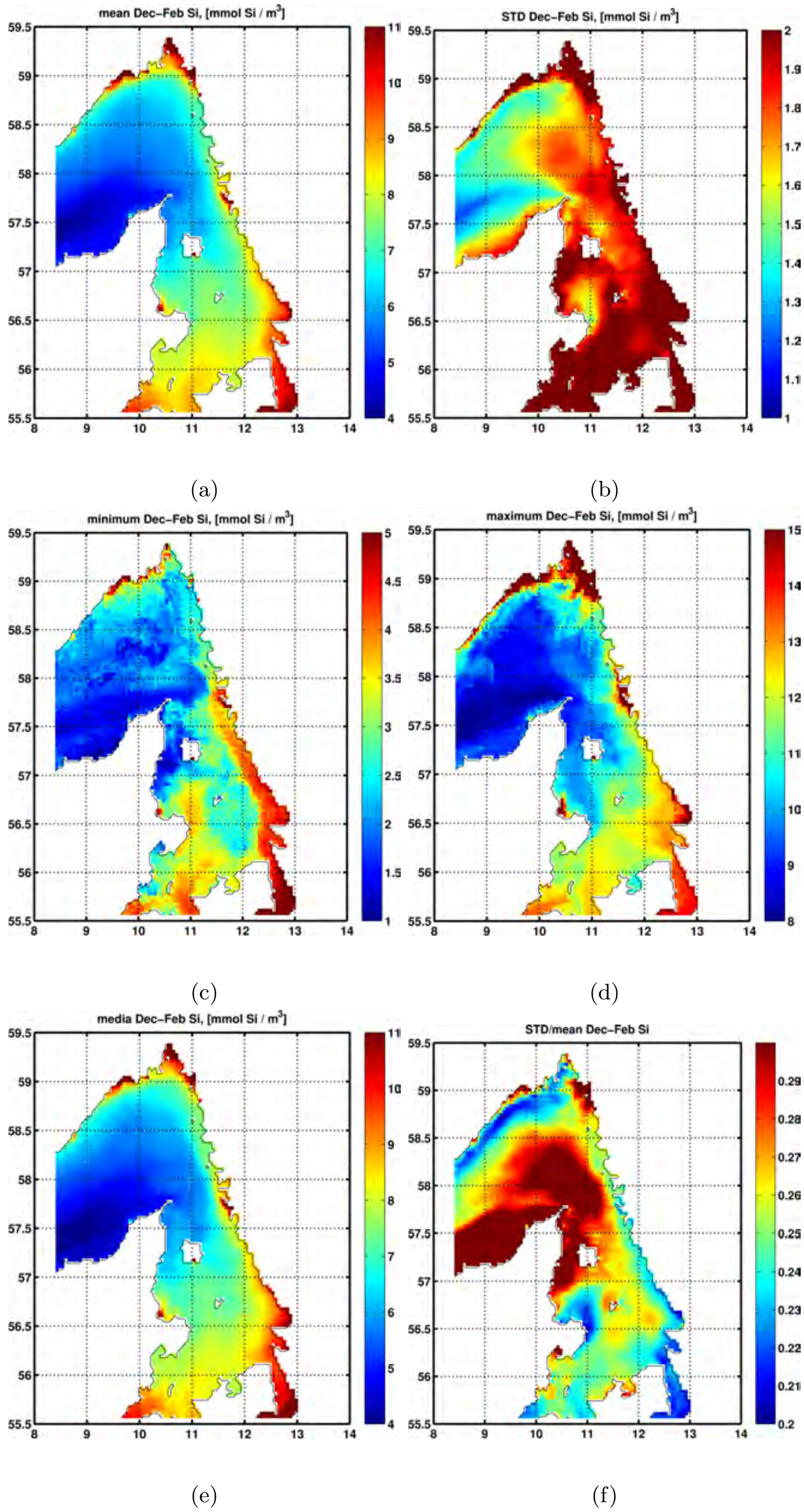

Figure 35: Winter (DJF) sea surface (10m mean) Si. Mean, std, minimum, maximum, median and std/mean for 2007–2011 years of BSAP run.

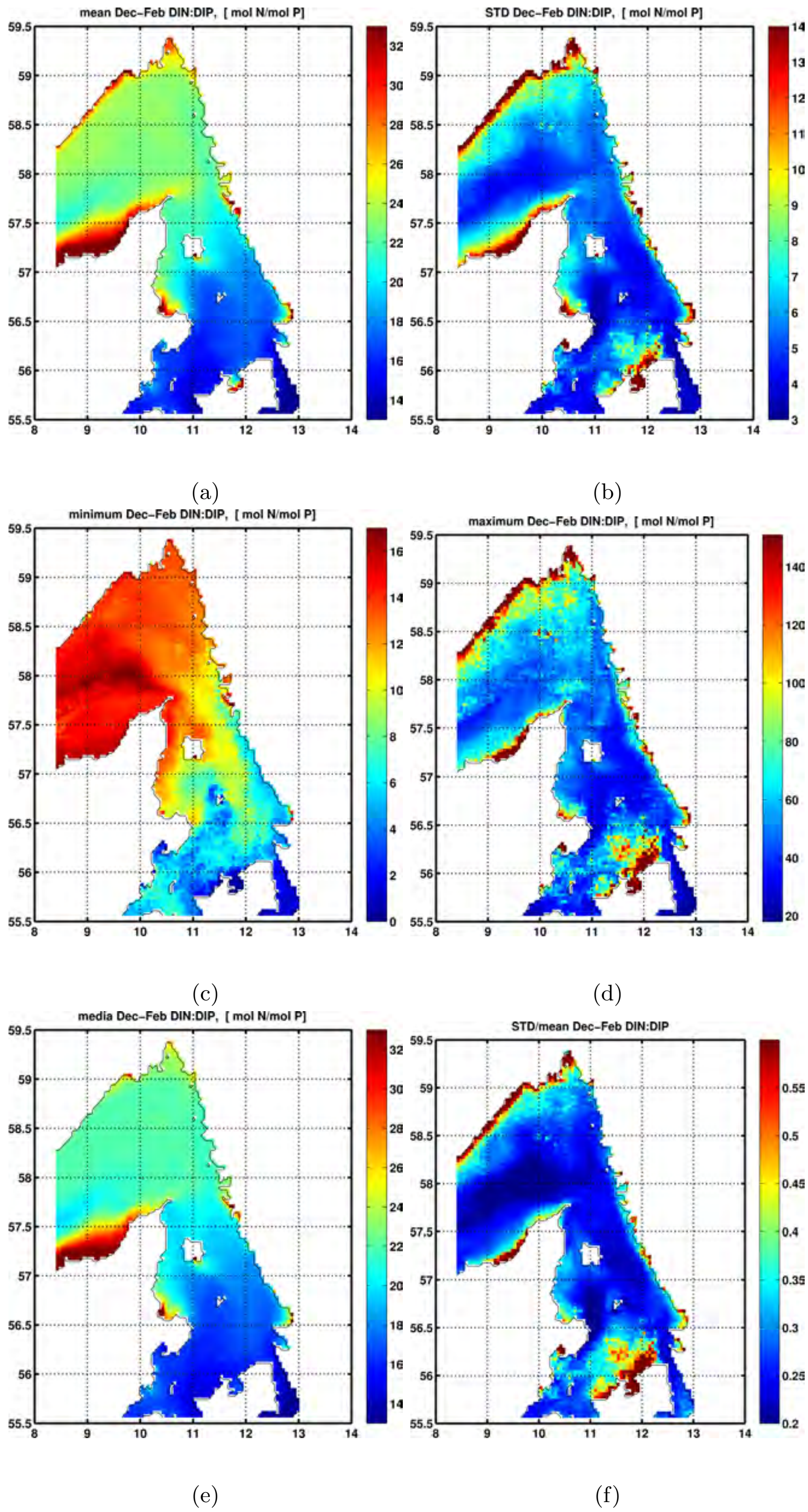

Figure 36: Winter (DJF) sea surface (10m mean) DIN:DIP. Mean, std, minimum, maximum, median and std/mean for 2007–2011 years of BSAP run.

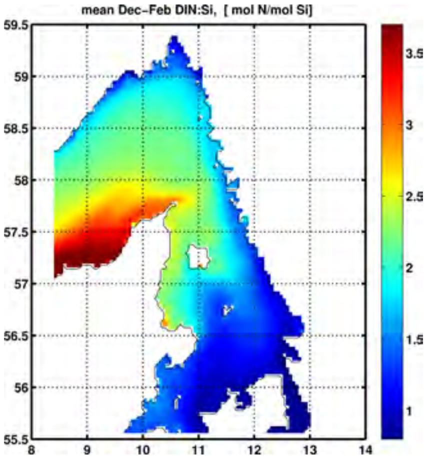

(a)

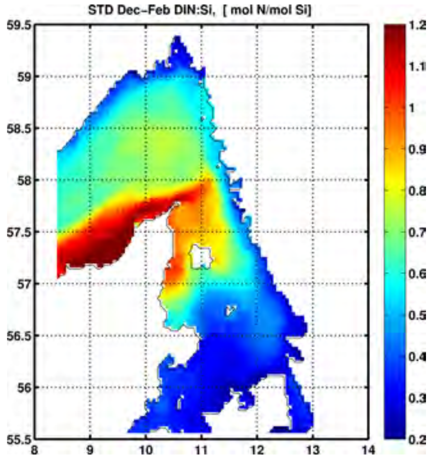

(b)

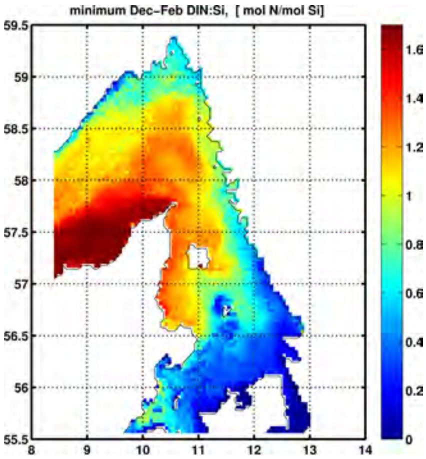

(c)

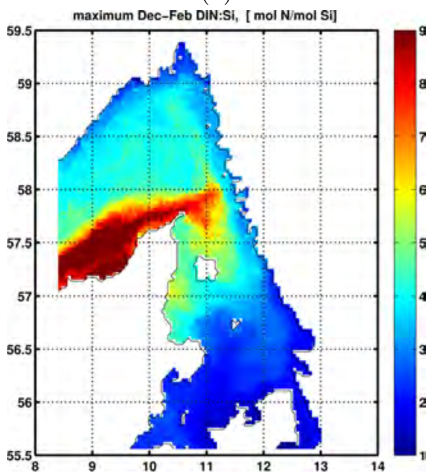

(d)

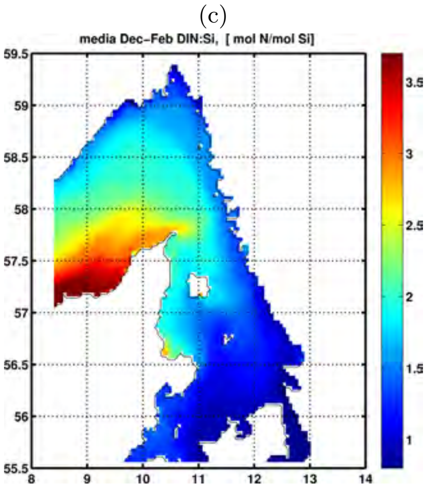

(e)

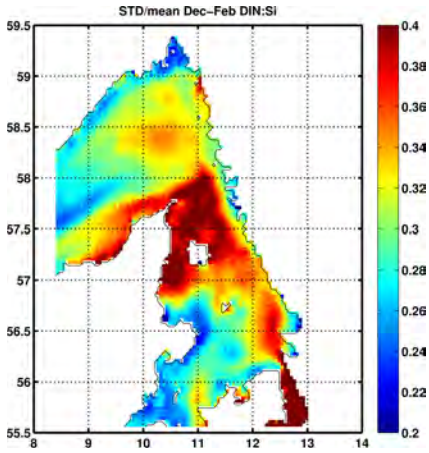

(f)

Figure 37: Winter (DJF) sea surface (10m mean) DIN:Si. Mean, std, minimum, maximum, median and std/mean for 2007–2011 years of BSAP run.

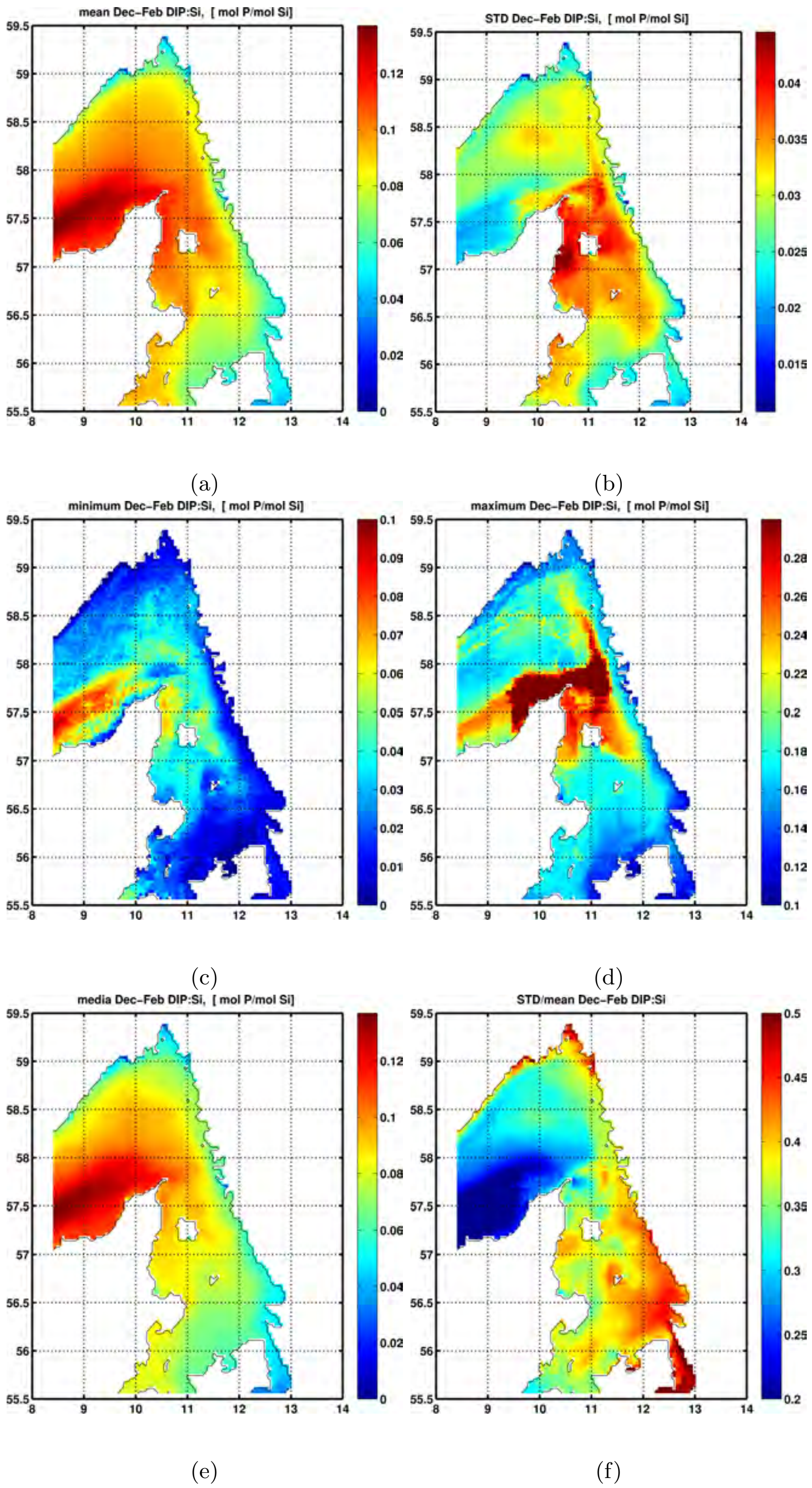

Figure 38: Winter (DJF) sea surface (10m mean) DIP:Si. Mean, std, minimum, maximum, median and std/mean for 2007–2011 years of BSAP run.

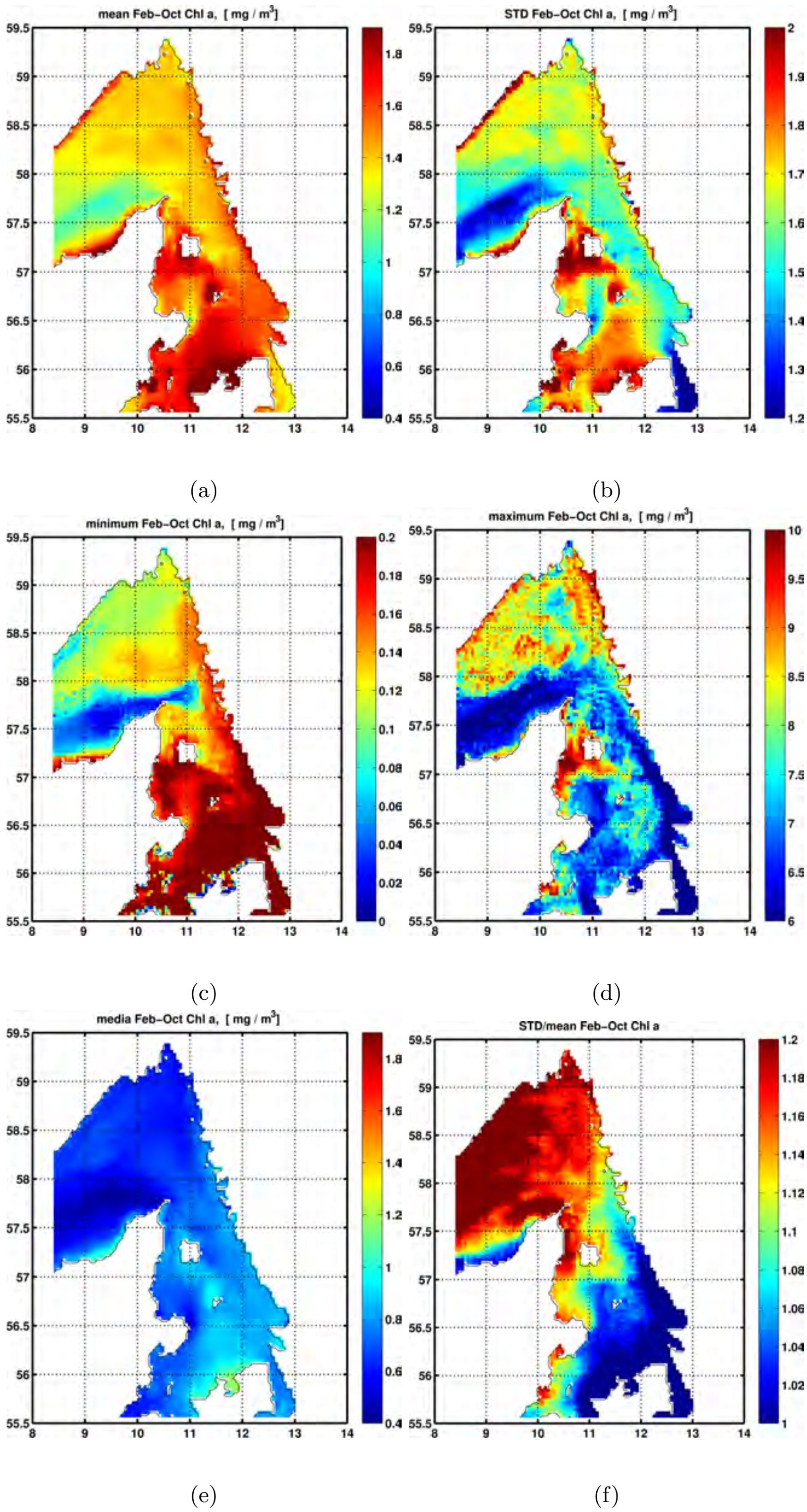

Figure 39: Concentrations of chlorophyll-a in the growing season (February to October) at sea surface (10m mean) Mean, std, minimum, maximum, median and std/mean for 2007–2011 years of BSAP run.

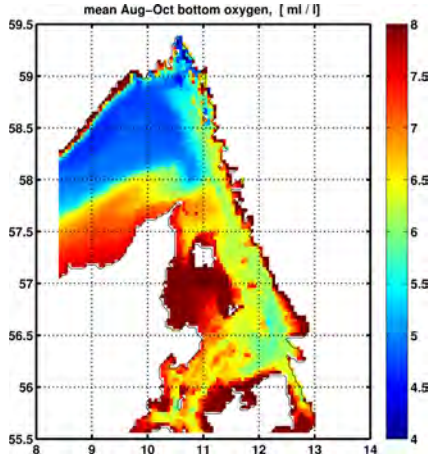

(a)

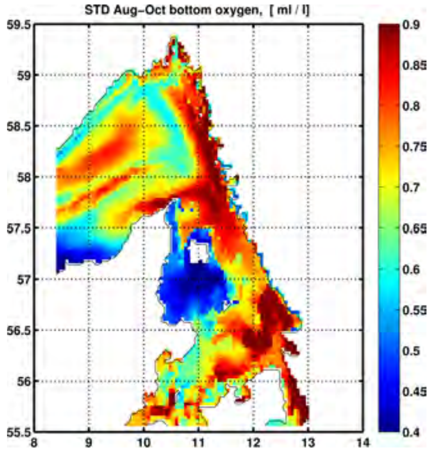

(b)

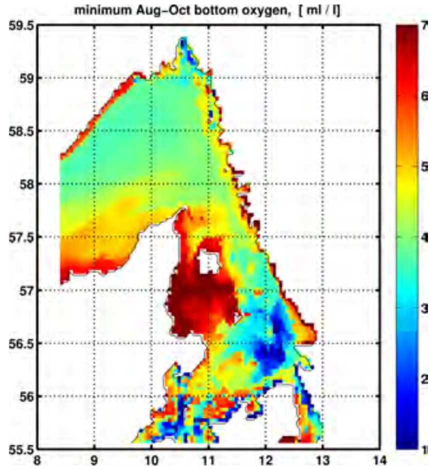

(c)

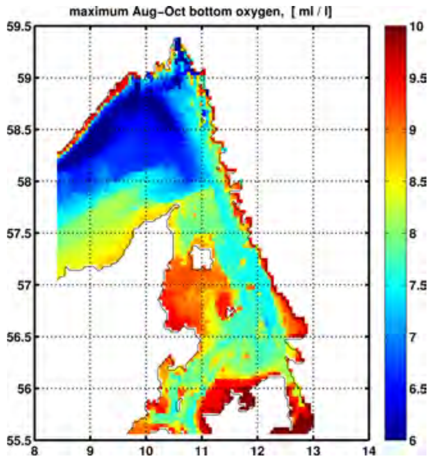

(d)

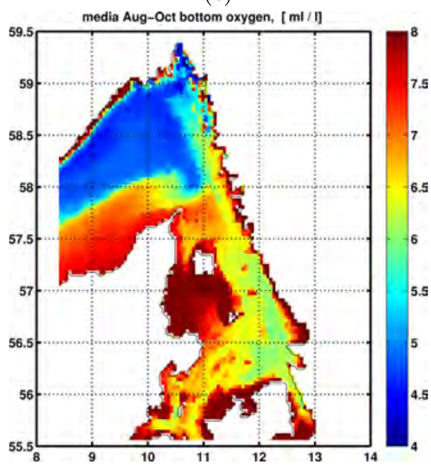

(e)

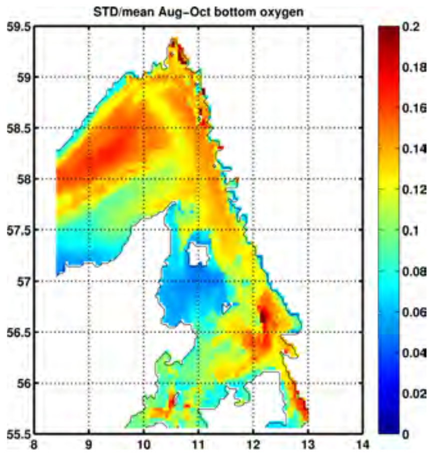

(f)

Figure 40: Concentrations of oxygen at sea bottom (grid cell and layer nearest the sea floor) during late summer-autumn (August-October). Mean, std, minimum, maximum, median and std/mean for 2007–2011 years of BSAP run.

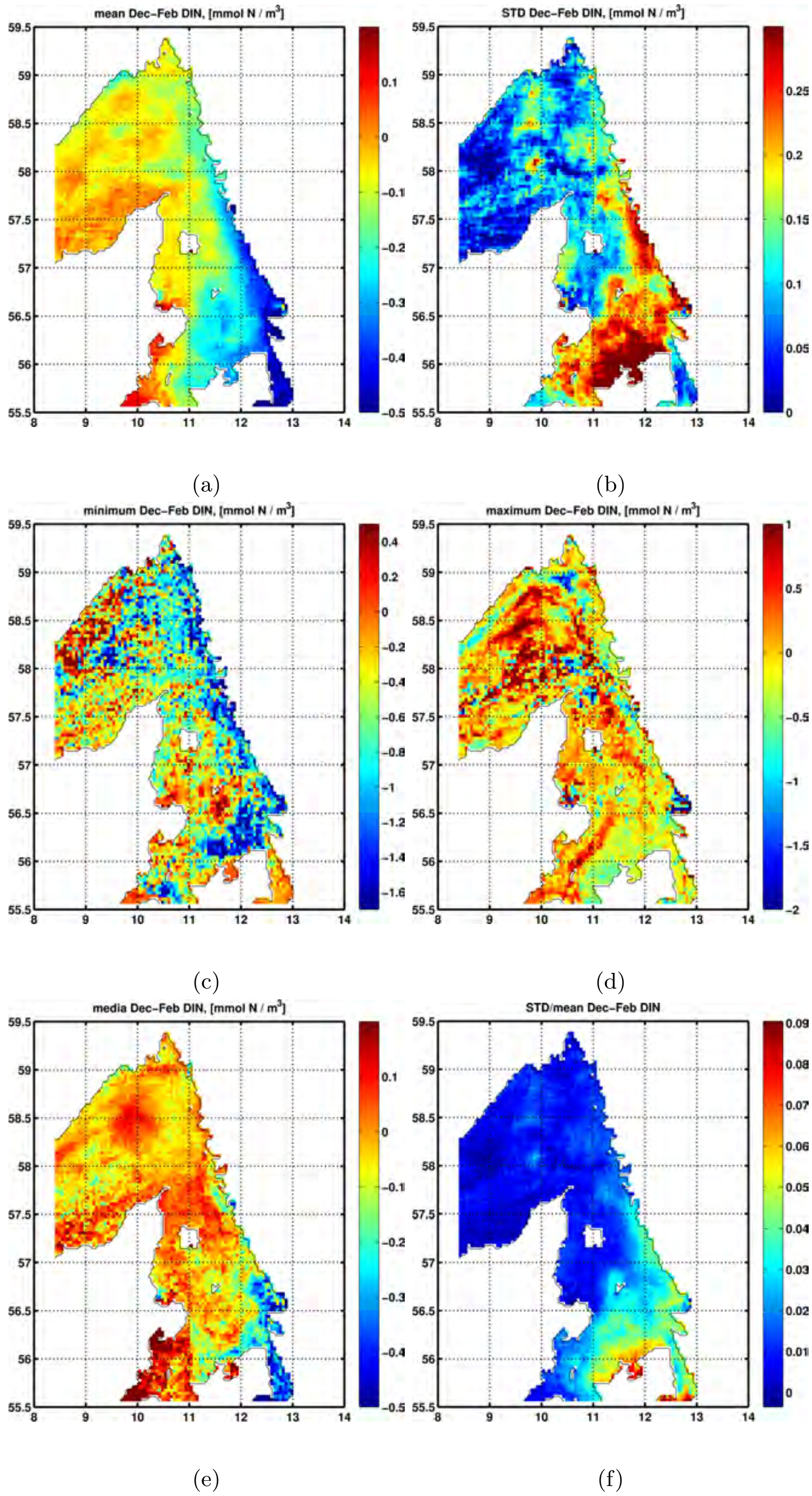

Figure 41: Changes between reference and BSAP runs (reference run - current run) in winter (DJF) sea surface (10m mean) DIN. Mean - (a), std - (b), minimum - (c), maximum - (d), median - (e) and std/mean - (f) for 2007–2011 years of BSAP run.

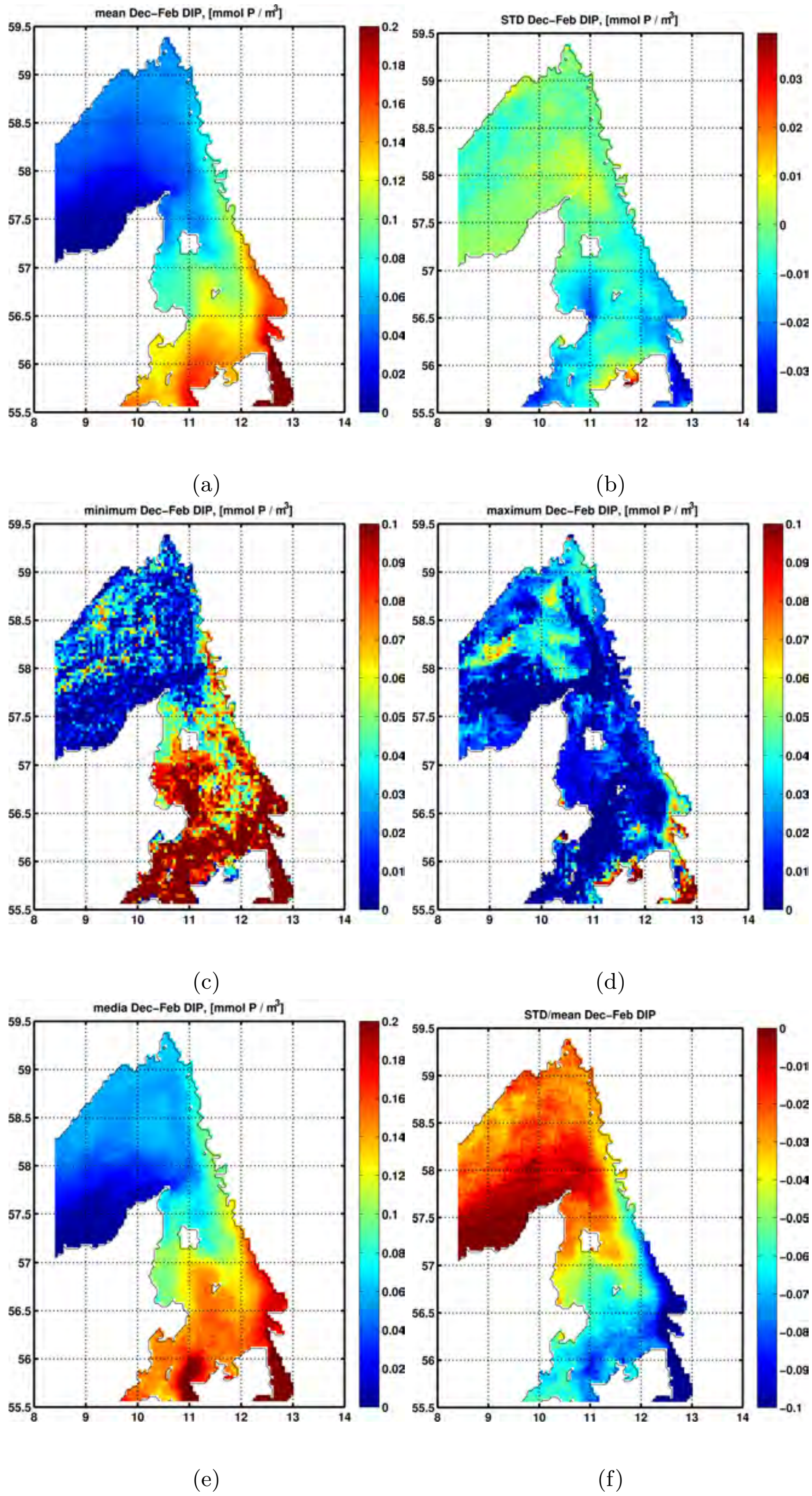

Figure 42: Changes between reference and BSAP runs (reference run - current run) in winter (DJF) sea surface (10m mean) DIP. Mean - (a), std - (b), minimum - (c), maximum - (d), median - (e) and std/mean - (f) for 2007–2011 years of BSAP run.

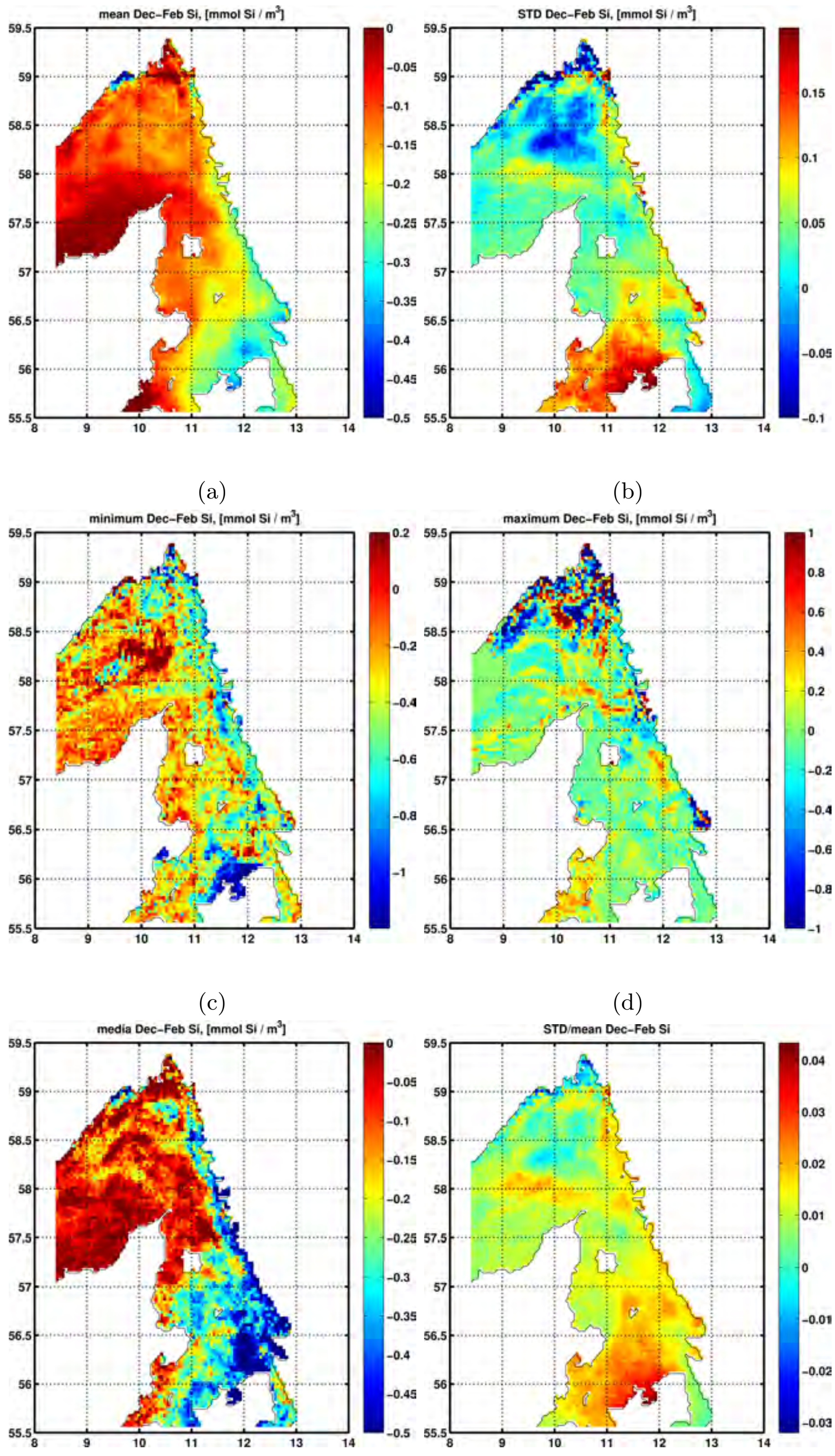

(a) (b) (c) (d) (e) (f)

Figure 43: Changes between reference and BSAP runs (reference run - current run) in winter (DJF) sea surface (10m mean) Si. Mean - (a), std - (b), minimum - (c), maximum - (d), median - (e) and std/mean - (f) for 2007–2011 years of BSAP run.

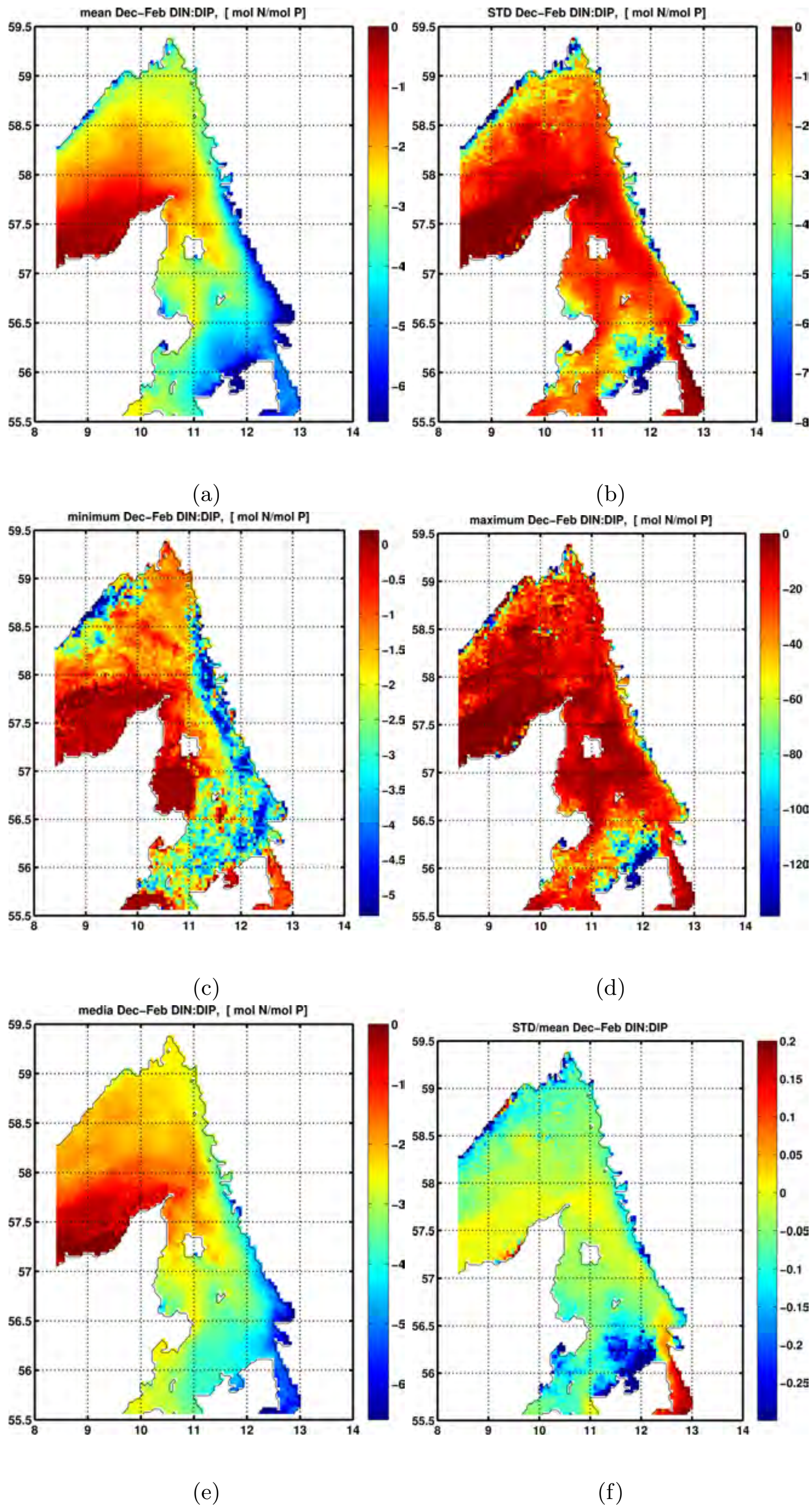

Figure 44: Changes between reference and BSAP runs (reference run - current run) in winter (DJF) sea surface (10m mean) DIN:DIP. Mean - (a), std - (b), minimum - (c), maximum - (d), median - (e) and std/mean - (f) for 2007–2011 years of BSAP run.

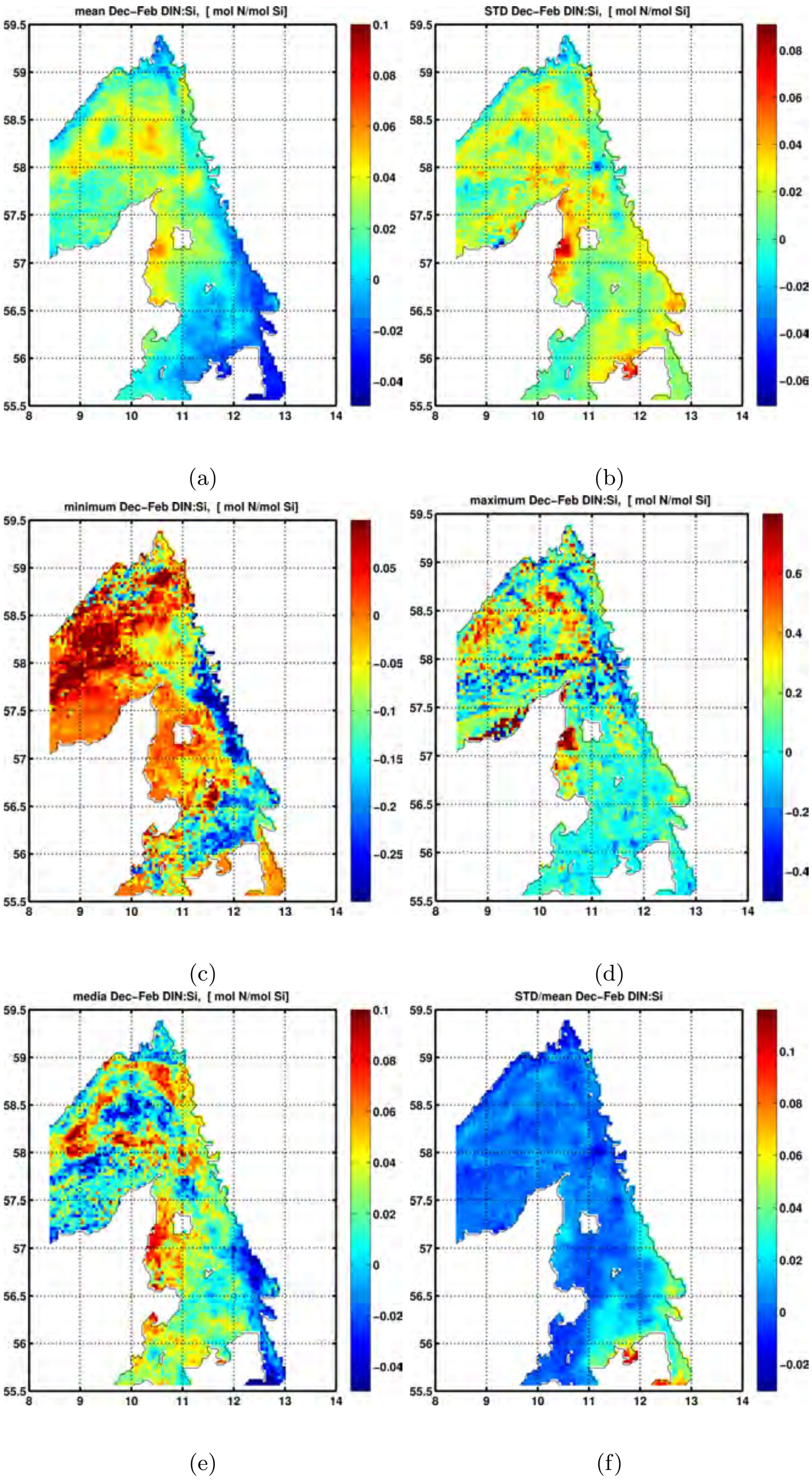

Figure 45: Changes between reference and BSAP runs (reference run - current run) in winter (DJF) sea surface (10m mean) DIN:Si. Mean - (a), std - (b), minimum - (c), maximum - (d), median - (e) and std/mean - (f) for 2007–2011 years of BSAP run.

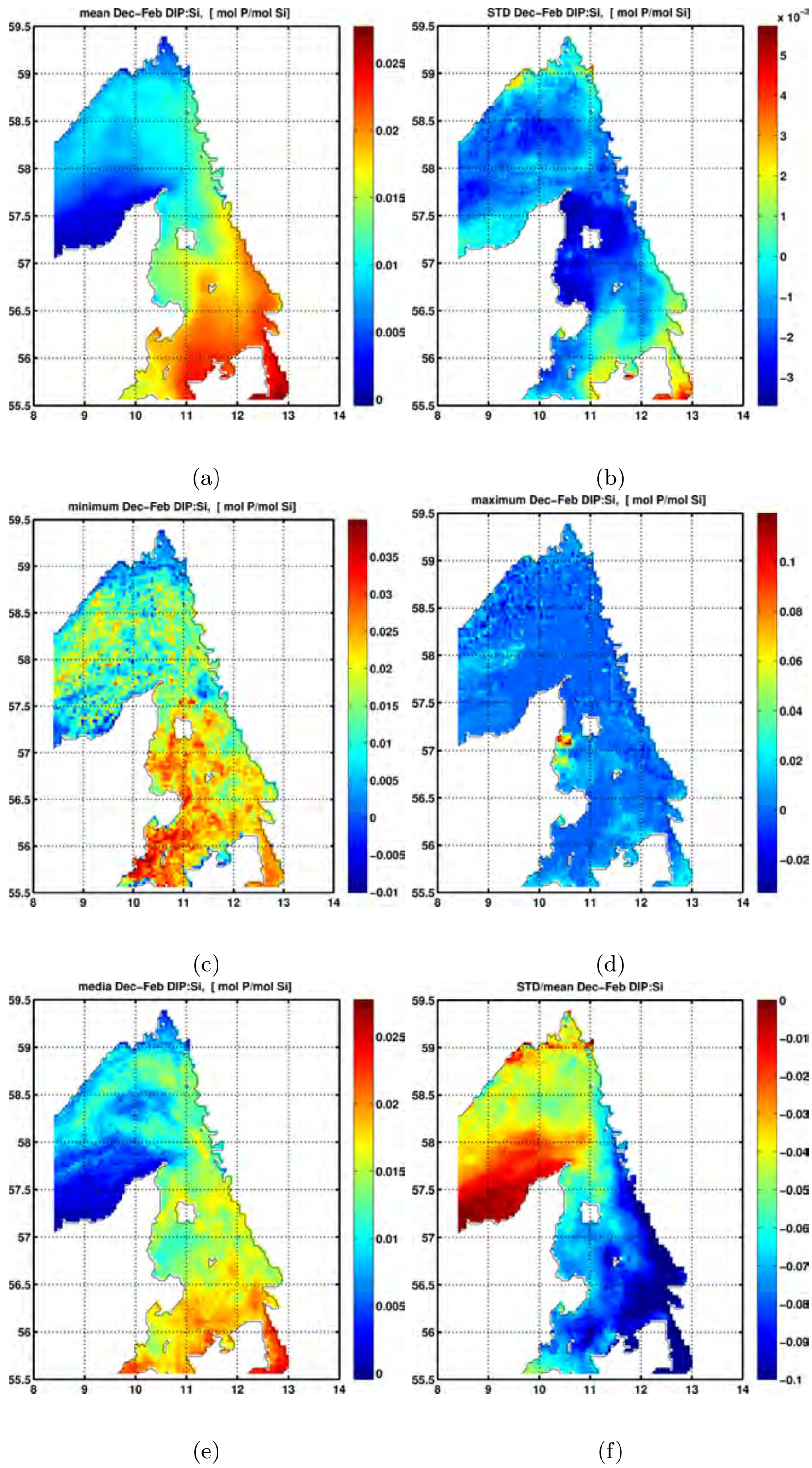

Figure 46: Changes between reference and BSAP runs (reference run - current run) in winter (DJF) sea surface (10m mean) DIP:Si. Mean - (a), std - (b), minimum - (c), maximum - (d), median - (e) and std/mean - (f) for 2007–2011 years of BSAP run.

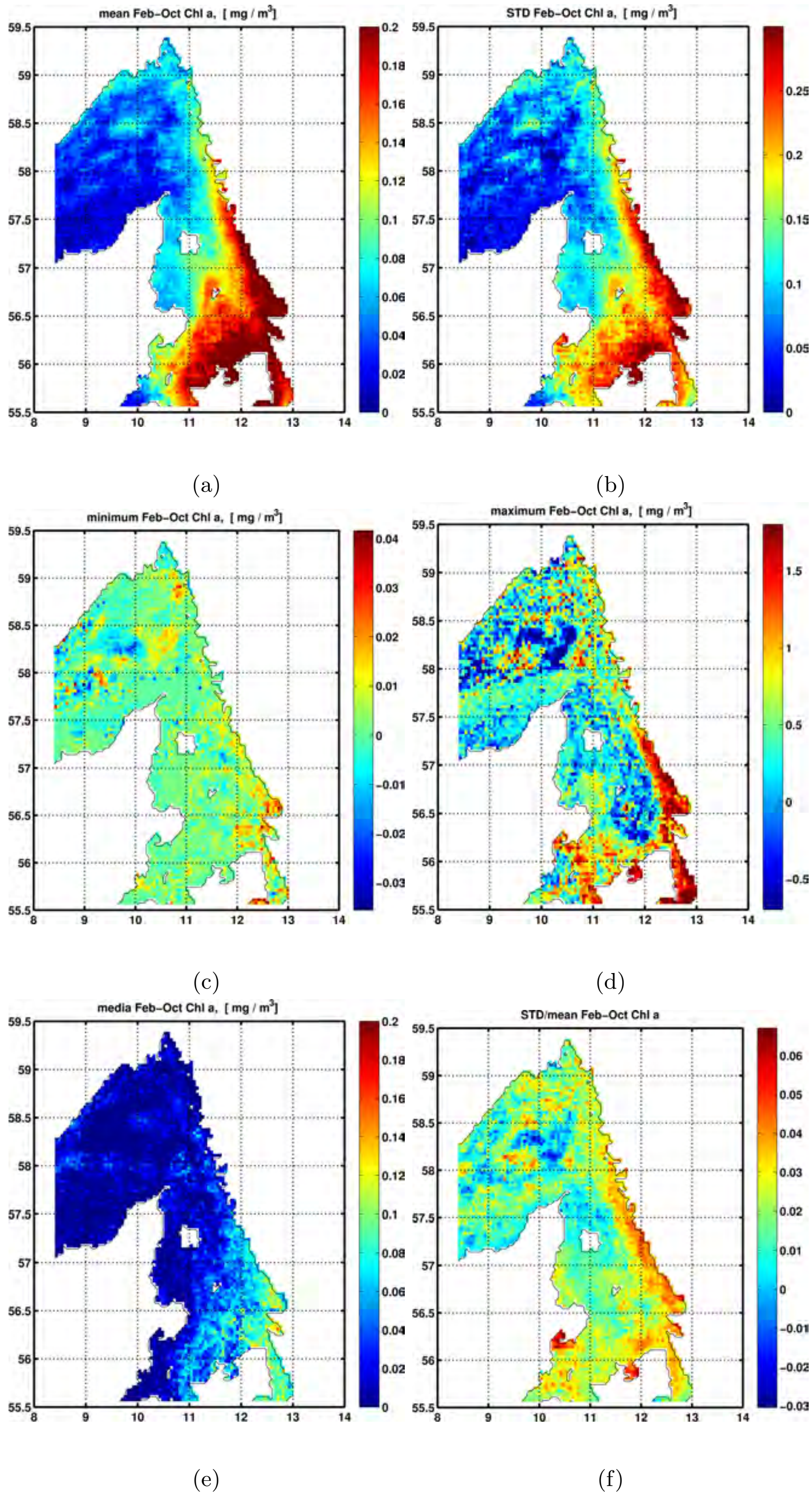

Figure 47: Changes between reference and BSAP runs (reference run - current run) in concentrations of chlorophyll-a in the growing season (February to October) at sea surface (10m mean) Mean - (a), std - (b), minimum - (c), maximum - (d), median - (e) and std/mean - (f) for 2007–2011 years of BSAP run.

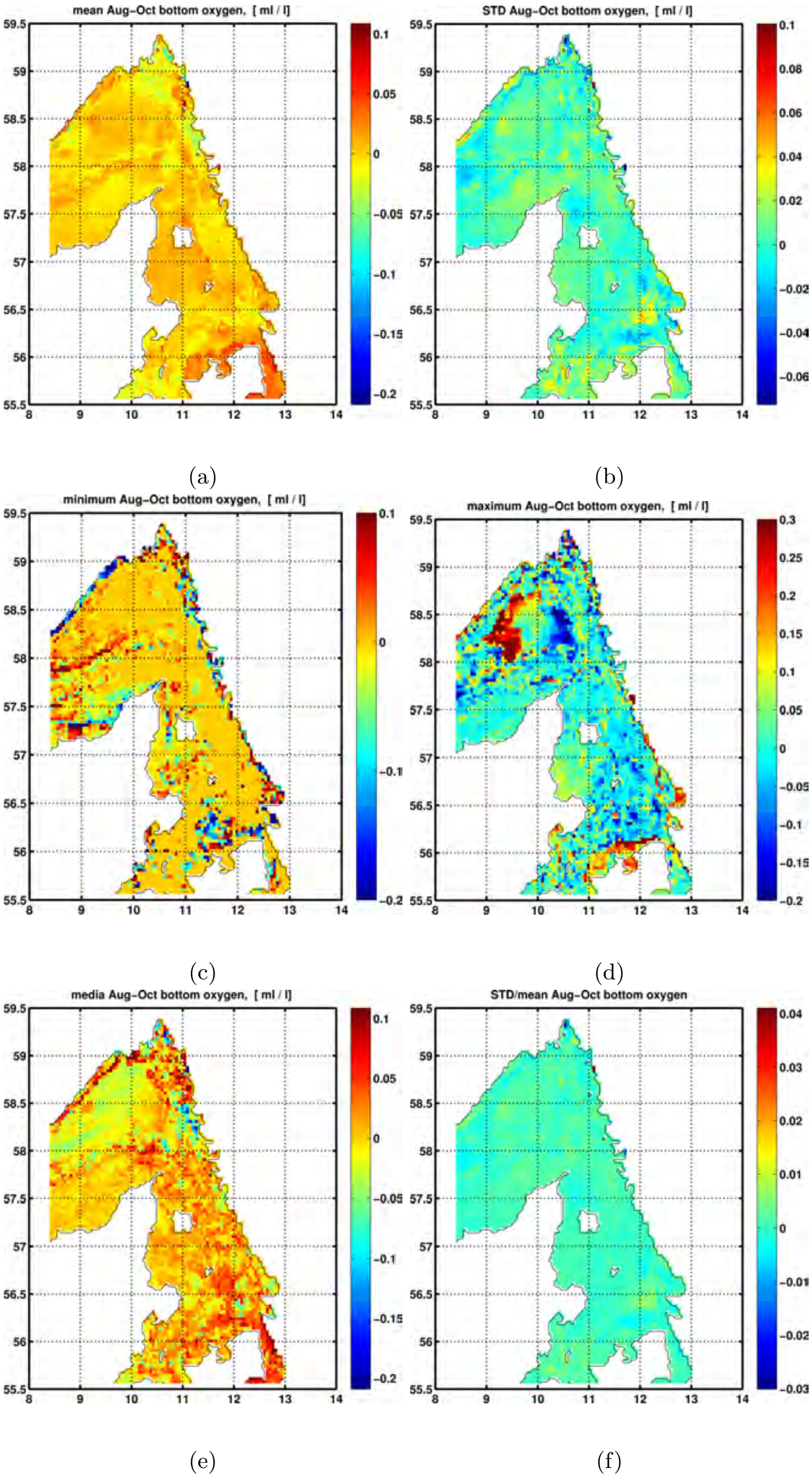

Figure 48: Changes between reference and BSAP runs (reference run - current run) in concentrations of oxygen at sea bottom (grid cell and layer nearest the sea floor) during late summer-autumn (August-October). Mean - (a), std - (b), minimum - (c), maximum - (d), median - (e) and std/mean - (f) for 2007–2011 years of BSAP run.

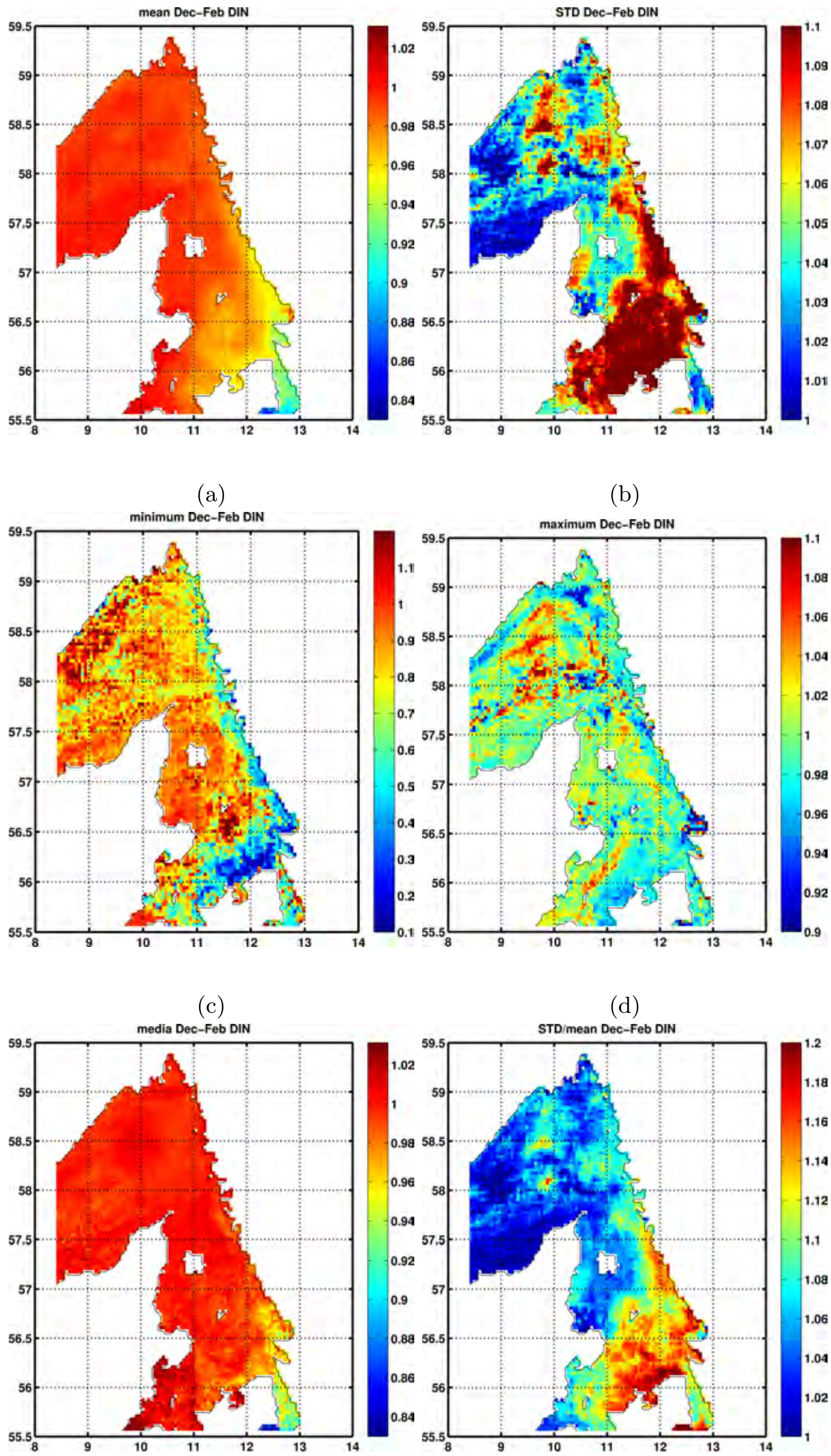

(a) (b) (c) (d) (e) (f)

Figure 49: Relative change in BSAP run (reference run / current run) in winter (DJF) sea surface (10m mean) DIN. Mean - (a), std - (b), minimum - (c), maximum - (d), median - (e) and std/mean - (f) for 2007–2011 years of BSAP run.

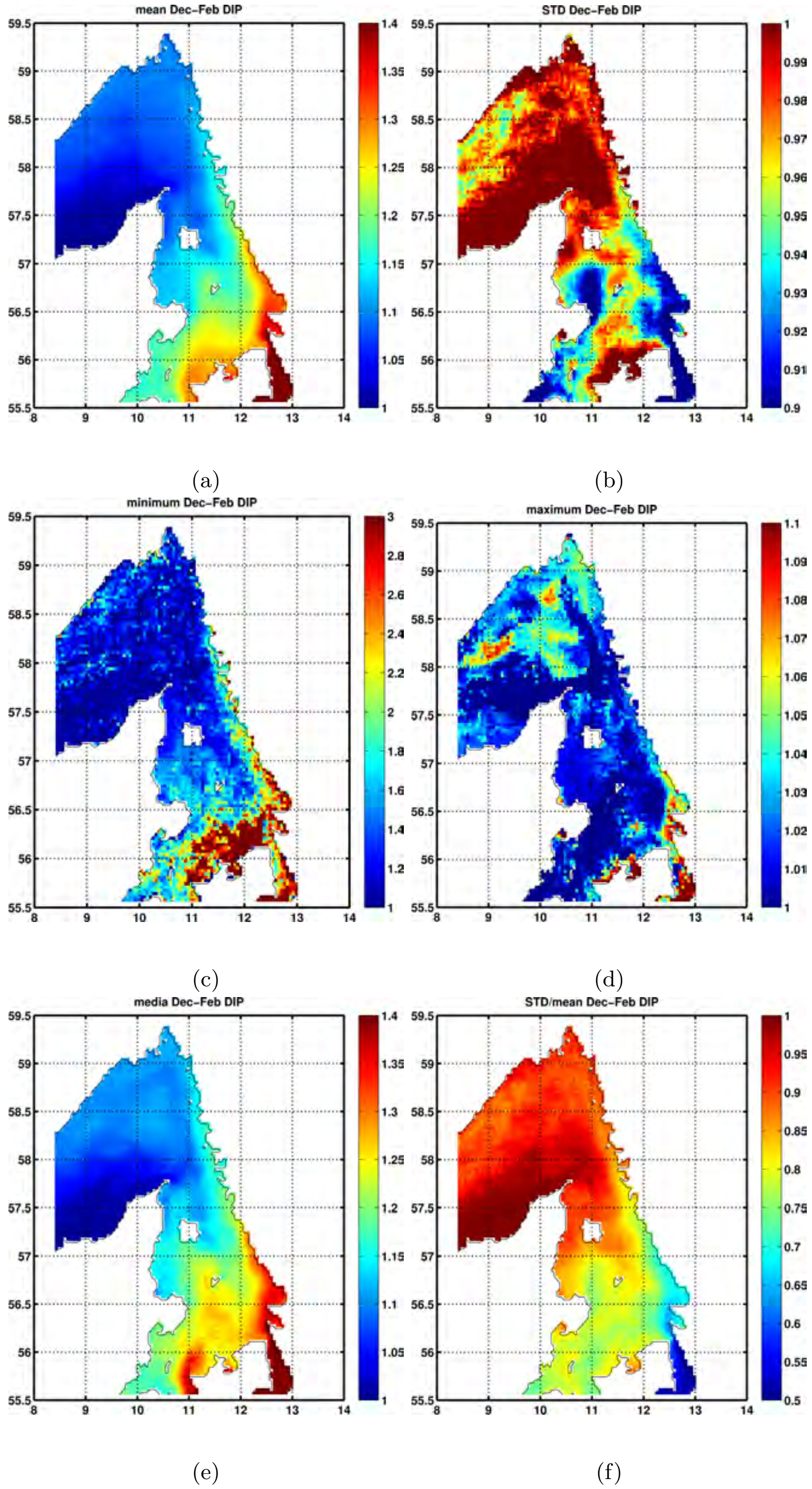

Figure 50: Relative change in BSAP run (reference run / current run) in winter (DJF) sea surface (10m mean) DIP. Mean - (a), std - (b), minimum - (c), maximum - (d), median - (e) and std/mean - (f) for 2007–2011 years of BSAP run.

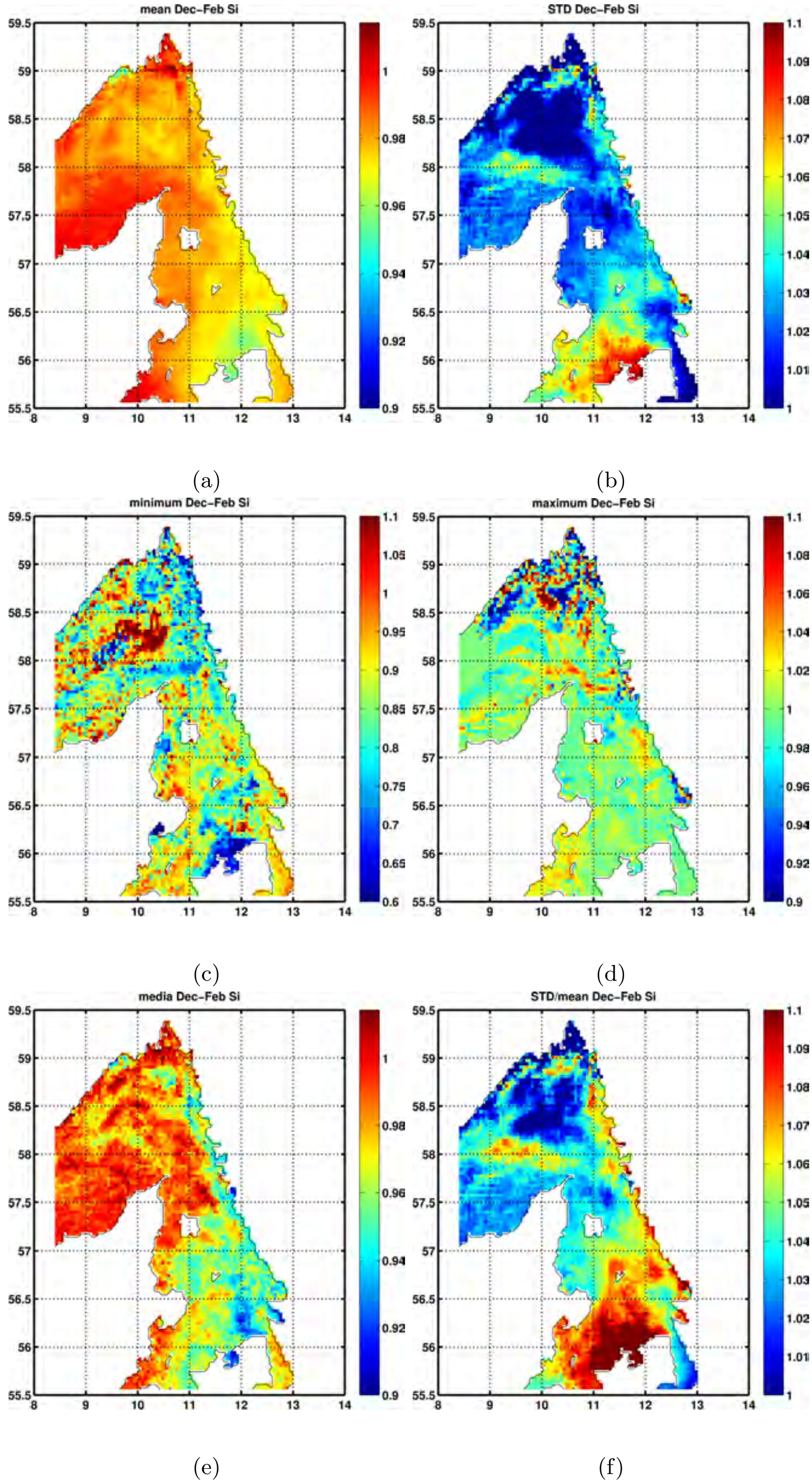

Figure 51: Relative change in BSAP run (reference run / current run) in winter (DJF) sea surface (10m mean) Si. Mean - (a), std - (b), minimum - (c), maximum - (d), median - (e) and std/mean - (f) for 2007–2011 years of BSAP run.

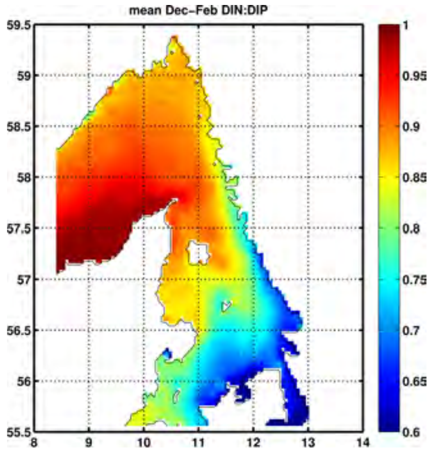

(a)

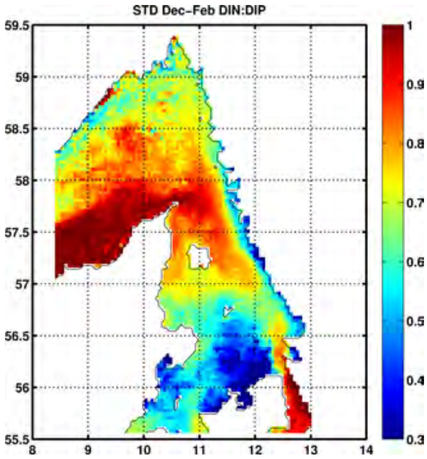

(b)

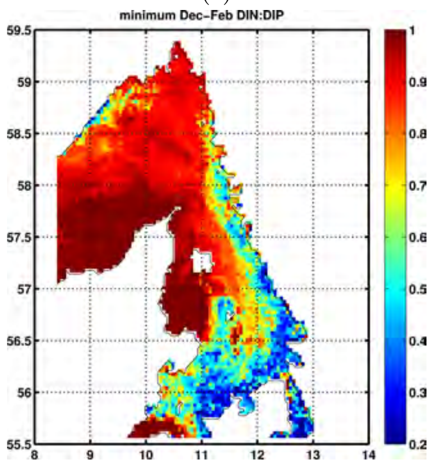

(c)

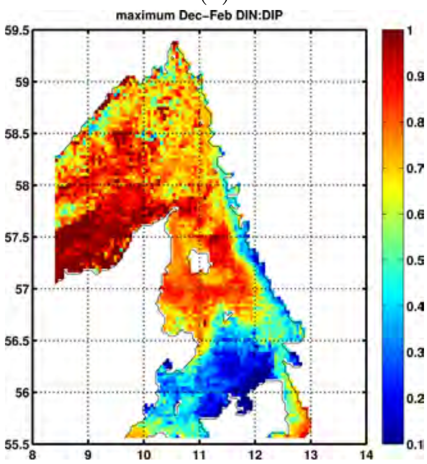

(d)

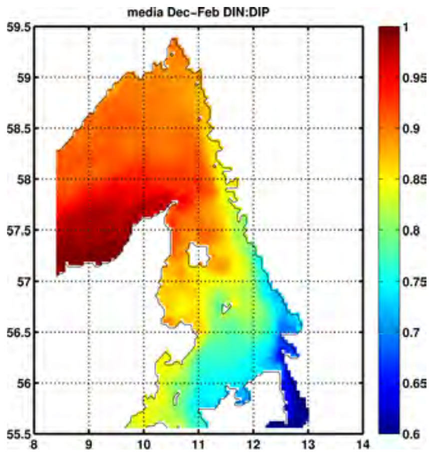

(e)

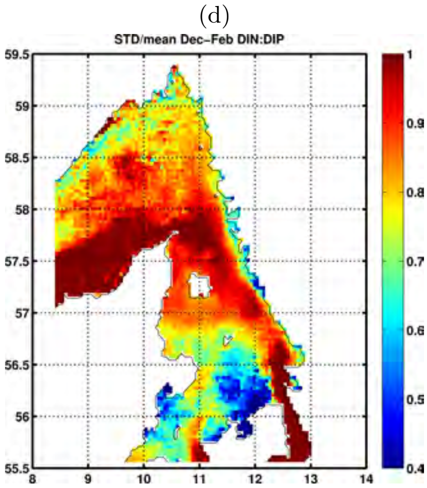

(f)

Figure 52: Relative change in BSAP run (reference run / current run) in winter (DJF) sea surface (10m mean) DIN:DIP. Mean - (a), std - (b), minimum - (c), maximum - (d), median - (e) and std/mean - (f) for 2007–2011 years of BSAP run.

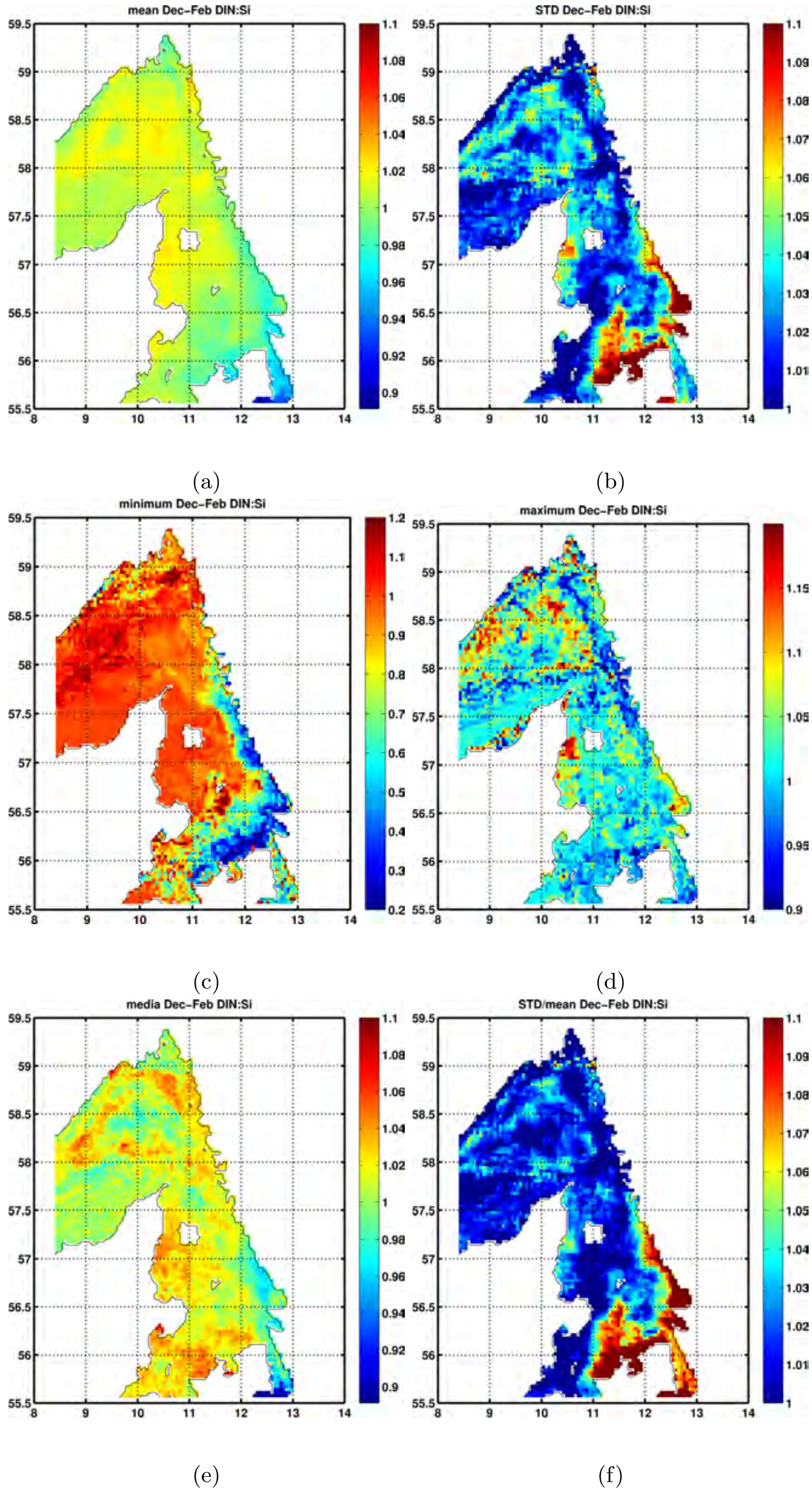

Figure 53: Relative change in BSAP run (reference run / current run) in winter (DJF) sea surface (10m mean) DIN:Si. Mean - (a), std - (b), minimum - (c), maximum - (d), median - (e) and std/mean - (f) for 2007–2011 years of BSAP run.

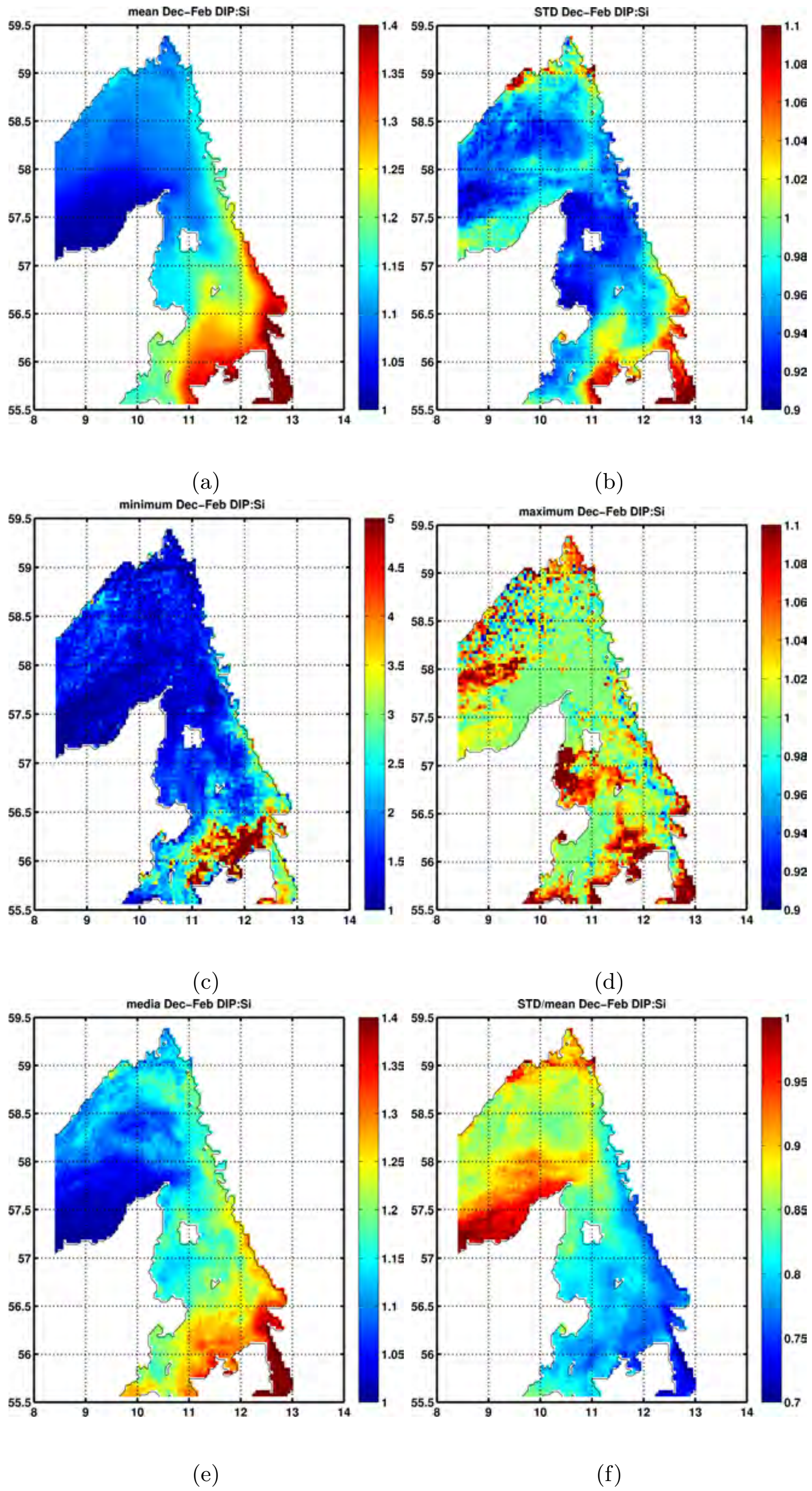

Figure 54: Relative change in BSAP run (reference run / current run) in winter (DJF) sea surface (10m mean) DIP:Si. Mean - (a), std - (b), minimum - (c), maximum - (d), median - (e) and std/mean - (f) for 2007–2011 years of BSAP run.

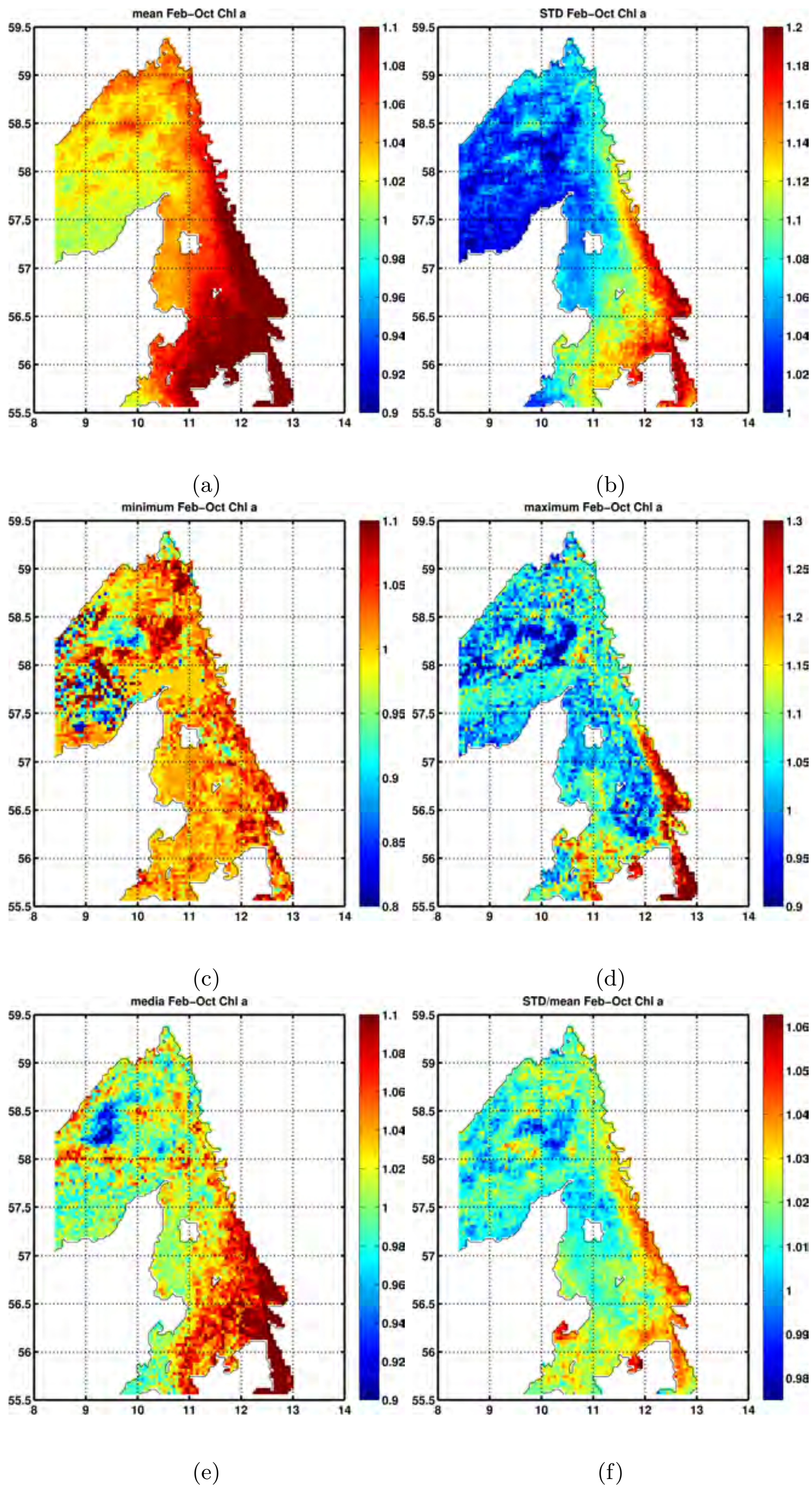

Figure 55: Relative change in BSAP run (reference run / current run) in concentrations of chlorophyll-a in the growing season (February to October) at sea surface (10m mean) Mean - (a), std - (b), minimum - (c), maximum - (d), median - (e) and std/mean - (f) for 2007–2011 years of BSAP run.

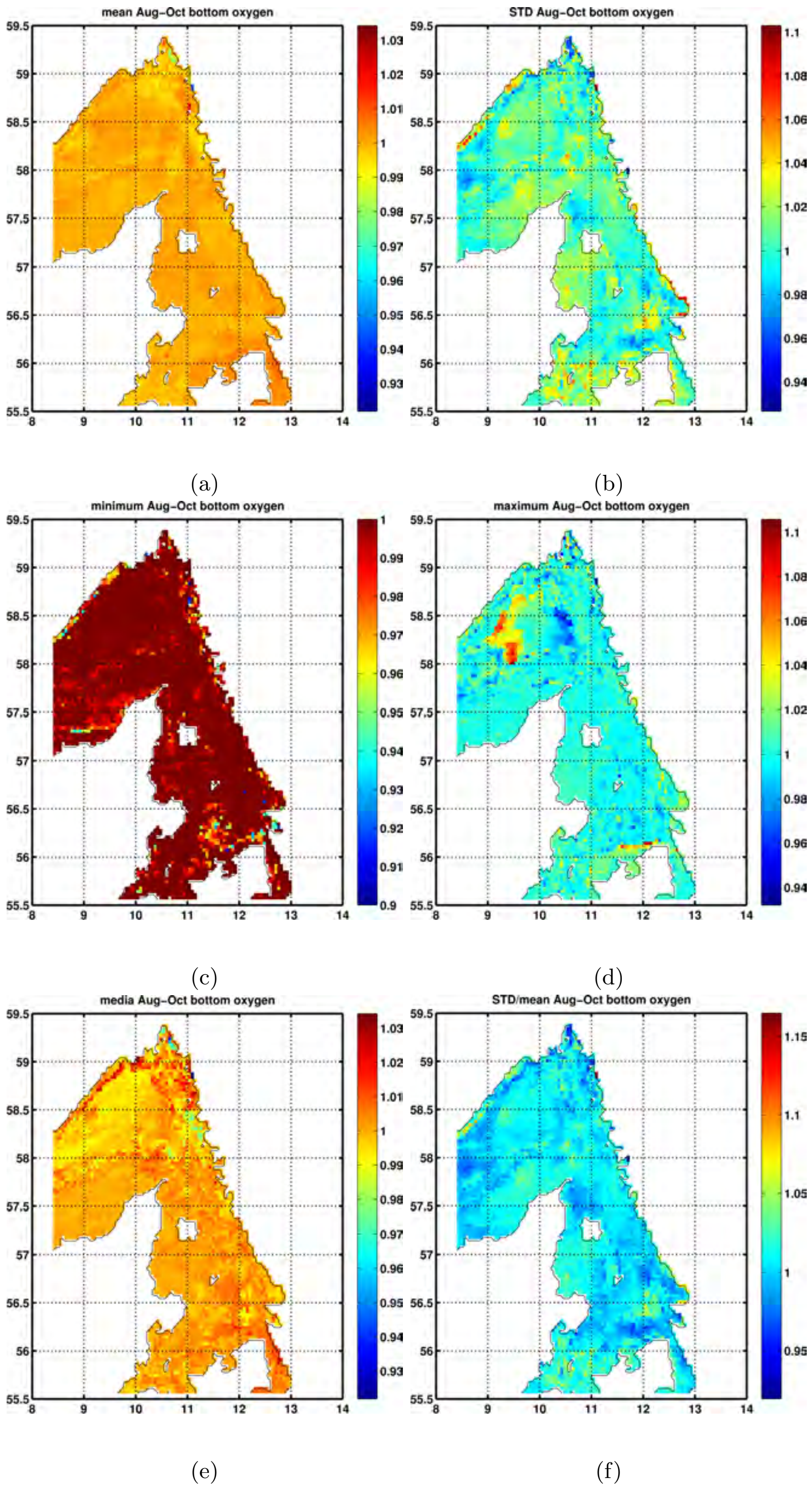

Figure 56: Relative change in BSAP run (reference run / current run) in concentrations of oxygen at sea bottom (grid cell and layer nearest the sea floor) during late summer-autumn (August-October). Mean - (a), std - (b), minimum - (c), maximum - (d), median - (e) and std/mean - (f) for 2007–2011 years of BSAP run.

SMHI Publications

SMHI publishes seven report series. Three of these, the R-series, are intended for international readers and are in most cases written in English. For the others the Swedish language is used.

Names of the Series Published since

RMK (Report Meteorology and Climatology) 1974
RH (Report Hydrology) 1990
RO (Report Oceanography) 1986
METEOROLOGI 1985
HYDROLOGI 1985
OCEANOGRAFI 1985
KLIMATOLOGI 2009

Earlier issues published in serie OCEANOGRAFI:

1 Lennart Funkquist (1985)
En hydrodynamisk modell för spridnings- och cirkulationsberäkningar i Östersjön Slutrapport.

2 Barry Broman och Carsten Pettersson. (1985)
Spridningsundersökningar i yttre fjärden Piteå.

3 Cecilia Ambjörn (1986).
Utbyggnad vid Malmö hamn; effekter för Lommabuktens vattenutbyte.

4 Jan Andersson och Robert Hillgren (1986).
SMHIs undersökningar i Öregrundsgrepen perioden 84/85.

5 Bo Juhlin (1986)
Oceanografiska observationer utmed svenska kusten med kustbevakningens fartyg 1985.

6 Barry Broman (1986)
Uppföljning av sjövärmepump i Lilla Värtan.

7 Bo Juhlin (1986)
15 års mätningar längs svenska kusten med kustbevakningen (1970 - 1985).

8 Jonny Svensson (1986)
Vågdata från svenska kustvatten 1985.

9 Barry Broman (1986)
Oceanografiska stationsnät - Svenskt Vattenarkiv.

10 ***Vakant – kommer ej att utnyttjas!***

11 Cecilia Ambjörn (1987)
Spridning av kylvatten från Öresundsverket

12 Bo Juhlin (1987)
Oceanografiska observationer utmed svenska kusten med kustbevakningens fartyg 1986.

13 Jan Andersson och Robert Hillgren (1987)
SMHIs undersökningar i Öregrundsgrepen 1986.

14 Jan-Erik Lundqvist (1987)
Impact of ice on Swedish offshore lighthouses. Ice drift conditions in the area at Sydostbrotten - ice season 1986/87.

15 SMHI/SNV (1987)
Fasta förbindelser över Öresund - utredning av effekter på vattenmiljön i Östersjön.

16 Cecilia Ambjörn och Kjell Wickström (1987)
Undersökning av vattenmiljön vid utfyllnaden av Kockums varvsbassäng. Slutrapport för perioden 18 juni - 21 augusti 1987.

17 Erland Bergstrand (1987)
Östergötlands skärgård - Vattenmiljön.

18 Stig H. Fonselius (1987)
Kattegatt - havet i väster.

19 Erland Bergstrand (1987)
Recipientkontroll vid Breviksnäs fiskodling 1986.

20 Kjell Wickström (1987)
Bedömning av kylvattenrecipienten för ett kolkraftverk vid Oskarshamnsverket.

21 Cecilia Ambjörn (1987)
Förstudie av ett nordiskt modellsystem för kemikaliespridning i vatten.

22 Kjell Wickström (1988)
Vågdata från svenska kustvatten 1986.

23 Jonny Svensson, SMHI/National Swedish Environmental Protection Board (SNV) (1988)
A permanent traffic link across the Öresund channel - A study of the hydro-environmental effects in the Baltic Sea.

24 Jan Andersson och Robert Hillgren (1988)
SMHIs undersökningar utanför Forsmark 1987.

25 Carsten Peterson och Per-Olof Skoglund (1988)
Kylvattnet från Ringhals 1974-86.

26 Bo Juhlin (1988)
Oceanografiska observationer runt svenska kusten med kustbevakningens fartyg 1987.

27 Bo Juhlin och Stefan Tobiasson (1988)
Recipientkontroll vid Breviksnäs fiskodling 1987.

28 Cecilia Ambjörn (1989)
Spridning och sedimentation av tippat lermaterial utanför Helsingborgs hamnområde.

29 Robert Hillgren (1989)
SMHIs undersökningar utanför Forsmark 1988.

30 Bo Juhlin (1989)
Oceanografiska observationer runt svenska kusten med kustbevakningens fartyg 1988.

31 Erland Bergstrand och Stefan Tobiasson (1989)
Samordnade kustvattenkontrollen i Östergötland 1988.

32 Cecilia Ambjörn (1989)
Oceanografiska förhållanden i Brofjorden i samband med kylvattenutsläpp i Trommekilen.

33a Cecilia Ambjörn (1990)
Oceanografiska förhållanden utanför Vendelsöfjorden i samband med kylvatten-utsläpp.

33b Eleonor Marmefelt och Jonny Svensson (1990)
Numerical circulation models for the Skagerrak - Kattegat. Preparatory study.

34 Kjell Wickström (1990)
Oskarshamnsverket - kylvattenutsläpp i havet - slutrapport.

35 Bo Juhlin (1990)
Oceanografiska observationer runt svenska kusten med kustbevakningens fartyg 1989.

36 Bertil Håkansson och Mats Moberg (1990)
Glommaälvens spridningsområde i nord-östra Skagerrak

37 Robert Hillgren (1990)
SMHIs undersökningar utanför Forsmark 1989.

38 Stig Fonselius (1990)
Skagerrak - the gateway to the North Sea

39 Stig Fonselius (1990)
Skagerrak - porten mot Nordsjön.

40 Cecilia Ambjörn och Kjell Wickström (1990)
Spridningsundersökningar i norra Kalmarsund för Mönsterås bruk.

41 Cecilia Ambjörn (1990)
Strömningsteknisk utredning avseende utbyggnad av gipsdeponi i Landskrona.

42 Cecilia Ambjörn, Torbjörn Grafström och Jan Andersson (1990)
Spridningsberäkningar - Klints Bank.

43 Kjell Wickström och Robert Hillgren (1990)
Spridningsberäkningar för EKA-NOBELs fabrik i Stockviksverken.

44 Jan Andersson (1990)
Brofjordens kraftstation - Kylvattenspridning i Hanneviken.

45 Gustaf Westring och Kjell Wickström (1990)
Spridningsberäkningar för Höganäs kommun.

46 Robert Hillgren och Jan Andersson (1991)
SMHIs undersökningar utanför Forsmark 1990.

47 Gustaf Westring (1991)
Brofjordens kraftstation - Kompletterande simulering och analys av kylvattenspridning i Trommekilen.

48 Gustaf Westring (1991)
Vågmätningar utanför Kristianopel - Slutrapport.

49 Bo Juhlin (1991)
Oceanografiska observationer runt svenska kusten med kustbevakningens fartyg 1990.

50A Robert Hillgren och Jan Andersson (1992)
SMHIs undersökningar utanför Forsmark 1991.

50B Thomas Thompson, Lars Ulander, Bertil Håkansson, Bertil Brusmark, Anders Carlström, Anders Gustavsson, Eva Cronström och Olov Fäst (1992).
BEERS -92 Final edition

51 Bo Juhlin (1992)
Oceanografiska observationer runt svenska kusten med kustbevakningens fartyg 1991.

52 Jonny Svensson och Sture Lindahl (1992)
Numerical circulation model for the Skagerrak - Kattegat.

53 Cecilia Ambjörn (1992)
Isproppsförebyggande muddring och dess inverkan på strömmarna i Torneälven.

54 Bo Juhlin (1992)
20 års mätningar längs svenska kusten med kustbevakningens fartyg (1970 - 1990).

55 Jan Andersson, Robert Hillgren och Gustaf Westring (1992)
Förstudie av strömmar, tidvatten och vattenstånd mellan Cebu och Leyte, Filippinerna.

56 Gustaf Westring, Jan Andersson, Henrik Lindh och Robert Axelsson (1993)
Forsmark - en temperaturstudie. Slutrapport.

57 Robert Hillgren och Jan Andersson (1993)
SMHIs undersökningar utanför Forsmark 1992.

58 Bo Juhlin (1993)
Oceanografiska observationer runt svenska kusten med kustbevakningens fartyg 1992.

59 Gustaf Westring (1993)
Isförhållandena i svenska farvatten under normalperioden 1961-90.

60 Torbjörn Lindkvist (1994)
Havsområdesregister 1993.

61 Jan Andersson och Robert Hillgren (1994)
SMHIs undersökningar utanför Forsmark 1993.

62 Bo Juhlin (1994)
Oceanografiska observationer runt svenska kusten med kustbevakningens fartyg 1993.

63 Gustaf Westring (1995)
Isförhållanden utmed Sveriges kust - isstatistik från svenska farleder och farvatten under normalperioderna 1931-60 och 1961-90.

64 Jan Andersson och Robert Hillgren (1995)
SMHIs undersökningar utanför Forsmark 1994.

65 Bo Juhlin (1995)
Oceanografiska observationer runt svenska kusten med kustbevakningens fartyg 1994.

66 Jan Andersson och Robert Hillgren (1996)
SMHIs undersökningar utanför Forsmark 1995.

67 Lennart Funkquist och Patrik Ljungemyr (1997)
Validation of HIROMB during 1995-96

68 Maja Brandt, Lars Edler och Lars Andersson (1998)
Översvämningar längs Oder och Wisla sommaren 1997 samt effekterna i Östersjön.

69 Jörgen Sahlberg SMHI och Håkan Olsson, Länsstyrelsen, Östergötland (2000).
Kustzonsmodell för norra Östergötlands skärgård.

70 Barry Broman (2001)
En vågatlas för svenska farvatten.
Ej publicerad

71 ***Vakant – kommer ej att utnyttjas!***

72 Fourth Workshop on Baltic Sea Ice Climate
Norrköping, Sweden 22-24 May, 2002
Conference Proceedings
Editors: Anders Omstedt and Lars Axell

73 Torbjörn Lindkvist, Daniel Björkert, Jenny Andersson, Anders Gyllander (2003)
Djupdata för havsområden 2003

74 Håkan Olsson, SMHI (2003)
Erik Årnefelt, Länsstyrelsen Östergötland
Kustzonssystemet i regional miljöanalys

75 Jonny Svensson och Eleonor Marmefelt (2003)
Utvärdering av kustzonsmodellen för norra Östergötlands och norra Bohusläns skärgårdar

76 Eleonor Marmefelt, Håkan Olsson, Helma Lindow och Jonny Svensson, Thalassos Computations (2004)
Integrerat kustzonssystem för Bohusläns skärgård

77 Philip Axe, Martin Hansson och Bertil Håkansson (2004)
The national monitoring programme in the Kattegat and Skagerrak

78 Lars Andersson, Nils Kajrup och Björn Sjöberg (2004)
Dimensionering av det nationella marina pelagialprogrammet

79 Jörgen Sahlberg (2005)
Randdata från öppet hav till kustzons-modellerna (Exemplet södra Östergötland)

80 Eleonor Marmefelt, Håkan Olsson (2005)
Integrerat Kustzonssystem för Hallandskusten

81 Tobias Strömgren (2005)
Implementation of a Flux Corrected Transport scheme in the Rossby Centre Ocean model

82 Martin Hansson (2006)
Cyanobakterieblomningar i Östersjön, resultat från satellitövervakning 1997-2005

83 Kari Eilola, Jörgen Sahlberg (2006)
Model assessment of the predicted environmental consequences for OSPAR problem areas following nutrient reductions

84 Torbjörn Lindkvist, Helma Lindow (2006)
Fyrskeppsdata. Resultat och bearbetnings-metoder med exempel från Svenska Björn 1883 – 1892

85 Pia Andersson (2007)
Ballast Water Exchange areas – Prospect of designating BWE areas in the Baltic Proper

86 Elin Almroth, Kari Eilola, M. Skogen, H. Søiland and Ian Sehested Hansen (2007)
The year 2005. An environmental status report of the Skagerrak, Kattegat and North Sea

87 Eleonor Marmefelt, Jörgen Sahlberg och Marie Bergstrand (2007)
HOME Vatten i södra Östersjöns vattendistrikt. Integrerat modellsystem för vattenkvalitetsberäkningar

88 Pia Andersson (2007)
Ballast Water Exchange areas – Prospect of designating BWE areas in the Skagerrak and the Norwegian Trench

89 Anna Edman, Jörgen Sahlberg, Niclas Hjerdt, Eleonor Marmefelt och Karen Lundholm (2007)
HOME Vatten i Bottenvikens vatten-distrikt. Integrerat modellsystem för vattenkvalitetsberäkningar

90 Niclas Hjerdt, Jörgen Sahlberg, Eleonor Marmefelt och Karen Lundholm (2007)
HOME Vatten i Bottenhavets vattendistrikt. Integrerat modellsystem för vattenkvalitets-beräkningar

91 Elin Almroth, Morten Skogen, Ian Sehsted Hansen, Tapani Stipa, Susa Niiranen (2008)
The year 2006
An Eutrophication Status Report of the North Sea, Skagerrak, Kattegat and the Baltic Sea
A demonstration Project

92 Pia Andersson editor and co-authors[1]
Bertil Håkansson[1], Johan Håkansson[1], Elisabeth Sahlsten[1], Jonathan Havenhand[2], Mike Thorndyke[2], Sam Dupont[2] *Swedish Meteorological and Hydrological Institute[1] Gothenburg University, Sven Lovén, Centre of Marine Sciences[2]* (2008)
Marine Acidification – On effects and monitoring of marine acidification in the seas surrounding Sweden

93 Jörgen Sahlberg, Eleonor Marmefelt, Maja Brandt, Niclas Hjerdt och Karen Lundholm (2008)
HOME Vatten i norra Östersjöns vatten-distrikt. Integrerat modellsystem för vattenkvalitetsberäkningar.

94 David Lindstedt (2008)
Effekter av djupvattenomblandning i Östersjön – en modellstudie

95 Ingemar Cato[1], Bertil Håkansson[2], Ola Hallberg[1], Bernt Kjellin[1], Pia Andersson[2], Cecilia Erlandsson[1], Johan Nyberg[1], Philip Axe[2] (2008)
[1]Geological Survey of Sweden (SGU)
[2]The Swedish Meteorological and Hydrological Institute (SMHI)
A new approach to state the areas of oxygen deficits in the Baltic Sea

96 Kari Eilola, H.E. Markus Meier, Elin Almroth, Anders Höglund (2008)
Transports and budgets of oxygen and phosphorus in the Baltic Sea

97 Anders Höglund, H.E. Markus Meier, Barry Broman och Ekaterina Kriezi (2009)
Validation and correction of regionalised ERA-40 wind fields over the Baltic Sea using the Rossby Centre Atmosphere model RCA3.0

98 Jörgen Sahlberg (2009)
The Coastal Zone Model

99 Kari Eilola (2009)
On the dynamics of organic nutrients, nitrogen and phosphorus in the Baltic Sea

100 Kristin I. M. Andreasson (SMHI), Johan Wikner (UMSC), Berndt Abrahamsson (SMF), Chris Melrose (NOAA), Svante Nyberg (SMF) (2009)
Primary production measurements – an intercalibration during a cruise in the Kattegat and the Baltic Sea

101 K. Eilola, B. G. Gustafson, R. Hordoir, A. Höglund, I. Kuznetsov, H.E.M. Meier T. Neumann, O. P. Savchuk (2010)
Quality assessment of state-of-the-art coupled physical-biogeochemical models in hind cast simulations 1970-2005

102 Pia Andersson (2010)
Drivers of Marine Acidification in the Seas Surrounding Sweden

103 Jörgen Sahlberg, Hanna Gustavsson (2010)
HOME Vatten i Mälaren

104 K.V Karmanov., B.V Chubarenko, D. Domnin, A. Hansson (2010)
Attitude to climate changes in everyday management practice at the level of Kaliningrad region municipalities

105 Helén C. Andersson., Patrik Wallman, Chantal Donnelly (2010)
Visualization of hydrological, physical and biogeochemical modelling of the Baltic Sea using a GeoDome™

106 Maria Bergelo (2011)
Havsvattenståndets påverkan längs Sveriges kust – enkätsvar från kommuner, räddningstjänst, länsstyrelser och hamnar

107 H.E. Markus Meier, Kari Eilola (2011)
Future projections of ecological patterns in the Baltic Sea

108 Meier, H.E.M., Andersson, H., Dieterich, C., Eilola, K., Gustafsson, B., Höglund, A., Hordoir, R., Schimanke, S (2011)
Transient scenario simulations for the Baltic Sea Region during the 21st century

109 Ulrike Löptien, H.E. Markus Meier (2011)
Simulated distribution of colored dissolved organic matter in the Baltic Sea

110 K. Eilola[1], J. Hansen[4], H. E. M. Meier[1], K. Myrberg[5], V. A. Ryabchenko[3] and M. D. Skogen[2] (2011)
[1]Swedish Meteorological and Hydrological Institute, Sweden, [2]Institute of Marine Research, Norway, [3] St. Petersburg Branch, P.P.Shirshov Institute of Oceanology, Russia, [4] National Environmental Research Institute, Aarhus University, Denmark, [5]Finnish Environment Institute, Finland
Eutrophication Status Report of the North Sea, Skagerrak, Kattegat and the Baltic Sea: A model study
Years 2001-2005

111 Semjon Schimanke, Erik Kjellström, Gustav Strandberg och Markus Meier (2011)
A regional climate simulation over the Baltic Sea region for the last Millennium

112 Meier, H. E. M., K. Eilola, B. G. Gustafsson, I. Kuznetsov, T. Neumann, and O. P.Savchuk,(2012)
Uncertainty assessment of projected ecological quality indicators in future climate

113 Karlson, B. Kronsell, J. Lindh, H. (2012)
Sea observations using FerryBox system on the ship TransPaper 2011 – oceanographic data in near real time. (Ej publicerad)

114 Domnina, Anastasia[1]. Chubarenko, Boris[1] (2012) *Atlantic Branch of P.P. Shirhov Institute of Oceanology of Russian Academy of Sciences, Kaliningrad, Russia.*[1]
"Discussion on the Vistula Lagoon regional development considering local consequences of climate changes Interim report on the ECOSUPPORT BONUS+project No. 08-05-92421.

115 K. Eilola[1], J.L.S. Hansen[4], H.E.M. Meier[1], M.S. Molchanov[3], V.A. Ryabchenko[3] and M.D.Skogen[2] (2013)
[1]*Swedish Meteorological and Hydrological Institute, Sweden.* [2]*Institute of Marine Research, Norway.* [3]*St. Petersburg Branch, P.P. Shirshov Institute of Oceanology, Russia.* [4]*Department of Bioscience, Aarhus University, Denmark*
Eutrophication Status Report of the North Sea, Skagerrak, Kattegat and the Baltic Sea: A model study. Present and future climate

116 ***Vakant – kommer ej att utnyttjas!***

117 Kari Eilola[1], Elin Almroth-Rosell[1], Moa Edman[1], Tatjana Eremina[3], Janus Larsen[4], Urszula Janas[2], Arturas Razinkovas-Basiukas[6], Karen Timmermann[4], Letizia Tedesco[5], Ekaterina Voloshchuk[3] (2015)
[1]*Swedish Meteorological and Hydrological Institute, Norrköping, Sweden.* [2]*Institute of Oceanography, Gdansk University, Poland.* [3]*Russian State Hydrometeorological University, Sankt-Petersburg, Russia.* [4]*Aarhus University, Roskilde, Denmark.* [5]*Finnish Environment Institute, Helsinki, Finland.* [6]*Coastal and Planning Research Institute, Klaipeda, Lithuania.*
Model set-up at COCOA study sites

118 Helén C. Andersson, Lena Bram Eriksson, Niclas Hjerdt, Göran Lindström Ulrike Löptien och Johan Strömqvist. (2016)
Översikt av beräkningsmodeller för bedömning av fiskodlingars näringsämnesbelastning på sjöar, vattendrag, magasin och kustvatten

SMHI
Sveriges meteorologiska och hydrologiska institut
601 76 NORRKÖPING
Tel 011-495 80 00 Fax 011-495 80 01

ISSN 0283-7714